KfK 4276
EUR 10535 e
Mai 1987

Nuclear Fusion Project Semi-annual Report of the Association KfK/EURATOM

October 1986 — March 1987

Projekt Kernfusion

Kernforschungszentrum Karlsruhe

KERNFORSCHUNGSZENTRUM KARLSRUHE
Projekt Kernfusion

KfK 4276
EUR 10535e

Nuclear Fusion Project

Semi-annual Report of the Association KfK/EURATOM

October 1986 - March 1987

Compiled by
G. Kast

Kernforschungszentrum Karlsruhe GmbH, Karlsruhe

Kernforschungszentrum Karlsruhe GmbH
Postfach 3640, 7500 Karlsruhe 1

ISSN 0303-4003

CONTENTS

B1 Blanket Design Studies

Two design concepts are studied by KfK: a helium cooled ceramic blanket and a blanket with Pb-17Li eutectic as breeder material and coolant. The study includes smal scale experiments and collaboration with industry for special feasibility problems. The studies are coordinated with efforts of CEA and UKAEA in a common working group.

In both of the designs blanket and first wall (F.W.) form a unit with a common coolant flow. Thus, the first wall studies are included here and described in more detail under Task N 1, Plasma Facing Components.

Helium Cooled Ceramic Breeder Blanket

A number of design improvements have been done on the canister concept since the last reporting period:
- new first wall design which allows a higher heat load (40 W/cm^2 instead of 20 W/cm^2);
- simplified canister design with the consequence of smaller temperature variation in the breeder material, easier fabricability, and significantly reduced probability and consequence of broken pebbles;
- Principal design for emergency cooling

In addition three-dimensional neutronics calculations were done with the Monte Carlo code MCNP which allows a geometrical representation very close to reality.

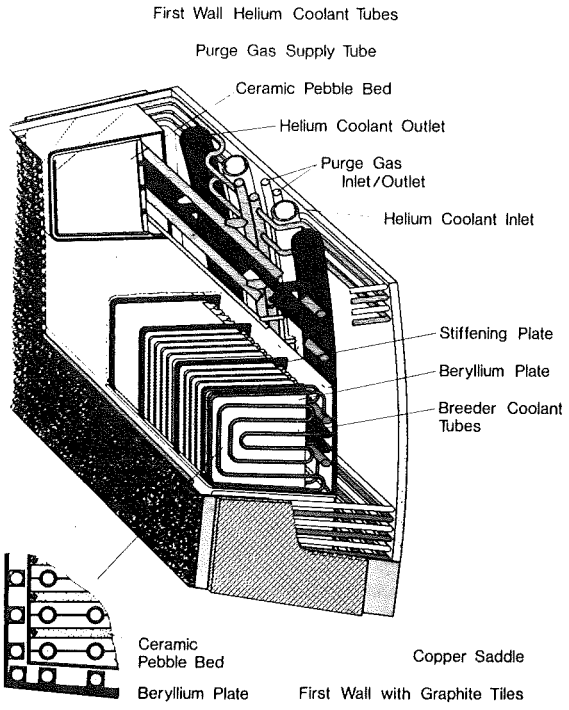

Fig. 1: Pebble Bed Breeder Canisters

Fig. 1 gives an artists view of the new outboard blanket canister design.

Fig. 2 shows a torodial mid plane cross section of the new inboard blanket which has poloidal coolant tubes. Basically the canister consists of beryllium plates with grooves for the coolant tubes.Two plates are sandwiched on each coolant coil. The rectangular slit between beryllium plates is filled with a Li_2SiO_4 pebble bed.

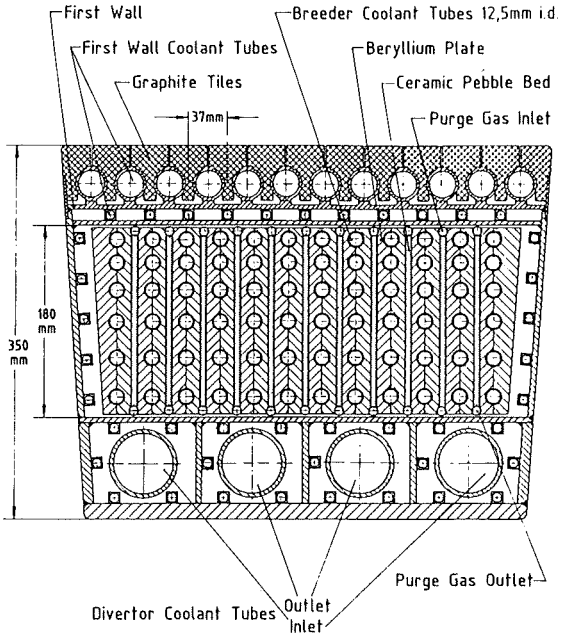

Fig. 2 Helium Cooled Inboard Breeder Blanket Segment

Purge flow supply tubes are foreseen at each end of the slit. No movement of pebbles is possibble or needed to account for differential thermal expansion effects.

To assure blanket cooling in case of loss of flow the blanket was modified to have two independent cooling systems which sequentially feed first wall as well as breeder coolant tubes. First wall and breeder cooling again is in series.

Because of the limited space on the inboard side the canister concept was abandoned here and a completely poloidal coolant tube arrangement was chosen (Fig.2). The inboard blanket has no curved surfaces and a smaller heat load what simplifies the design. Coolant flows downward in a first wall tube and upward in a corresponding blanket tube array. The large diameter tubes on the back side are supply tubes for the helium cooled divertor which is located below. The previous first wall design led to unacceptable stresses on the

blanket facing side. The improved version is indicated on Fig. 2. For the outboard blanket this design has the problem that the coolant tubes are outside the box on the front side but have to be inside of the box on the side walls. How this is solved is illustrated in Fig. 3.

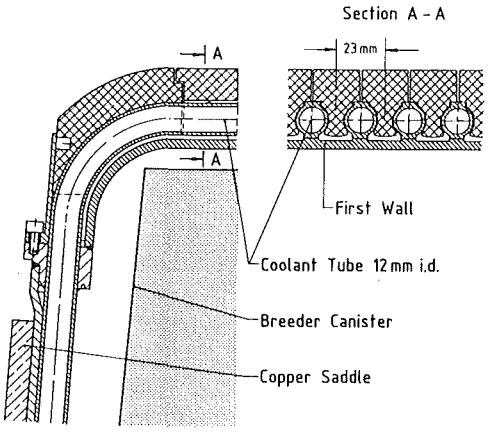

Fig. 3 Outboard First Wall with Graphite Tiles

With the three-dimensional neutronics calculations a tritium breeding ratio of 1.0 could just be obtained when all segments of NET are occupied by ceramic breeder blankets and a ^{6}Li-enrichment of 90% is taken (for details see description under B2). For larger fusion reactors tritium self sufficiency would be no problem.

Liquid Metal Cooled Blanket

The development of a blanket concept where the eutectic lithium-lead alloy Pb-17Li serves both as breeder material and as coolant has been continued. The present design is based on the NET double null configuration and on the arrangement of breeding blankets at the outboard side only. There are water or gas-cooled shielding segments arranged at the inboard side serving as neutron reflector.

Blanket design work has been concentrated on two subjects:

- Analysis of mechanical stresses in the steel structure,
- Design of an independent auxiliary cooling system for afterheat removal.

The stress analysis has been performed together with the Nuklear-Ingenieur-Services (NIS) company. This first phase of the analysis has been restricted to scoping calculations using linear elastic models. The aim was to find critical regions or components requiring design changes. The analysis was based on the use of austenitic steel SS 316 L as structural material. This is a change compared to the previous design where the martensitic steel 1.4914 had been considered. The roughly 50% lower allowable stress of solution annealed SS 316 L compared to the martensitic steel requires one major design change. In the previous design, the side walls are curved in order to avoid bending stress. A thickness of 20 mm would be necessary using austenitic steel to acommodate the membrane stress. However, an increase to 25 mm is sufficient to allow flat side walls which are easier to fabricate. Figure 4 shows the modified blanket cross-section with an increased thickness of the beryllium multiplier as recommended by neutronic calculations. The thickess of some walls had to be adjusted slightly to the results of the stress analysis which will be continued and more detailed.

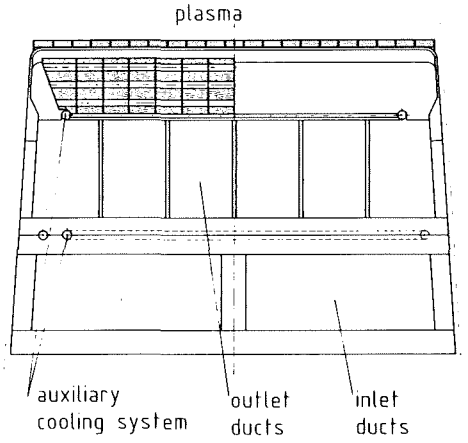

Fig. 4 : Cross section of the blanket segment

Afterheat removal by natural convection in the primary loop is an important inherent feature of both liquid metal as well as water cooled blankets. Natural convection, however, requires a closed primary loop which is not the case i.e. during blanket exchange.Therefore, a completely independent auxiliary cooling system is proposed as indicated in Figure 5 and 6. Small cooling tubes are arranged in each toroidal channel and in the plate between the inlet and outlet poloidal ducts.

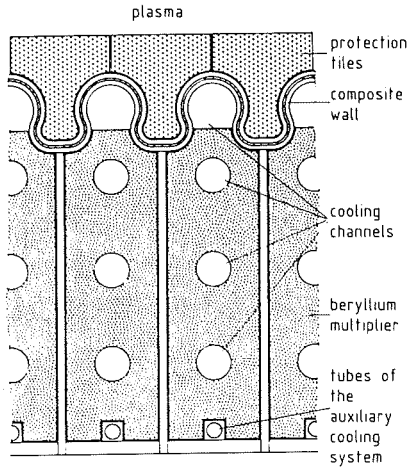

Fig. 5: Cooling tubes of the auxiliary cooling system in the toroidal channels

The eutectic liquid metal alloy NaK has been selected as coolant because it offers the possibility to use a thermopump. This is an electromagnetic pump using thermo-electricity as current source and permanent magnets in order to become independent from power upply.

Such pumps have been used successfully in inpile loops for fuel pin irradiation tests. The pump design will be modified and tested in this blanket development program.

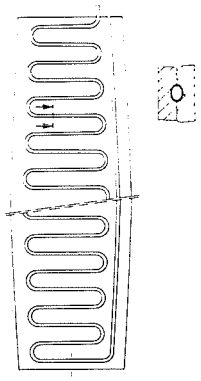

Fig. 6: Cooling tubes of the auxiliary cooling system in the plate between inlet-and outlet ducts

Staff:

K. Arheidt	M. K üchle
E. Bojarsky	W. Link
V. Casal	S. Malang
M. Dalle Donne	J. Reimann
U. Fischer	H. Reiser
C. Günther	K. Rust
B. Haferkamp	G. Schumacher
H. John	G. Sordon

B 2 Development of Computational Tools for Neutronics

The activities at KfK to improve the computational tools for fusion neutronics comprise the evaluation and processing of nuclear data, the development of new techniques, as the adoption and application of existing methods and programmes(e.g. Monte Carlo methods) for use in fusion neutronics.

For a rigorous treatment of the anisotropic neutron scattering, a general transport code system GANTRAS, making full use of double-differential cross-sections (DDX), is under development. The one-dimensional module, ANTRA 1, treating plane and spherical geometry, already had been set up and documented /1/ Furthermore, ANTRA 1 has been extended to include the cylindrical geometry option. The introduction of a new interpolation scheme for the angular fluxes, needed for the calculation of the scattering source, also necessitated the introduction of a new quadrature set being more appropriate for the applied procedure. The cylindrical geometrical option has been tested numerically meanwhile.

A comparative study of the neutron multiplication of a 14MeV neutron source in a spherical lead assembly has been performed. For this purpose, the ANTRA 1 programme has been used, together with a newly developed processing system for the provision of the angular-dependent transfer matrices, generated from the lead single- and double-differential data contained on the European Fusion File EFF-1. It is seen from Fig. 7 that, for the same geometrical assembly, there is no significant difference when using different procedures and data. On the other hand, it is concluded from this comparison, that the experimental values by Takahashi et al. are still too high, because the calculations refer to an ideal spherical assembly. Taking into account the real geometry(beam channels, target etc.),however, there will be a significant decrease of the neutron multiplication. This is also confirmed by the experiment of Hansen et al (see Fig.7).

Monte-Carlo methods have been proven to be very powerful for treating complex geometrical arrangements in fusion reactor blankets in two and three dimensions.The Los Alamos code MCNP has been used for analyzing the ceramic "pebble bed canister blanket"(see task B1) in the NET double null configuration /2/. A true geometrical model of a torus sector without any idealizing approximations has been used.

Fig. 8 shows a poloidal cross-section of a sector as it is used in these calculations. Table 1 presents the tritium breeding ratio gained in the one-, two- and three-dimensional MCNP-calculations. An important subject of such calculations is the determination of the total power production and the spatial distribution of the power density. However, the nuclear data describing the energy release are not very reliable in the MCNP library. Based on one dimensional calculations using the same geometrical model, there is, on the average, an underprediction of the power production by ca. 10%, as compared to deterministic 1d-calculations with nuclear data based on the VITIMIN-C library. Therefore, the efforts to improve the data base of MCNP have been intensified. Programmes for printing and plotting the neutron and photon data in the MCNP library have been written. This enables the handling and judging of these data in a convenient way. The programme ACER, a module of the nuclear data processing system NJOY converting the data from the ENDF-representation (as it is used in the nuclear data files, including EFF) to the representation in the MCNP-library, is under intense testing. Be-9 on EFF-1 presently is used as test sample.

For the calculation of the activation and afterheat of fusion reactor blanket components the DKR activation code, developed at the University of Wisconsin, together with its data library based on ENDF/B-IV, has been implemented at KfK (Siemens 7890 computer). DKR has been coupled with the ONETRAN transport code in a twofold way: ONETRAN provides the spatially varying neutron spectra for DKR and finally it performs the transport calculation for the photons created by the radioactive decay of the activation products. The source strength of the decay photons is calculated by DKR. In a first step this procedure already has been applied to a NET blanket design. At present this analysis is deepend and, furthermore, some more improvements are incorporated into the DKR-code in order to improve the data input.

	3d 7.5°-sector	2d radial-toroidal (torus mid-plane)	1d radial (torus mid-plane)
M	1.66	1.63	1.72
TBR	0.95	1.15	1.27

Table 1: Neutron multiplication (M) and tritium breeding ratio (TBR) of the "canister blanket"(see task B1) in the NET-III/DN configuration gained by 1d-,2d- and 3d-Monte Carlo calculations with MCNP.

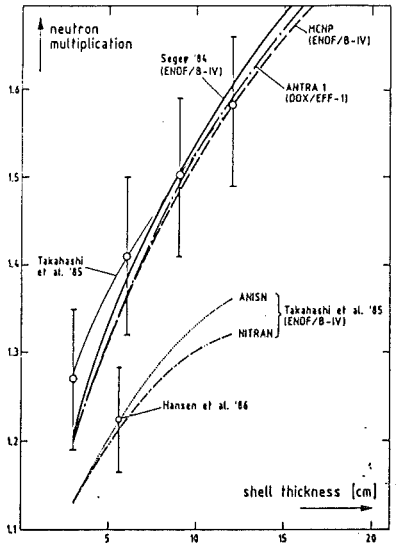

Fig. 7: Neutron multiplication in lead: a comparison between calculated values using different procedures and data and experimental values.

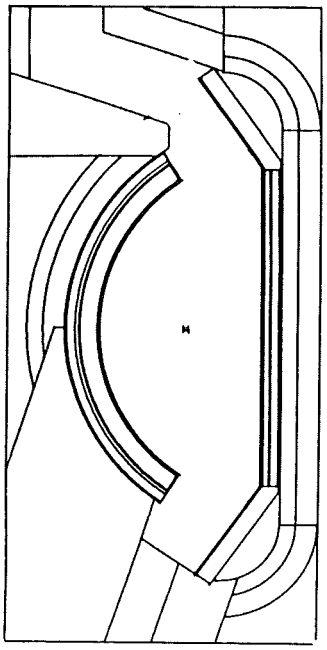

Fig. 8: Poloidal-radial cross section of a sector in the NET double null configuration, used in the MCNP calculation for the "canister blanket".

Publications:

1. A. Schwenk-Ferrero:GANTRAS, A System of Codes for the Solution of the Multigroup Transport Equation with a Rigorous Treatment of Antisotropic Neutron Scattering-Plane and Spherical Geometry, KfK-4163(1986).

2. U. Fischer : Multi-dimensional Neutronics Analysis of the "Canister Blanket" for NET, KfK-4255 (1987)

Staff

U. Fischer
H. Küsters
A. Schwenk-Ferrero
E. Stein
E. Wiegner

B 6 Corrosion of Structural Materials in Flowing Pb-17Li

Staff:
Ch. Adelhelm
H.U. Borgstedt
G. Drechsler
G. Frees
Z. Perić
G. Streib
S. Winkler

The corrosion loop PICOLO has been completed and commissioned in February 1987 (see Fig. 9). After measurements of the liquid metal flow in the test section as a function of the hydraulic diameter, the corrosion specimens have been inserted in the test section. These specimens are of steel 1.4914 (X 18 CrMoVNb121) in the state of recommended heat treatment. The temperature in the test section is maintained at 550 ± 2°C, the minimum temperature in the loop is in the range of 280 - 320°C. The first corrosion test has been started on March 6, 1987. The corrosion studies will be accompanied by chemical analytical examinations of the molten metal.

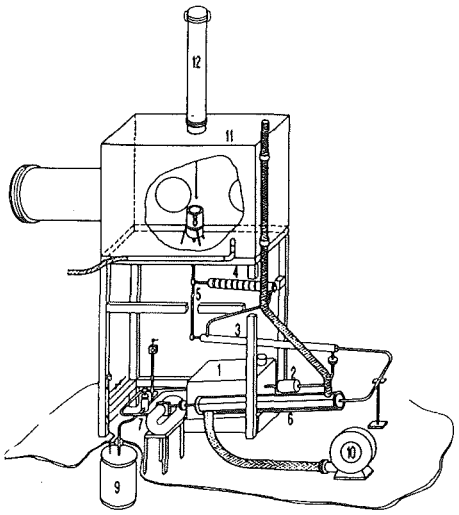

Fig. 9: The PbLiCorrosion Loop PICOLO

1 EM pump	2 EM flow meter
3 heat exchanger	4 electr. heater
5 test section	6 air cooler
7 magnetic trap	8 expansion vessel
9 drain tank	10 blower
11 glove box	12 equipment for changing of specimens

Publication: H.U. Borgstedt, G. Frees and G. Drechsler
J. Nucl. Mat. 141-143 (1986) 561-565

B 6.3. Fatigue of Structural Steel in Pb-17Li

The low cycle fatigue behaviour of the martensitic steel X 18CrMoVNb 12 1 (1.4914) will be tested at 550°C in the liquid alloy Pb-17Li. The electromechanical testing machine (INSTRON 8062, 125kN) was put into operation and some room-temperature tests with austenitic steels have been performed to check the testing machine. Capsules for the in liquid metal tests are already prepared. Hour glass shaped specimens for LCF tests are under preparation. The tests with and without hold time at the strain maximum will be started in October 1986.

The development of the testing method for lcf tests in Pb-17Li environment has been finished, the calibration of the equipment is under the and first tests with hour glass shaped specimens of 1.4914 steel will follow.

Staff
H.U. Borgstedt
M. Grundmann
Z. Peric

B 9 Tritium Extraction from Liquid Pb-17Li by the Use of Solid Getters

Several Methods were proposed to extract tritium from the liquid blanket material. Task B9 wil study the possibility to use solid getter materials. An advantage of this method will be its simplicity and the possible very low tritium inventory in the blanket.

For the studies the loop TRITEX is under construction. In parallel laboratory studies especially for compatibilities of different metals with the liquid alloy are under way.

The loop TRITEX will be a pumped stainless steel loop with about 60 kg of Pb-17Li circulating. The most important data are given in the table, the flow diagramm in the figure.

Loop TRITEX

construction material	steel 4922 (similar to HT9)
total inventory Pb-17Li	75 Kg
circulating Pb-17Li	60 Kg
flow rate	0 to 0.4 kg/s
temperature range	250 to 550 °C
purification systems	cold trap (bypass) magnetic trap
cover gas	argon

Hydrogen will be dissolved in the liquid metal within the expansion tank via the free surface. Tritium will be simulated by deuterium, only traces of tritium will be used in later experiments. Experiments for hydrogen extraction will be performed in the test section, which is inside of an argon-glove box. Two sampling stations before and after the test section allow liquid metal sampling for hydrogen determination. Other special features of the loop are a magnetic trap and a bypass cold trap with possibilities to investigate deposited impurities, and several corrosion sample positions. Furhtermore static tests can be performed using an experimental plug at the drain tank.

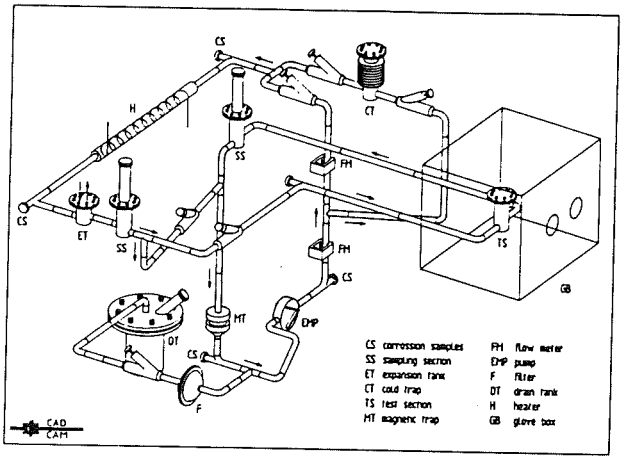

Fig. 10 : The loop TRITEX

During the next reporting period the loop will be completed and the Pb-17Li filled in. Experiments for the extraction of hydrogen behavior will start in 1988, after investigating the hydrogen behavior in the system without extraction. Because as well the test section and the sampling stations are very flexible tools, also other extraction techniques can be studied at a later time.

Tritium Extraction by cold Traps and Permeation Windows

The choice of the tritium extraction technique is dependent on the blanket concept. Two different techniques are investigated:

For a self-cooled Pb-17Li blanket with an intermediate Na or NaK loop a promising method is to have the tritium permeating into the fluid into the fluid of the intermediate loop and o separate it by precipitation as tritide in a cold trap. To recover the tritium, the cold trap is decoupled from the flow, the fluid is drained and the cold trap is heated up. The elemental tritium which results from thermal decomposition at about 400 °C is pumped off and stored, e.g. with a getter bed.

The surface of the ferritic heat exchanger is sufficient as permeation window. The compatibility of steel swith Na or NaK is well known. Oxygen impurities do not build up permeation barriers. Oxygen in the Pb-17 Li may cause a permeation impediment, which, for the ferritic steels, appears to be acceptable. Other open questions are related to the tritium precipitation and decomposition kinetics (for details see KfK 4105, Oct. 1986). However, none of this problems appear to be a feasibility issue. The WAWIK-programme (WAWIK = Wasserstoff-Abtrennung und Wiedergewinnung in Kaltfallen) has been started to investigate experimentally these effects. First experiments to decompose tritide (simulated by hydride) are presently carried out.

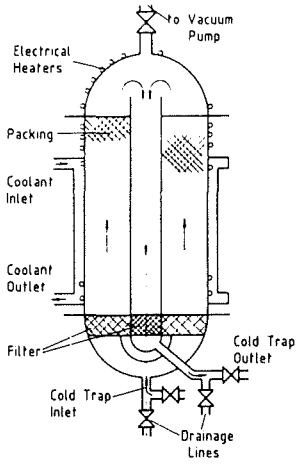

Fig. 11: Conceptional Design of cold Trap for Tritium Precipitation and Recovery

Fig. D shows a conceptional design of such a cold trap: The NaK with dissolved tritium (Sieverts range) flows upward in an annulus and is cooled counter currently to a temperatue below the tritium saturation temperature. Tritium precipitates as tritide on the surface of the packing. A homogeneous precipitation on the entire packing surface is anticipated. In the central tube the NaK flows downward and is heated up. The filters shown in the figure prevent the plugging of the drainage lines due to break-off of cristals.

The other method is attractive for a water-cooled Pb-17Li blanket. The tritium permeates through a wall with a high permeability, coated at the downstream side with a catalyst layer to oxidize the tritium which then diffuses into a He stream for further processing. The open problems were studied in the frame of a NET contract (223/86-2FUD NET). Critical problems are associated with the "permeation window" and not with the subsequent processing steps.

Problems are the compatibility of structural materials with Pb-17Li, the influence of impurities in Pb-17Li on tritium permeation, and the mechanical stability of the intermetallic bond. Experiments are planned in order to investigate the critical problems.

Staff:
H. Feuerstein
H. Gräbner
G. Kieser

B 11-16 Development of Ceramic Breeder Materials

The KfK contribution concentrates on the Li-Silicates and includes all the steps necessary to achieve a product to be used in the helium cooled blanket design. The development starts with fabrication and characterization of pellets and pebbles. Physical, mechanical and chemical properties are measured before and after irradiation. The irradiation program makes use of several reactors within the European and the Beatrix Cooperation. Lithium-Orthosilicate has been proven as the most promising candidate for the NET reference ceramic breeder material.

1. Fabrication and Characterization of Ceramic Breeder Materials (B 11, B 12)

The preparation and fabrication of lithium containing monosilicates, especially Li_2SiO_3 and Li_4SiO_4, are under development to be used as breeder materials. Monosilicate powders, normally sintered to pellets with cylindrical shape or fabricated as nearly spherical granules, were prepared for basic material studies. The preparation of pure monophase and sinterable Li_4SiO_4 powder from alcoholic suspensions has been worked out in detail.

Preparation of Li_2SiO_3 and Li_4SiO_4 Pellets and Powders

50 orthosilicate and 30 metasilicate disks with different diameters and a central hole were prepared to test the compatibility behavior of the silicate ceramics in contact with beryllium within a French - German experiment. A batch of 600 g spray-dried Li_4SiO_4 powder calcinated at elevated temperature was produced for further basic material compatibility studies at KfK.

Fabrication of Li_4SiO_4 Powders from Alcoholic Suspensions

Within the preparation technique to process pure Li_4SiO_4 powders from alcoholic suspensions an organic phase is obtained from amorphous SiO_2 ("Aerosil") and lithium hydroxide suspended in methanol and boiled under reflux conditions for about 3 to 5 hours. A very fine dispersed powder with a high flowability character is obtained from suspension by spraydrying after methanol is distilled-off with subsequently addition of water. In Fig. 12 a picture is given, obtained from scanning electron microscopy, showing spherical granules of a spray-dried powder. Most of the granules are in the size of 10 µm, the larger ones with 20 to 30 µm in size are mostly broken or damaged. Calcination of this loose powder in air leads at temperatures of about 600 to 650 °C to the formation of pure monophase Li_4SiO_4 from which sintered bodies r nearly spherical granules can be processed by usual powder metallurgical methods without any further milling steps. This preparation technique can easily be scaled-up to larger batches. The production of a 70 kg of Li_4SiO_4 fabricated by this method under industrial conditions is foreseen to be realized in the coming months.

Characterization of Ceramic Breeder Materials

At the end of 1986 the LISA experiment series proceeded with the second inpile test. This test concentrates on the investigation of orthosilicate amples (see last report). Three of these samples consist of spherical particles, one of granules and one of pellets. These pellets can be compared with those of the LISA 1 experiment. The results of the structure analysis (Table 2) show differences in specific surface area and in density and pore structure, which are reflected in sound velocity. The mean diameters of cross sections through grains as well as the frequency distributions of the diameters (Figure 13) are slighty different. The densities of the granules and the spherical particles measured by means of He stereopycnometry are in accordance with the theroretical density. This means, there is no closed porosity within these materials. The mean diameter of cross sections trough grains of the granules was 36 µm, significantly larger than that of the pellets.

Staff:
B. Dörzapf
H. Elbel
E. Günther
R. Hanselmann
J. Heger
W. Jahraus
E. Kaiser
W. Laub
H. Nagel
R. Scherwinsky
D. Vollath
Dr. H. Wedemeyer
M. Wittmann

Table 1 : Geometric and structure data of the Li_4SiO_4 pellets of the first two LISA experiments

		LISA 1	LISA 2
Mean diameter	(mm)	7.88	8.04
Geometric density	(g/qm^3)	2.22	2.16
	(% th.d. [1])	92.9	90.4
Hg porosimeter density	(g/cm^3)	2.27	2.18
He pycnometer density	(g/cm^3)	2.30	2.22
Total porosity [2]	(%)	5.0	8.8
Closed Porosity [3]	(%)	3.8	7.1
Relative open porosity	(%)	24	19
Effective channel diameters [2]	(µm)	< 0.02	< 0.03
Permeability coefficient	(cm^2/s)	< 0.02	< 0.02
Sound velocity	(km/s)	6.14	6.03
Mean diameter of cross sections through grains	(µm)	26	21
Specific surface area	(m^2/g)	0.77	0.20

1) $\rho th = 2.39$ g/cm^3
2) according to Hg porosimetry
3) according to He pycnometry

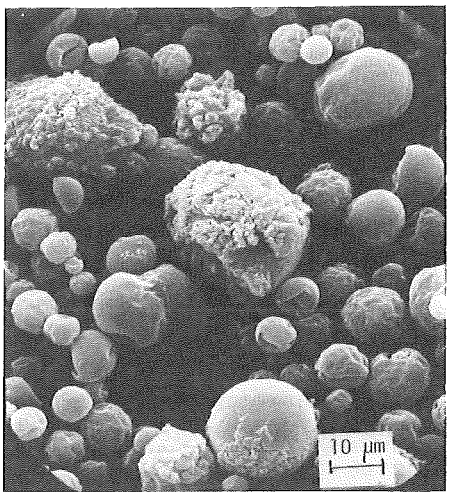

Figure 12: Scanning electron micrograph of a "Li_4SiO_4" powder obtained from a suspension of "Aerosil" and LiOH in methanol after spray-drying

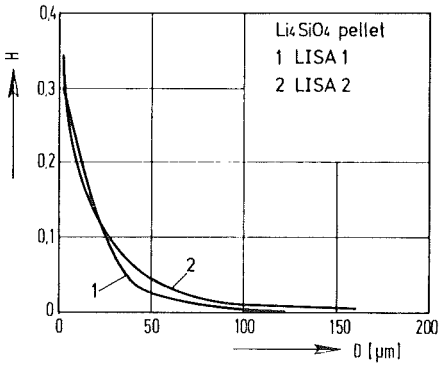

Figure 13: Grain size distribution in the cut surface of a pellet of the orthosilicate samples from LISA 1 and 2

2. Measurement of Physical, Mechanical and Chemical Properties (B13)

Constitution and Thermodynamics

Li_4SiO_4 seems to be a promising ceramic breeder candidate, especially regarding its tritium release behaviour which is an important criterion. It is known from literature that doping of Li_4SiO_4 with Al_{3+} or P_{5+} ions increases its Li_+ ion conductivity. By this way, also the tritium release rate could be possibly increased, assuming some parallelity between Li_+ ion and tritium diffusion. Therefore the ternary phase relations of the subsystem Li_2O-Li_2SiO_3-$LiAlO_2$ were reinvestigated with respect to ternary solid solutions of Li_4SiO_4. Two series of solid solutions were localized: 1) between Li_4SiO_4 and Li_5AlO_4:$Li_{4+x}(Si_{1-x}Al_xO_4)$, $0 \leq x \leq 0.06$; 2) between Li_4SiO_4 and $LiAlSiO_4$: $Li_{4-3x}Al_x(SiO_4)$, $0 \leq x \leq 0.15$. In addition, a range of homogeneity was found only for $LiAlO_2$ on the join $LiAlO_2$-Li_4SiO_4: $Li_{1+x}Al_{1-x}Si_{0.5x}O_2$, $0 \leq x \leq 0.03$. The results are shown in fig.14.

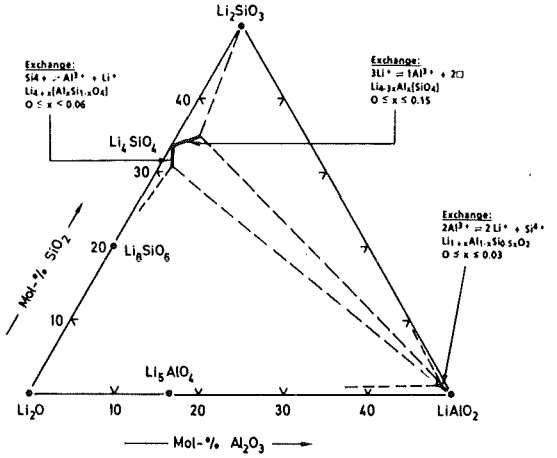

Fig. 14 : Ternary phase diagram of the subsystem Li_2O-Li_2SiO_3-$LiAlO_2$(isothermal section at 800°C)

The continuous isothermal experiments on the interaction of Li_4SiO_4 with water vapour were continued. After annealing 3 months at 500°C, ∿ 100 ppm H_2O in Ar (flow rate 25 l/h), the loss of weight was insignificant, but the formation of an unidentified phase was proved by SEM micrographs. Transient experiments (10 K/min) at 97 ppm H_2O showed a changing moisture content depending on the temperature. For Li_4SiO_4, desorption of water vapour occurred in the range 100 - 435°C. Above - 720°C, consumption of water vapour was observed in connection with evaporation processes.

Physical and Mechanical Properties

The thermal diffusivity of γ-$LiAlO_2$ samples prepared from Li_2O_2 and γ-Al_{203} (ENEA-Italy) with a density of 95% was measured in the laser flash apparatus. The results fit the equation

$$\alpha_{95} = \frac{1}{-16.6 + 0.135\,T} = cm^2/sec., \quad [T] = K$$

which has to be compared with data of samples of 78% density prepared from powders fabricated with the same chemical procedure and corrected for 100% density:

$$\alpha_{100} = \frac{1}{-7.42 + 0.120\,T} = cm^2/sec., \quad [T] = K$$

Additionally, the thermal diffusivity was measured on Li_2SiO_3 samples prepared by isostatic hot-pressing. Within the margin of error the data for α agree with those obtained on axially hot-pressed samples. The data fit the equation (with [T] = K):

$$\alpha_{95} = +6.335\times10_{-2} - 1.844\times10_{-4}T + 2.016\times10_{-7}T_2 - 7.405\times10_{-11}T_3 \; cm_2/sec$$

For the determination of mechanical properties of Li_4SiO_4, pellets of two manufacturing series with diameters of 9mm and densities of 90 and 78% were available. The Young's modulus was evaluated from the ultrasonic velocity determined by the pulse-echo-method. It was found to be 80±5 GPa for the 90% dense Li_4SiO_4 and 40±5 GPa for the 78% dense material. For the determination of the compressive strength the load was applied at a rate of 100 N/s. The strength of the 90% dense material is very low.

It was found to be 85±20 MPa. For the 78% dense material a value of 200±25 MPa was found. It is not yet clear wether this density dependence of the strength can only be accounted for by the different grain sizes of the two materials (about 100µm for the 90% dense material and about 15µm for the 78% dense material).

Different manufacturing parameters may have contributed to this phenomena, too.

The thermal shock resistance, defined as the lowest temperature difference at which under given boundary conditions cracking occurs, was determined by dipping the pellets into liquid tin. At a temperature difference of 240 K the lowest difference which could be realized, all pellets of the two materials cracked. Compared with Li_2SiO_3 the thermal shock resistance of Li_4SiO_4 is significantly lower. This is primarily caused by higher thermal expansion coefficient of the Li_4SiO_4. The influence of the mechanical data of the two materials on their different thermal shock behaviour cannot yet be discussed because the data base is too small.

High Temperature Mass Spectrometry and Solubility Measurements

Among the ceramic materials presently under discussion for use in the breeder blanket of a fusion reactor lithium silicates appear to be promising candidates. Considerable effort has already been invested into the characterization of these species. However, two important psychochemical properties, i.e. the solubility of hydrogen and the stability towards thermal decomposition, have so far received inadequate attention.

For the measurement of solubilities a stainless steel ultra high vacuum apparatus has been constructed and installed in a glove box. Complete thermostatization of the equipment is therefore possible and at the same time the requirements for work with radioactive tritium are fulfilled. Typically about 800 pellets of the silicate ($\sim$ 45 g Li_2SiO_3) having approx. 92% theoretical density were stacked inside an externally heated alumina vessel. Solid samples were carefully dehydrated and only very dry gases used. For the determination of solubilities a volumetric procedure was employed. Within a temperature range of 450-550°C and pressures up to 550 mbar the solubility of hydrogen Li_2SiO_3 were found to have values between 1 x 10^{-5} and 2 x 10^{-5}mol/mol. These values are substantially lower than those reported previously by this laboratory. The discrepancy may have its origin in impurities present in the tablets of the first runs.

In addition to the volumetric measurements tracer experiments with tablets placed in an autoclave are in progress. This technique allows pressure equilibration studies up to several bar. Solubility data are obtained by quenching without depressurizing and dissolving the tablets in acid. The amount of incorporated H_2/HT is determined by low level LSC of the supernatant liquid. First results with this highly sensitive method substantiate the volumetric findings. However, there are indications that some hydrogen trapping in the silicate ceramics is taking place.

The thermal stability of solid Li_2SiO_3 is being investigated by high temperature mass spectrometry. For solid/gas equilibrium studies a Pt Knudsen cell with an effusion aperture of 0.5 mm is employed. The thermal decomposition study has been tentatively described by the following reaction.

Li_2SiO_3 (s) $\rightarrow$ 2 Li (g) + 1/2 O_2 (g) + SiO_2 (s)

Gaseous lithium oxides could not be detected over solid Li_2SiO_3. Therefore, from detection limit considerations, the partial pressures of these species must be lower than those of lithium by at least a factor of 100. From the above it may be concluded that the contribution of lithium oxides to the total thermal lithium losses from a fusion reactor breeder blanket are small.

Complete evaluation of the data will deliver equations for the partial pressure of oxygen and lithium over solid and liquid Li_2SiO_3 in the temperature range 1170-1470 K. Another result will be the reaction heat for the above shown chemical equation. From the present still preliminary evaluation it appears that an extrapolation of Li partial pressures measured over the liquified silicate yields blanket partial pressures that are substantially lower than those obtained from an extrapolation of the present solid/gas studies.

Staff:

Ch. Adelhelm
M. Blumhofer
G. Haase
E. Nold
H.J. Ritzhaupt-Kleissl
V. Schauer
G. Schlickeiser
B. Schulz
A. Skokan
H. Zimmermann
M. Glugla
H. Ihle
R.-D. Penzhorn
H.E. Noppel
P. Schuster
K.-H. Simon

3. Compatibility with metallic materials (B 14)

The compatibility tests between Li_2O, Li_2SiO_3, Li_4SiO_4 and the stainless steels 1.4914 and 1.4919 (AISI 316) were extended to higher temperatures (800 - 1000°C). In addition, the compatibility behavior of Ni, Cr-base alloys (Inconel 625, Hastelloy X) has been examined. In the experiments the Li compounds were used in two different conditions:

a) as-dried (900°C/2h),
b) containing 1 mol % NiO per 1 mol Li_2O to simulate a controlled oxygen potential.

The results of the compatibility experiments are shown in Figure 15 together with literature data. The extent of interaction between Li_2SiO_3 or Li_4SiO_4 and the stainless steels between 800 and 1000°C correlates reasonably well to the extrapolated results from lower temperatures. This is not the case for Li_2O where a higher activation energy for the reaction rate is determined above 800°C. Li_2O causes the strongest chemical attack followed by Li_4SiO_4 and Li_2SiO_3 in the as-dried condition causes no chemical interactions at all, even not at 1000°C. Concerning the cladding materials, there was no considerable difference in the reaction rates of the austenitic steel 1.4919 and the Ni, Cr-alloys, Hastelloy X and Inconel 625. But the martensitic-ferritic steel 1.4914 was clearly more attacked at temperatures 800°C, in contrast to its behavior at lower temperatures. Assuming that a cladding attack to a maximum depth of 200 µm after 10000 hours is acceptable, the following provisional maximum cladding temperatures can be determined for the examined Li compounds according to Figure 15: for Li_2O about 700°C, for Li_4SiO_4 about 850-900°C, and for Li_2SiO_3 about 1000°C.

First compatibility tests have been performed with metallic beryllium, which is of interest as a neutron multiplier, and Li_2SiO_3 at 600, 750, and 900°C. The maximum annealing time was 1000 Hours. Two Be disks were sandwiched by three Li_2SiO_3 disks, packed in a welded 1.4919 capsule. At 600°C after 1000 Hours the compatibility behavior between Be and Li_2SiO_3 as well as between Be and stainless steel was acceptable. At 750°C strong chemical interaction between Be and Li_2SiO_3 takes place already after 100 h. As a result of the chemical reduction of the Li_2SiO_3 by metallic Be, Li-silicates form which are liquid at 750°C and penetrate into the Li_2SiO_3 up to 500µm. At 900°C the chemical interactions are disastrous. Further experiments are needed to determine in more detail the reaction behavior between 600 and 750°C and to determine the maximum allowed temperature for practical applications.

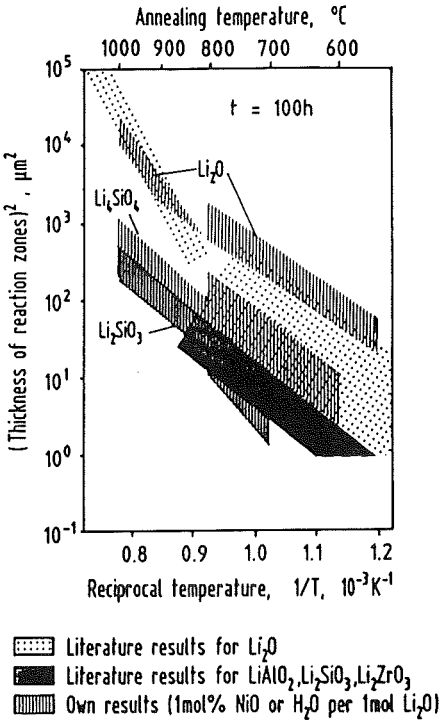

Fig. 15: Chemical reaction of oxide breeder materials with stainless steels, normalized to 100 h

Staff:
W. Dienst
P. Hofmann
K.H. Kurz
H. Metzger

4. Irradiation Testing of Ceramic Breeder Materials (B15 and B15.3)

After a number of start up difficulties (licensing, sample handling, sample decanning equipment), post irradiation examination has been started with the tritium annealing of low activation (1-10 mC/g) samples. Different types of metasilicate samples irradiated in the DIDO reactor at KfA Jülich and the meta- and orthosilicate pellets of the first inpile test LISA-1 have been annealed.

In agreement with inpile results it was found that release from metasilicate is insensitive to the type of purge gas (Ar or Ar + 0.1%H_2) and in most cases is inconsistent with diffusion. For the orthosilicate pellets of LISA-1 release during out of pile annealing

was quite different from inpile behaviour: A large fraction (≈90%) of the tritium is released (probably in the oxdized form) at a very low temperature (150-300°C) in a very short time (=ten minutes), whereas the release of the residual tritium seems to be similar as in the inpile tests. The LISA-1 samples were at air for several hours during unloading and afterwards stored in the closed capsules under air for several months. It is tentatively assumed that the tritium release behaviour during annealing is caused by absorbed water vapor. Weight losses of several °/oo during annealing support this assumption.

After the examination of the LISA-1 samples some high activity samples from the first irradiation in the OSIRIS reactor, DELICE 01 (45 stacks lithium metasilicate pellets) will be studied during the next months. In addition, the 20 lithium silicate sample stacks (Li_2SiO_3 and Li_4SiO_4) from DELICE 02, which have been irradiated in the first half of 1986 wait for post-irradiation examination. The transport from Saclay to Karlsruhe is now envisaged for summer 1987. As the KNK II reactor has been shut down for some month in order to allow fuel element defects to be analyzed, it has not yet been possible to start the first ELIMA 1 in-pile experiment exposed to a fast neutron flux and involving 24 sample stacks.

Consequently, also the ELIMA 2 irradiation to be conducted by five partner institutions and compared with the DELICE 03 thermal irradiation in the OSIRIS reactor is retarded. (For more details see the two preceding semi-annual reports.) Sample fabrication for the ELIMA 2/DELICE 03 comparative irradiation has begun; the date of irradiation cannot be definitely fixed for the time being.

Staff:
E. Bojarsky
W. Breitung
H. Elbel
H.E. Häfner
K. Heckert
J. Lebkücher
P. Norajitra
K. Philipp
G. Schumacher
H. Wedemeyer
H. Werle

5. Tritium Recovery from Ceramic Breeder Material (B16)

Because of the fast tritium release from lithium orthosilicate observed in the first inpile test LISA-1 (1), the second (LISA-2) concentrated on this material. Test parameters were chosen to match the requirements of the present KfK blanket design: Samples mainly in the form of spheres or pebbles (Tab. 1), low temperature down to 350°C. In addition, the effect of adding a small amount of oxygen (10ppm) to the purge gas on tritium release and on tritium permeation will be studied. Irradiation of LISA-2 started November 24, 1986 and was stopped December 2, 1986 because of a leak in the tank of the SILOE reactor. It is expected that the test can be continued September 1987. During this first 9-day-cycle purge gas was He + 0.1% H_2. Neutron flux and purge gas flow rate were changed and the sample temperature was varied between 600 and 350°C. Measured tritium production agreed within 20% with predicted values. Out-of-flux tritium extraction was performed after irradiation using the electrical heaters of the CHOUCA furnace. The released amount of tritium was found to be in excellent agreement with end-of-irradiation inventory estimated from the difference between tritium production and release during irradiation. If during irradiation the sample temperature is changed, the release temporarily deviates from production. The difference between release and production decreases with time and is approximately exponential for longer times. The exponential region was used to estimate tritium residence times according to

$$\tau = \pi_2 (t_2 - t_1)/15(\ln r_1 - \ln r_2)$$

(t time, r release rate).

Some values are given in Tab. 3.

Residence times for the various orthosilicate samples differ up to two orders of magnitude. The pellet (P5) has the smallest residence time and is also much faster (factor 50) than the orthosilicate pellet investigated in LISA-1 (1).

All orthosilicate samples have a faster response than the aluminate pellet. Out of flux residence times generally agree with influx values, except for P3 and possibly P6, for which the influx values are remarkably lower. Above 450° the residence times of all orthosilicate samples are less than 10h. They increase strongly with decreasing temperature, achieving values of about 100 h at 350°C. This

increase is stronger than expected from out of pile annealing studies. Therefore, after restart of LISA-2, release at low temperatures will be studied in detail.

References

(1) H. Werle et al. "The LISA-1 Experiment: In-situ Tritium Release Investigations", J. Nucl. Mater. 141 - 143 (1986)

Staff:

H. Elbel

H.E. Häfner

H. Wedemeyer

H. Werle

	sample	P1	P3	P5	P2	P4	P6	LISA-1
Characteristics	Material	Ortho	Alu (1% Mg)	Ortho	Ortho	Ortho	Ortho	Ortho
	Type	Granules	Pellet	Pellet	Spheres not. temp.	Spheres temp.	Spheres temp.	Pellet
	Dimensions (mm)	0.45-0.56	8 Ø	8 Ø	0.45-0.56	1-1.5	0.45-0.56	8 Ø
	% TD	85-90	84	92	97	97	97	94
	% open porosity	–		14	–	–	–	31
	Grain size (η)	–	0.8	21	-	-	-	26
Residence time τ (h)	Out of flux, 500°	5.7	23.4	0.13	1.3	0.84	1.00	-
	Influx, 500°	4*	9*	0.2*	1.23	1.00	0.57	4.8
	≈360°	–	–	–	169	114	105	–

* values interpolated

Tab. 3: LISA-2 samples, characteristics and residence times

M 1 The Large Coil Task (LCT)

The Large Coil Task entered 1986 in its important experimental phase. After a successfull running down of the single coil tests preparations for tests in the toroidal configuration were started. The first test in the toroidal configuration (Standard I) with the General Dynamics (GD) coil as test coil was successfully started on August 14, 86, followed by the Japanese coil.

As the third in the series of Standard I tests the Euratom LCT coil was tested in the second half of October. The goal of the test was to demonstrate a safe operation of the coil up to 8 T at the rated current. The mass flow rate was reduced in 4 steps to explore the stable operation of the coil under these conditions (Table 4).

Case m [g/s]	Winding m [g/s]	Heat Transfer Coefficient* h [mWcm²/K]
54	161	60
76	101	41
48	55	25
32	33	17

Table 4: Helium mass flow rate for winding and case used for the test runs of the Euratom Standard I test.
(* if the coil goes normal at rated current and 8 T)

For all mass flow rates the coil could be operated without any sign of thermo-hydraulic or electrical instabilities.

The originally specified current distribution for the single coils of the torus had to be changed. The ampere turns of the single coils were so different that as well too high field values as also too big out-of-plane loads would be generated in the torus. For the Euratom coil the out-of-plane forces varied during Standard I testing from 0.6MN to 10 MN. The biggest out-of-plane force occurred during the Standard I test of the Westinghouse coil. For this test the field strength was 8T equal in all coils (symmetrical torus in field). The out-of-plane force of 10 MN for the Euratom LCT-coil was already 35% of the maximum out-of-plane load if one of the torus coils would be without current.

Such a load case will be tested in the extended test program. Some key values of the Euratom Standard I-test are summarized in Table 5.

- Coil current		11,7kA
- Field at reference point in the central plane		8,0T
- Max. field at the smallest curvature		8,2T
- Total force on the bucking post		- 40 MN
- Out-of-plane force		- 0,61MN
	TORUS	SINGLE COIL
- Static losses of the winding	∿ 25 W	18 W
- Static losses of the case	∿ 90 W	80 W
- Gap winding-case in the central plane	2,22mm	1,28mm
- Maximum von Mises stresses	131N/mm²	137N/mm²

Table 5: Some characteristic data of the Euratom-coil for the Standard I-Test.

The measured von Mises stresses at all points are for the torus test lower than for the single coil test (Fig.16.) The increasing gap between winding and coil case bahaved as expected (Fig. 17). An explanation for the increasing static losses in the torus test is the higher force of the coils against the bucking post. The additional heat flux by this force was impressively demonstrated by the increase of the bucking post temperature when the torus was powered.

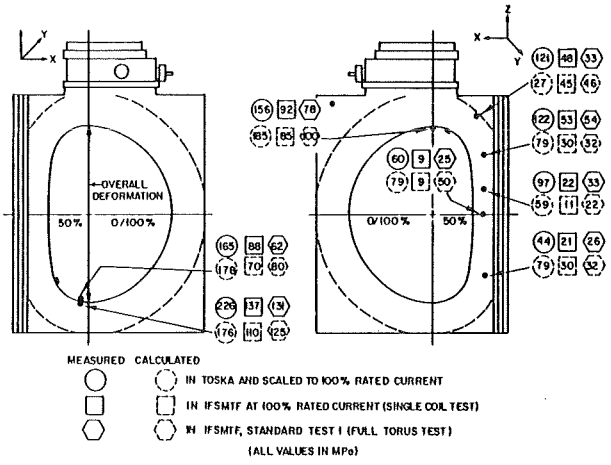

Fig. 16: Comparison of the measured and calculated van Mises stresses for the TOSKA-test, single coil test in ORNL and the test in the toroidal configuration.

Coil	Max. discharge power (MW)	Dissipated Energy in the dump resistor (MJ)
EU	28,2	122,0
WH	7,2	46,5
GE	4,2	95,2
GD	1,8	106,0
JA	8,2	91,1
CH	16,5	64,5
Total		525,3
Stored energy in the torus		554MJ
Dissipated energy in the dump resistor		525MJ
Losses at 4,2K		29MJ

Table 6: Discharge power and energy balance of a dump off the full torus

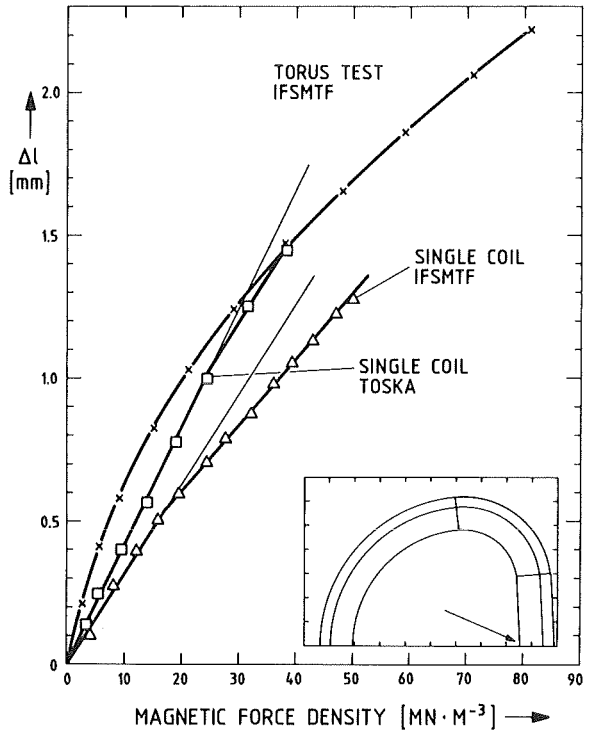

Fig.17: The gap between winding and coil case as function of the averaged Lorentz force density for the same load cases like Fig.16.

At the first ramping up to the Standard I the whole torus was dumped at the rated current of the Euratom coil by an unexpected quench in an adjacent coil. The analysis of this dump is given in the table 6.

The scaling up of the dump losses of the single coil test led to losses of 25MJ which is in fair agreement with the measured losses. The measured maximum temperatures in winding (6.1K) and case (15.8K) were somewhat lower than for the single dump. After the successful test of all coils in the Standard I test series the pulse coil system was brought in operation. The pulse coil was positioned in the Euratom coil before closing the lid of the vacuum vessel. The Euratom coil was the first test coil in the Standard II test series (toroidal arrangement with external pulse field). Some problems had to be overcome with the electrical power supply and the LN_2 cooling circuit (the pulsed coils are LN_2 cooled cooper coils) until the test could start. The limitation of the pumping power required a reduction of the flat top of the pulse from 30s to 15s. Investigations showed that the losses were independent of the length of the flat top of the pulse. The losses were measured as a function of the coil current with different mass flow rates as parameter. About 15-20 pulses were needed to get steady state conditions. The results (Fig.18) could be summarized as follows:

- The losses decrease in the lower current region (< 500A) strongly.
  After this decrease the change with increasing current is weak.

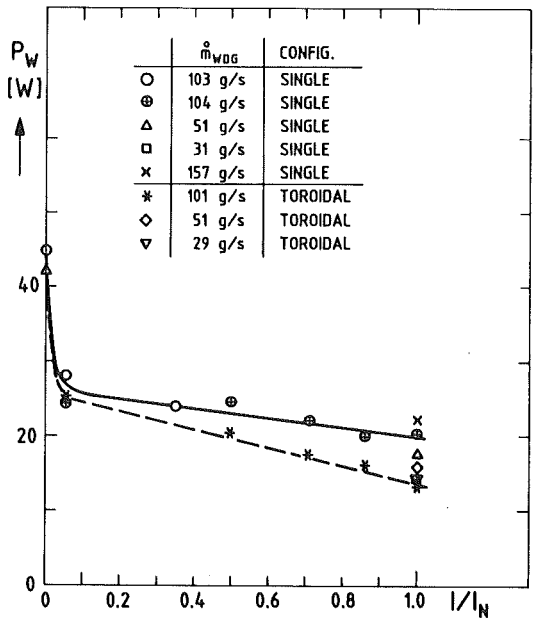

Fig.18: Measured losses of the Euratom LCT coil in the Standard 2 test series.

- The single coil losses are slightly higher than the losses in the toroidal configuration
- The measured losses were between 14 W and 22 W. They are in good agreement with the estimation of 18 W derived from short samples of the cable.
- The same was valid for the case losses measured: (6-11W, estimated: 8W).
- The coil could also be operated under the load of an external pulse field down to a mass flow rate of 30g/s without any sign of thermohydraulic or electric instabilities.
- A temperature minimum was found for a certain mass flow as expected (Fig.19).

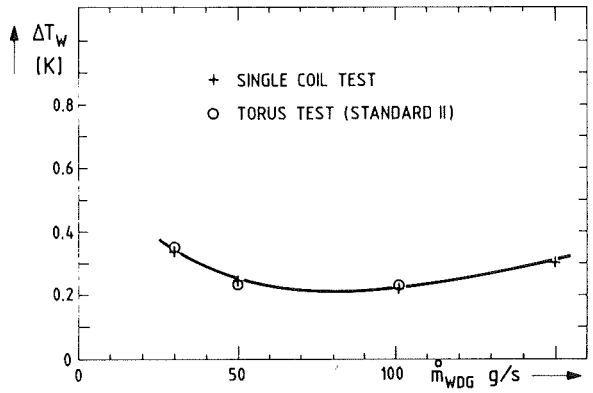

Fig. 19: The existence of a temperature minimum for a certain mass flow

- The compensation circuit of the quensch detection system for the Euratom coil was only slightly influenced by the pulse coil operation (∿ some mV at a level setting of 50 mV). The ORNL system was made more sensitive against pulse coil operation. The level setting had to be about 1 V to avoid a dump.

In the whole Standard II test of the Euratom-LCT coil the coil was loaded with 328pulse field cycles. The Standard II test was successfully continued by testing the Swiss and Japanese coil with external pulsed field. Some problems with the pneumatic drive mechanism, which caused also a breakdown of the vacuum could be successfully handled. Some changes in the test sequence to minimize risks were proposed by the Operating Agent. The extended single coil tests shall be performed before the Standard II tests of the remaining 3 US-coils. With the successful test of three LCT coils under pulse field conditions it was demonstrated that poloidal field transients need not to be a problem for superconducting coils.

M 3 Development of Composite High Field Superconductors

Experiments in the HOMER High Field Test Facility

The HOMER test facility is a magnet system offering a magnet field of 11,5 T in an experimental volume of 260 mm diameter which can be run at different temperatures down to 1,8 K. One goal was to achieve fields in the range of 18 T by means of insert coils wound from commercial high field Nb_3Sn conductors. Because it is a general tendency to look at higher fields in the technical application of magnetic fields in particular in fusion technology, adequate test facilities are needed.

The insert magnet system was designed for magnetic fields of about 18 T in a bore of 55 mm id.. It consists of three coaxial coils covering field ranges of 14,5 T in 160 mm i.d., 17 T in 100 mm i.d. and 18,7 T in 55 mm i.d.. For both innermost coils ternary Nb_3Sn conductors were provided. Because of the small size of these coils they had to be built in the well known wind and react technique, i.e. the heat treatment for forming $(NbTa)_3$ Sn e.g. was performed after winding the coil. The bigger 14.5 T coil has LHe-cooling at the windings for a cryostable operation and must therefore be wound from a prereacted conductor. A special development was performed for manufacturing a convenient conductor consisting of a heat treated Nb_3Sn flat cable soldered to a copper coated aluminum tape as the electrical stabilizer.

After delivery of the ordered conductors the coils were finished and tested at the end of the last year. With a $(NbTa)_3Sn$ insert coil a field of 18,7 T was generated in a free bore of 55 mm. At an operating temperature of 1,8K a maximum field of 19,3T was achieved by a $(NbTi)_3Sn$ insert coil with a free bore of 22 mm. This was the highest field strength achieved so far in any set of superconducting magnets.

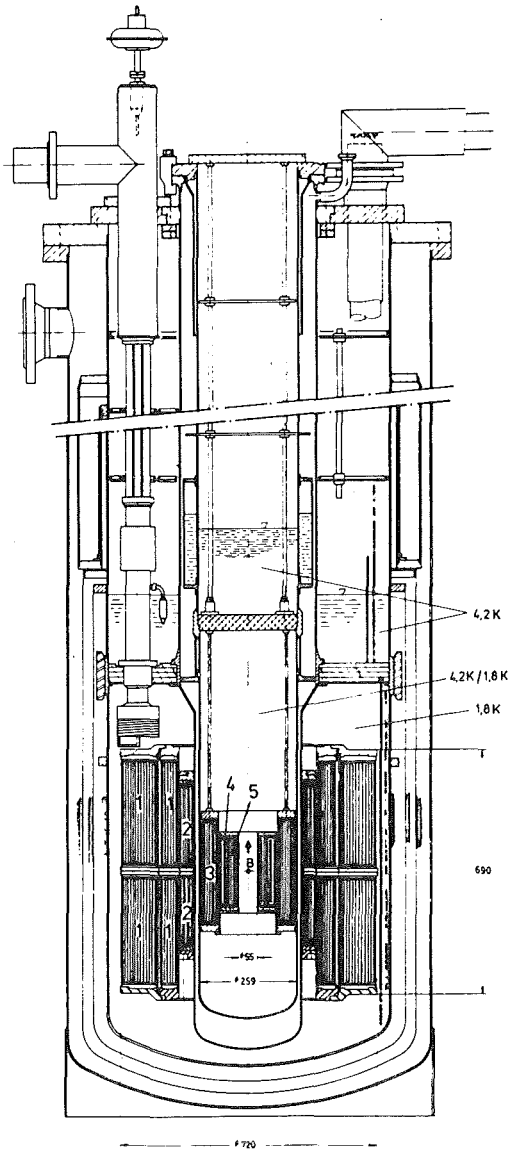

HOMER - Magnetsystem

SL		B [T]	T [K]	freie Bohrung ø [mm]
1	Nb Ti	10	1,8	390
2	Nb Ti Hf	12	1,8	290
3	Nb_3Sn	15/~16	4,2/1,8	160
4/5	$(Nb Ta)_3Sn$ / $(Nb Ti)_3Sn$	~18/~19	4,2/1,8	55

Fig. 20 : A cross section trough the complete HOMER magnet system

Mechanical tests on internally cooled conductors

Heat treated conductor loops of internally cooled conductors, s. Fig. 21, were carefully mounted to the test rig described in the last report. A first result to be expected was the strong precompression effect on the Nb_3Sn cable enclosed in the stainless steel madrel due to the differential thermal contraction coefficient, s. Fig. 22. The possibility to run the test loop simulantaneously under field, transport current and mechanical forces revealed differences between the two tested ICCS conductors in respect to premature quenching under increasing mechanical elongation. The cable in which pure bronze strands are surrounded by copper strands for electrical stabilization and protection purposes exhibited some kind of training effect during the increase of the mechanical load. A tight bonding of the stabilizer and the superconductor seems to be the better choice. A clear dependence on frequency of premature quenching and helium pressure in the conduit could not be stated by the few experiments because of poor statistics.

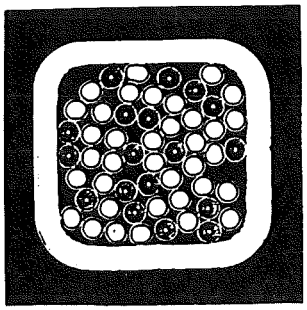

Fig. 21 : Cross section of the tested ICCS conductor containing 18 superconducting and 36 copper strands. Overall dimensions are 5 x 5 mm^2, void fraction is 32%.

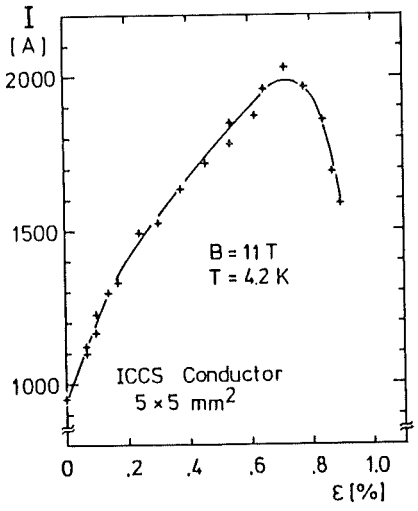

Fig. 22: The critical I_c of the ICCS conductor versus the strain of the test loop. The bending radius is 125 mm.

Development of Composite High Field Superconductors

The Composite Core Method

In the last years, the critical current density J_c of Nb_3Sn multifilamentary wires at fields above 11 T has considerably been enhanced by the addition of a third element. The upper critical field B_{c2} was raised about 3 T by adding Ti or Ta to Nb_3Sn. Ordinarily the Nb-Ta or Nb-Ti cores for multifilamentary superconductor wires are prepared by electron beam melting, remelting being necessary to reach a good homogeneity.

The critical current density J_c of $Nb_{3n}Sn$ wires below 11 T is mainly determined by the pinning forces. In Nb_3Sn the main pinning centers determing the critical currents are situated on the A 15 grain boundaries. However, no production process for Nb_3Sn wires has so far been effective in reducing the grain size or introducing precipitates or inclusions into the filaments in a comparable manner to the a-Ti wires. A first attempt to produce such "artifical" pinning centers by a powder metallurgical (P/M) process replacing simultaneously the electron beam melting of Nb-Ta cores has been undertaken.

The wires were produced by the bronze route replacing the conventional electron beam melted Nb-Ta rods by P/M prepared composites. All starting powders were produced by the hydride-dehydride process, ranging from 75µm to 150 µm for Nb and from 45µm to 75µm for Ta, respectively. Ta as addition element was used because of its plastic deformation similar to Nb. Nb/Ta powder mixtures with 0,3.5, 7.5, 15 and 20 wt% Ta were thoroughly mixed in argon atmosphere and filled in a Cu can (65 mm o.d., 55 mm i.d.). At that stage the grain density was between 50 - 60% but increased after compressing with 16 GPa to a density of more than 85%. This was followed by cold extrusion to 32mmØ and conventional swaging and rolling. The whole deformation was made at room temperature to avoid oxidation of the powders. At 1mmØ the Cu jacket was removed by echting in nitric acid. After the thermochemical treatment, the Nb/Ta composite rods were stacked in a Cu-Sn bronze tube (Cu 13 wt% Sn), followed by standard wire drawing and annealing procedures. At a later stage of deformation 19 single core wires were bundled in a second bronze tube and subsequently deformed to an areal reduction ratio of $R_a = 2 \times 10^7$ (Ø = 0.40 mm). Finally the wires were reacted at three different heat treatment conditions, i.e. 675°C/120h, 700°C/64h, and 750°C/64h, respectively.

To examine the workability of the Nb/Ta powder composite measurements of the Vickers microhardness (300g load) were carried out at different stages of the wire production process. Since former experiments showed a strong influence of the oxygen content on the ductility of the composite powders containing less than 300ppm Oxygen were used. At small area reduction a strong increase of the Vickers microhardness of the composite rods was observed. For R_a = 20 the hardness of the Nb powder particles nearly doubled its value from 850 to 1600 N/mm^2 (300g load). After further deformation the increase was slower and reached H_v = 2000 at R_a = 4200. The Ta powder particles had the same behavior but exhibited a stronger increase of the microhardness, from H_{v_2} = 1300N/mm^2 for the starting powder to H_v = 2850 N/mm^2 for Ra = 100.

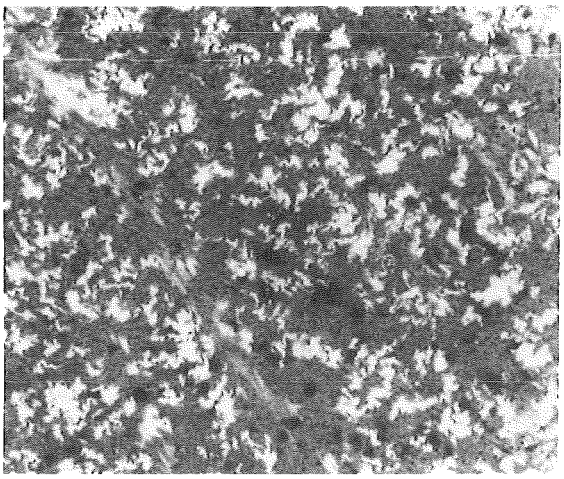

Fig. 23: Distribution of Ta inclusions (white) and Nb (dark) in Nb/Ta powder composite rod in a cross section perpendicular to the wire axis (the marks correspond to 10 µm at an intermediate wire diameter o 2 mm).

At lower area reduction ratios (Ra $\leq$ 100), the microhardness of the Nb/Ta composite corresponds to the mixing rule. The distribution of Ta in Nb can be seen on scanning electron micrographs of cross sections of the wire (Fig.23). The elongation of the inclusions in the Nb matrix could be observed down to a width of 150 mm, corresponding to an area reduction $R_a = 4 \times 10^4$.

The critical current measurements of the Nb/Ta composite core wires should answer two questions:

1. whether the electron beam melted Nb-Ta rods could be replaced by P/M rods and
2. whether the Ta inclusions serve as "artifical" pinning centers,thus increasing the critical current density at lower fields.

Figure 24 shows the J_c (A15 layer) vs. B curves for Nb/7.5 wt% Ta composite wires after different reaction heat treatments. The P/M composite core wires exhibited new characteristics. After a reaction heat treatment at - 675°C, the current carrying capacity is similar to that of binary Nb_3Sn wires. High values of J_c at intermediate fields (B - 11T) and a steep decrease at higher fields are observed.
The measured J_c values were 6.67 x 10^5 A/cm^2 at 8 T and 4.2 x 10^5 A/cm^2 at 10 T.

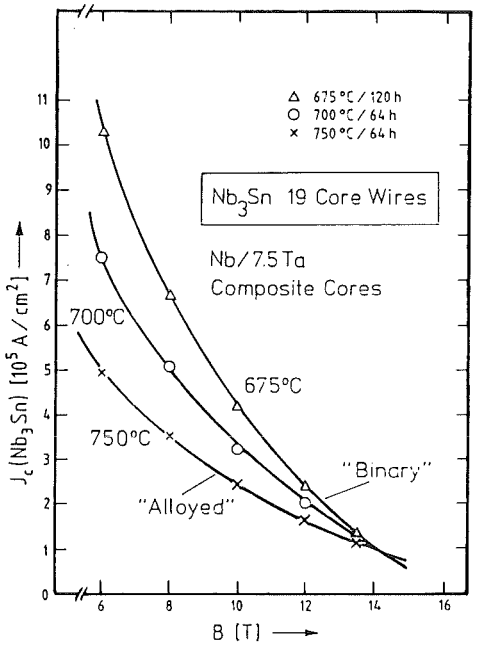

Fig. 24: J_c in the Nb_3Sn layer vs. B for a composite core wire after different heat treatment conditions.

After a reaction heat treatment at 750°C, however, the current carrying characteristics of the P/M composite core wires is comparable to that of ternary $(Nb\text{-}Ta)_3Sn$ wires produced by the conventional bronze technique showing in particular a slower decrease at high magnetic fields (B - 11T). This is illustrated by the vallues of J_c = 1.8 x 10^5 A/cm^2 at 12 and 13.5 T respectively. After a reaction at 700°C an intermediate behavior between that of binary and alloyed Nb_3Sn wires is observed.

The present P/M processing of Nb_3Sn wires width Nb/Ta composite cores leads to enhanced J_c values compared to conventional binary or alloyed Nb_3Sn wires, the main improvement being observed below 13T is expected by reducing the filament diameter and the matrix to core ratio, and by optimizing as well the amount of additive as the powder quality. The influence of other addition elements than Ta as well as the mechanical behavior of the new type of composite filaments (comprising ductile Ta dispersed in brittle Nb_3Sn) are actually investigated in our laboratory.

Staff:

W. Barth
M. Beckenbach
M. Brünner
P. Duelli
U. Fath
R. Flükiger
S. Förster
F. Gauland
S. Gauss
W. Goldacker
A. Kling
B. Lott
G. Nöther
A. Nyilas
H. Orschulko
H. Raber
T. Schneider
W. Specking
S. Stumpf
P. Turowski

M 4 Superconducting Poloidal Field Coil Development

The tasks aims at the development and test of all necessary components to build and operate a supercon ducting poloidal field coil in the real tokamak environment of TORE SUPRA in 1990. The development shall be relevant for NET.

In order to test the components under TORE SUPRA load conditions, a model coil of 3 m diameter is under design to be operated in the KfK-TOSKA test facility 1987/1988.

Model Coil Fabrication
Design of the model coil was teminated. The contract for industrial fabrication of the model coil has been placed to Alsthom (France). The procedures for establishing the coil winding , the component design and fabrication, the materials testing program and the mechanical and hydraulical calculations have been discussed with the manufacturer. The KfK design has been transfered to Alsthom and serves now as a basis for the future work.

For the materials test program, specific specimens for mechanical and high voltage testing (including partial discharges) of the insulation system have been designed and were fabricated by Alsthom for testing at KfK.

The insulation system between conductors is based on glassfiber and glassfiber/Kapton is the alternative. The outer high voltage insulation of the coil will be made out of the several layers of glassfiber and Kapton. The coil will be impregnated with epoxy resin using standard vaccum impregnating in techniques.

Conductor Development and Fabrication (Fig.25)
A call for tender for the conductor fabrication has been placed to the European industry based on the results of the conductor development. Two companies, offered for the conductor. The final decision will be taken at the beginning of the next reporting period.

Laser Welding
Four quarter sections will be joint around the cable using two laser beams simulanteously. The laser beam sharing device has been succesfully operated in a penetrating test of the laser beam on adjacent points of a round tube. The available CO_2 laser power was 1,5 kW at a welding velocity of 1.2m/min. Weldments using two CO_2 lasers of 3 KW each have been performed with velocities of 4-5m/min.

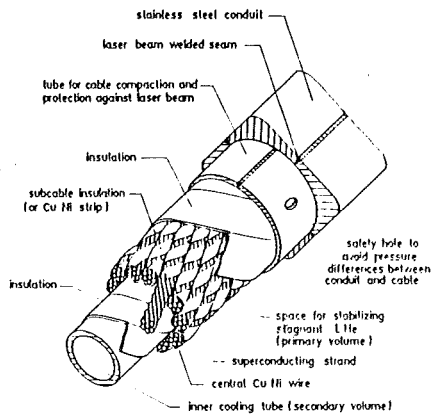

Fig. 25: Polo superconductor for poloidal field coil applications in Tokamaks

Steel Section Fabrication
Manufacturing of 6 m long quarter sections has been terminated. In parallel, the fabrication process has been established for 150 m long sections and the production has now been started.

Stability Experiment
Measuremements of the stability of the Polo-conductor will be carried out in a special test device. In the reporting period the assembly of the device has been completed. Bending tests of the conductor to produce the necessary needle shape have been performed with considerable effort. Buckling of the outer protection tube had to be avoided. During these bending tests, conductors with insulated subcables could be bent to a radius of 100 mm without any short between subcables. It is foreseen to have different He conditions in the primary channel (from bath cooling to supercritical He at 5 bar). The primary channel has therefore to be closed at the conductor ends where the subcables will be connected. It is a very complicated and time consuming task to manufacture the vacuumtight feed through for the 78 wires, which come out of the primary channel and to make the connections between the subcables.

High Voltage/Low Temperature Laboratory
The cryogenic installations have been started at the lab in order to be able to test the insulation materials and the coil components under high voltage conditions at low temperatures. The noise level of partial discharges of the whole high voltage supply of the Faraday cage has been measured with the help of the University of Karlsruhe. The discharge level is below 1 pC and we thus have excellent test conditions.

The design of various potential breaks is a continuing activity. Potential calculations of the breaks and optimisation considerations have been performed together with the University of Karlsruhe.

2 - Phase Flow Experiment in the Existing TOSKA Facility:
In a third test run pictures of the flowing helium have been taken in order to see what flow pattern occurs during different massflow and heating conditions. The necessary viewing section was designed by our french colleagues at Saclay. This group also participated in the experiment.

The test results are now being evaluated by the french group. A fourth test run is now under preparation. This test will mainly be done to gain experience with operation of a LHe pump.

For a first test we will use the LINDE pump although this pump is not really designed for this operating regime.

Current Leads for the model coil and the ES-ccil.
Because of limited personal it was decided not to proceed further with a new design for the mcdel coil current leads. Instead we will adapt the existing design which was used in the LCT and TESPE tests. For the ES- coil a special upgraded design of the TORE-SUPRA leads is made by Mr. Claudet from CEN Grenoble. We are currently preparing a cryostat and measuring equipment for the test of these leads.

Work for Installation of the model coil:
A first design of the necessary supports to hold the model coil and the short circuit ring inside the TOSKA vessel was completed (Fig.26). This design has now been improved by more detailed calculation of the forces etc.. A first draft for the cryogenic schematic was made. The design of special sensors (void measuring cell, venturi tubes) continued. A programmable control system was chosen and work will continue to get experience with this system.

Details of the new software for the VAX computer were discussed with the data acquisition group. The incorporation of the carbon glass sensors which will be used in the future was discussed in detail. Preliminary plans for the test procedure for the model coil were made and questions like quench detection, special sensors, pressure rise in the coil etc. have been discussed.

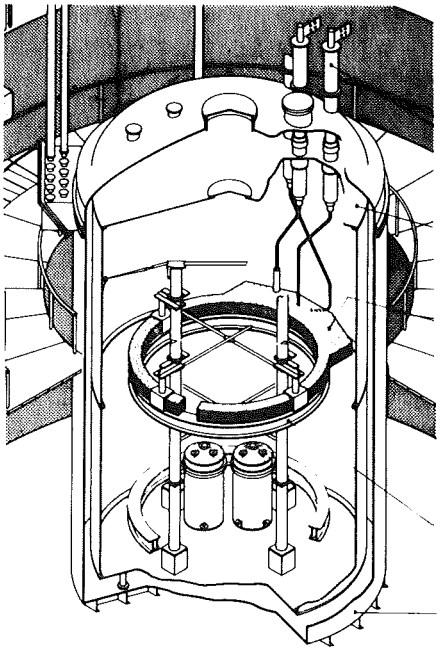

Fig. 26: Polo model coil in the TOSKA facility

Staff:

H. Bayer
F. Beckenbach
P. Duelli
S. Förster
U. Jeske
H. Katheder
J. Lühning
G. Nöther
A. Nyilas
L. Schappals
G. Schenk
C. Schmidt
K. Schweickert
E. Specht
H.-J- Spiegel
F. Süß
M. Süßer
A. Ulbricht
R. Wagner
D. Weigert
F. Wüchner

M 8 Design and Construction of a Poloidal Field Coil for TORE SUPRA as NET-Prototype Coil

1. Requirements

The objective of the task is the development and test of an Equilibrium Field Coil (EF Coil) with parameters relevant for NET. The reliable operation of a superconducting PF-coil shall be demonstrated in a real tokamak environment with the rapid field variations due to start up, plasma position control and disruptions. The development has to confirm the coil construction process proposed for NET on a fairly large scale.

For this purpose, the upper ring coil "E_h" of TORE SUPRA will be replaced by a superconducting coil "ES". Design and construction will be based on the results of the already running task M 4.

2. Design of the TORE SUPRA Coil "ES"

2.1 Components for Coil "ES"

The major components, which have to be developed and fabricated are:

- Coil winding and impregnation using an internally cooled superconducting cable. The cable is the same as developed now for the model coil in task M 4.
- Coil vacuum vessel and radiation shield (80 K) with low time constant against pulsed magnetic fields (= 5ms).
- Current leads for 12 kA, 23 kV using the experience of the developments done for so far at KfK and CEA.
- Mechanical support structure to bear the forces acting on the coil under normal load and fault conditions.
- Cryogenic supply system (preferably to be fitted into the existing TORE SUPRA cryogenic system).
- Coil diagnostics and protection.

2.2 Design of the coil ES

The design of coil "ES" has been started. Calculations of eddy-currents in the vacuum vessel and the associated forces have been continued.

Staff:

F. Beckenbach
S. Förster
U. Jeske
H. Katheder
L. Schappals
G. Schenk

M 9 Structural Materials Fatigue Characterization at 4 K

Joining of structural materials

The plate materials 1.4429, 1.4306 and 1.4435 with the dimensions 5000 x 1500 x 30 mm^3 had already been delivered. The plates were cut in lenghts of 1000 mm and 250 mm width. The joint preparation for the weld seams were completed. The consumable wires with a diameter of 1.2 mm were supplied from five different vendors. Tests with respect to hot cracking susceptibility of these consumable materials started in the reporting period. After evaluation of the hot cracking tests the preselection of the consumable wire will be done. For the TIG welding the application of a welding robot is foreseen. First preliminary tests with a newly adopted weld robot showed the feasibility of this welding process.

Bulk material characterization

For the 4 K material characterization fracture toughness tests and tensile tests were prepared. Machining of different types of compact tension specimens and tensile test specimens from the plate material 1.4429 is on the way. These plate material tests will be also a part of the exchange investigations (Round Robin tests) between NBS, oulder and KfK.

Staff:
S. Fischer
H.P. Raber
A. Nyilas

M 12 Development of Low Electrical Conductivity Structures

Joining of metallic structures by adhesives

Glued joints of certain metallic components of a superconducting magnet (superconductor/-superconductor joint in a winding pack e.g.) need careful selection of the used adhesives with respect to electrical and mechanical properties. To qualify the mechanical performance of such metallic/non-metallic joints a low temperature materials test program was established. For heavy loaded structures bonded by adhesives the key controlling parameter of the joints integrity is the joints shear bearing property. The determination of the joints shear strength value is an important design parameter. The common methods for shear strength determination are either the lap shear test (according to ASTM D2557-72) or shear test under beam loading (ASTM 2355-76). Numerical(FEM) and mechanical investigations show for lap shear measurements a lower bound value compared to the latter test method. The analysis for overlapped joints confirm high shear stresses at the very edge of the joint. The resulting hear strength is therefore a mean value of the joints overlapped area. This method yields a reasonable evaluation for the adhesive materials selection but it can't be recommended as shear strength determination for design purposes.

For beam test method the span length (L) and the height of the beam (D) determines the shear distribution. To evaluate the necessary (L/D) ratio, tests have been carried out with a 2 mm thick CFRP plate material. The apparent shear strength τ'vs. (L/D) ratio is given in Fig. 27. A ratio of ~ 5 seems to be suitable to measure proper shear strength without compression or bending type failure. According to this given ratio investigations were carried out to determine the adhesive joint performance of metallic sheated superconductors. Two square sections (sand blasted 304 type stainless steel) with 50 x 50 mm^2 cross section were wrapped around either with glass fabric or glass/Kapton fabric tapes. Joining was performed by vacuum impregnation of an epoxy compound supplied by Ciba-Geigy.Table 7 gives the measured shear strength values. The 77K mean shear strength of glass/glass and glass/Kapton joints are $\sim 62 \pm 5$ MPa and 55 ± 7 MPa respectively. The load vs. displacement records confirm also a ~20% lower stiffness of the glass/Kapton epoxy joint compared to the glass/glass joint.

Support strap development

For cryogenic application filament wound glass-epoxy support straps are developed. Such straps offer minimum heat conduction and can be used as load carrying structures between 295 K and 4 K. To lower the liquid helium consumption of the existing 200 kN mechanical testing machine the central pulling rod was replaced with such a special developed GFRP support strap. The strap consisted beside the unidirectional filaments also of six glass fabric tapes to ensure shear performance at the pin loaded ection. The 450 mm long strap cross section dimensions were 45 x 10 mm^2. Static tests resulted at 295 K and 77 K tension strengths of ~500 MPa and ~1000 MPa, respectively. The measured modulus was~50GPa at 295 K and 77 K.

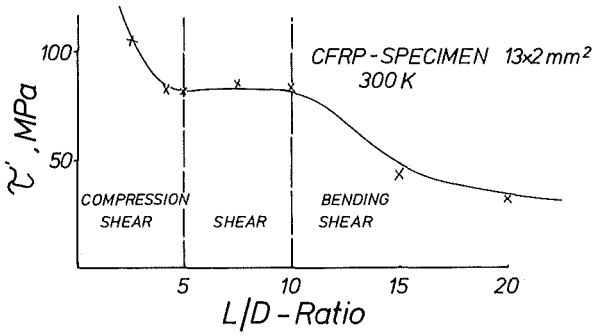

Fig. 27: Influence of span length L on the apparent shear strength values of a CFRP-plate material

Mat.	Temp. (K)	Load (kN)	Shear strength (MPa)
Glass/ Glass	295	89	51
	77	104	59
		105	60
		100	57
		122	70
		120	68
		109	62
Glass/ Kapton	295	98	56
	77	84	48
		114	65
		92	53
		98	56

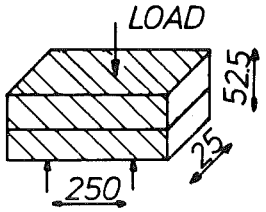

Table 7: Cryogenic shear strength measurements of stainless steel/ epoxy joints

Staff:
S. Fischer
H-P.Raber
A. Nyilas

MAT 1.6 Development and Qualification of Type 1.4914 Base Metal Properties

A fully martensitic steel (German denomination 1.4914) has been selected as a possible first wall and structural material for the Next European Torus.

The first NET- heat (Nr. 53645) of Type 1.4914, the composition of which has already been given in the previous report, has been used to produce rods and plates with dimensions requested by the different EC laboratories. Most of the EC labs and industrial partners associated with the research programme on Type 1.4914 material have in the meantime been supplied with material (see table). In order to recommend a final heat treatment for this fully martensitic steel investigations have been performed in which the influence of austenitizing temperature (varied between 1050 and 1175°C) and the follow-on tempering heat treatment (600 - 780°C) on microstructure and toughness were studied. Especially ferrite formation, prior austenite grain size, and structural homogenity have been investigated. The investigations indicate, that in addition to the above heat treatments, also the fabrication steps used in the production of plates with a thickness between 1 and 20 mm can influence the microstructure and the ferrite formation.

For the material in all dimensions the following heat-treatment 950°C/2 h + 1075°C/30 min + 750°C/2 h produces a δ - ferrite free fully martensitic structure. Therefore this heat treatment should be used in further experimental investigations as a reference heat-treatment for steel 1.4914 - NET.

Further investigations on the transformation diagramme, on tensile-, creep and impact properties have been started in the meantime.

Laboratories and industrial groups which have been supplied with 1.4914 material:

France, CEA, Fontenay
Belgium, CEN/SCK, Metallurgy Department, Mol
Italy, Euratom, MSD, Ispra
Netherlands, NERF, Petten
Great Britain, University , Birmingham
Great Britain, Tube Investments Research Lab., Essex
Great Britain, Culham Lab., Culham, Oxon
Switzerland, Sulzer, Winterthur
Switzerland, ElfR, Fusion Technology, Würenlingen
West Germany, KfK, IMF, Karlsruhe
West Germany, KFA, Jülich
West Germany, MAN, Technologie, München

MAT 1.9 Pre- and Post-Irradiation Properties of 1.4914 Martensitic Steel

The main objective of the present task is to investigate the influence of mechanical and thermal cycling upon the lifetime of first wall materials for conditions given by the NET matrix.

1. Mechanical Loading Equivalent

Because the preparation of the hollow test specimens (HGRIM) of 1.4914 is delayed, the optimizing procedures were started on solid specimens(SGRIM) of 1.4914.

On these specimens low cycle fatigue tests were conducted at 550 °C with a total strain range of 1.0%. The reproducibility of the cyclic deformation behaviour was very satisfactory irrespective whether the heat treatment was performed prior or subsequent to manufacturing. The lifetime of the non heat treated material (as delivered) is not very different from that of the heat treated specimens.

In Fig. 28 the maximum tensile stress σ_{max} is plotted versus the number of cycles N. For loading conditions given in Fig.28, in contrast to the results on AISI 316L, cyclic softening is observed for 1.4914 irrespective of the fabrication conditions. Nevertheless, the number of cycles to failure for both materials is nearly equal.

2. Thermal Loading (Thermal Fatigue)

As already reported in order to check the heating equipment, experiments on AISI 316L HGRIM specimens under "free-ends" conditions were conducted up to 20000 cycles. As expected, no cracks were observed under these conditions.

In a first series of experiments a sample was axially constrained in length at the lower test temperature of 250°C and then heated up to 550 °C. Since thermal expansion was not possible, this increase of temperature generated a plastic deformation of the sample. For technical reasons these experiments were terminated after 20000 cycles without any damage .

A second kind of tests under really conditions "fixed-ends", i.e. constrained both in tension and compression direction, is on the way in a mechanical LCF testing equipment as load frame which allows for

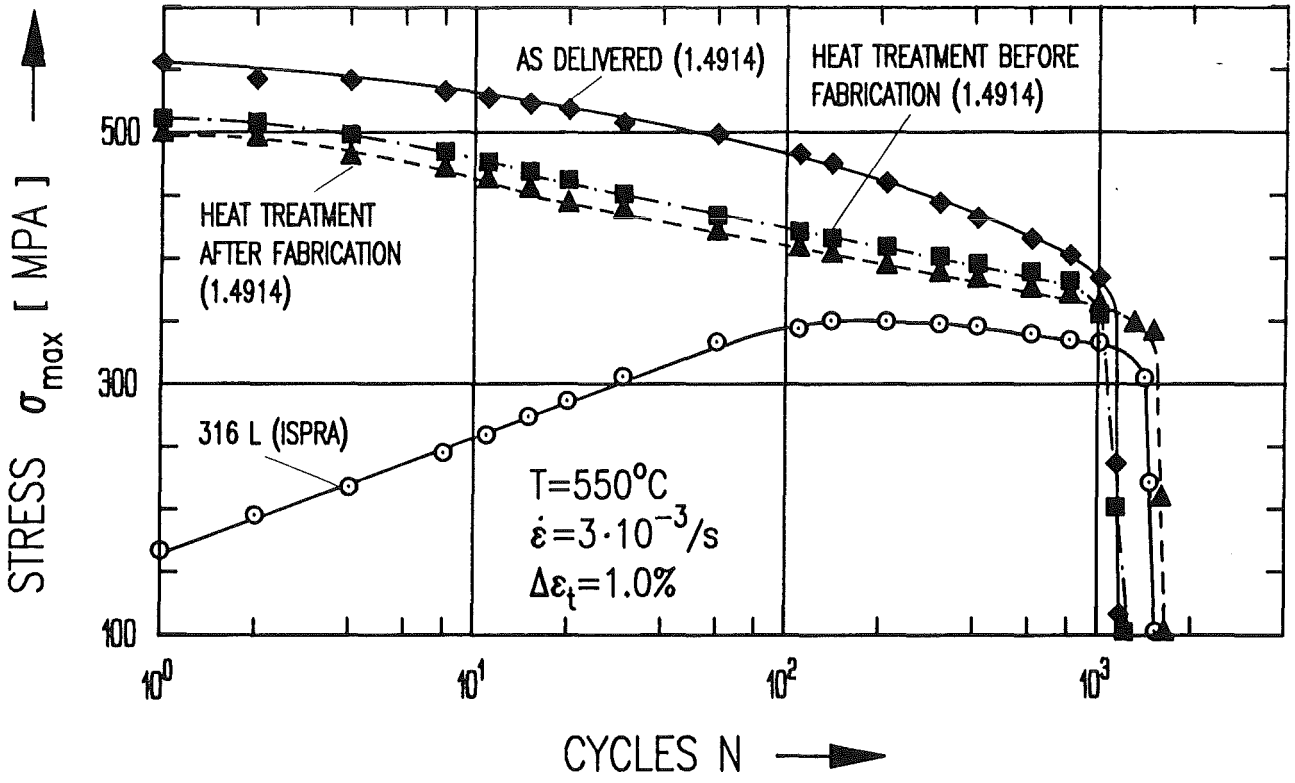

Fig. 28: Maximum tensile stress vs. number of cycles to failure for 1.4914 and AISI 316L (SGRIM specimens)

variable clamping conditions. These experiments will be used to specify the parameter field of future experiments.

Because of the long duration of the tests (several weeks) and the restriction given by the planned time schedule, it was decided to install 10 test facilities to be operated in parallel. With the experience from the preceding tests these facilities, consisting of the heating equipment, the load frame and an automatic data acquisition system, were designed and ordered.

3. Azimuthal Temperature

As it was shown by calculations, an azimuthal temperature distribution will be generated in the Dual Beam Experiment (MAT 9.2) during the planned in - beam low cycle fatigue test in addition to the radiation damage.This will change the mechanical behaviour of the HGRIM sample. To study this influence a simulation test facility was installed in a LCF machine. First tests are on the way to investigate the stability of the sample against buckling and its influence on the number of cycles to failure .

Staff:

W. Baumgärtner	W. Scheibe
M. Bocek	R. Schmitt
C. Petersen	H. Schneider
D. Rodrian	W. Schweiger

MAT 1.11 Post-Irradiation Fracture Toughness of Type 1.4914 Martensitic Steel

The target of the MAT 1.11 activities is to study the influence of fission neutron irradiations on the impact properties of 1.4914 material. Emphasis is given to the problem of DBT-temperature shift and to an eventual change of impact energy as a function of irradiation temperature and neutron fluence. In addition, radiation hardening and post irradiation annealing behaviour are studied by tensile and hardness tests.

In accordance with the planning schedule 90 minaturized Charpy-V-samples from the NET-heat 1.4914 have been prepared for the common JRC-ECN-KfK irradiation SIENA-E-198-14. In this experiment samples with the reference heat treatment as well as other metallurgical treatments, in which the tempering temperature has been varied between 600 and 750°C, are included. Also samples taken in different orientation to the rolling direction of the ingot material have been put into this experiment. Tensile samples with the reference treatment have been manufactured by our ECN cclleagues and have also been loaded into the irradiation rig. The irradiation should start in May 87.

Data from prerunning experiments with melts of Type 1.4914 and data of other 9-12%Cr steels taken from literature give a rather uniform behaviour of the DBT-temperature as a function of irradiation conditions. As can be concluded, the increase of DBTT from -50°C up to 150°C is the strongest in the temperature region below 300°C. In addition a reduction of the upper-shelf energy down to 50% of the initial value can be observed. The results are of great significance for the NET-design and the envisaged operational temperature region.

Staff:
B. Dafferner
K. Ehrlich
C. Wassilew

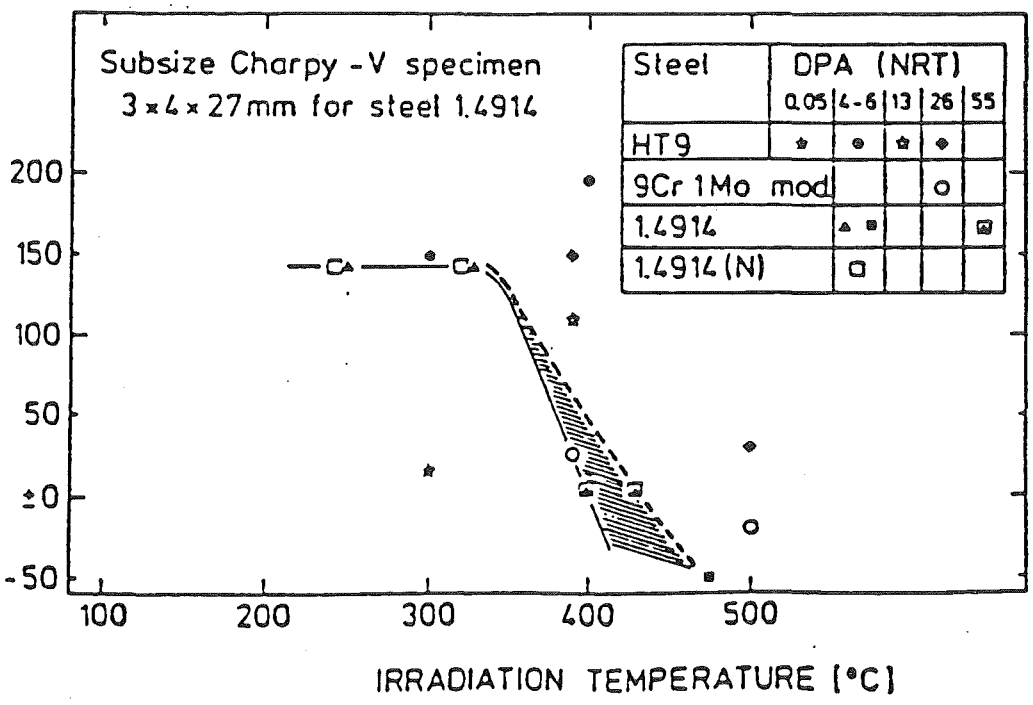

Fig. 29: DBT-temperature of irradiated 9-12% Cr steels determined by Charpy -V- tests.

MAT 2.2 In - Pile Creep-Fatigue Testing of Type 316 and 1.4914 Steels

It is intended to study the in-reactor deformation and the fracture behaviour of the two candidate structural materials for NET under load cycling in tension.

The irradiation will take place at the central position of the KNK-II-reactor Each irradiation rig will consist of eight pressurized tube samples which can individually be loaded by internal gas pressure and can be temperature controlled. The technique of these instrumented pressurized tubes has been tested.

The external parameters for these tests have now been specified. Sample temperatures will be constant between 400 and 550°C, dependent on the reactor position. The inner pressure is variable between 10 and 450 bar, which corresponds for the given geometry of tubes to a maximum tangential stress of 400 MPa. Pressure hold-times between 100 and 1000 s can be achieved. For the pressure control a first concept was developed and first experiments were started to measure the characteristic times for pressure increase and decrease. Typical values which have been achieved in prerunning tests are: Pressure increase velocities of about 40 bar/s and a pressure decrease of 10 to 20 bar/s.

The facility for the generation of such pressure transients has been technically specified and ordered. The delivery is expected around September 87. Out-of-pile-tests will then start in the fourth quarter of 87.

Staff:
K. Ehrlich
L. Schmidt

MAT 6 / MAT 13 Ceramics for First Wall Protection and for RF Windows

SiC qualities of industrial manufacturers are to be tested concerning the durability of tiles to protect the first wall against plasma instabilities and disruptions. Insulator materials (like Al_2O_3, $MgAl_2O_4$, AlN) are to be selected with regard to their resistance to thermal crack formation by dielectric loss in rf-windows. These windows shall be applied to separate wave guides for ECR heating from the plasma vacuum.

In order to test the neutron irradiation behaviour of ll the materials mentioned (together with graphite samples of other investigators), mainly with regard to changes of strength, thermal conductivity and dielectric loss, several irradiation experiments have been started or are being prepared. Table 8 gives the present state. The third HFR irradiation (bottom of the table) with SiC and graphite samples at very high emperature was again ordered by KfK, and its design and loading scheme are under discussion. Additionally, it is envisaged to insert SiC bending test samples into a HFR irradiation at 600°C.

Concerning the thermal operation conditions of protective tiles on the first wall, a critical temperature limitation may be given by the evaporation behaviour of SiC. Therefore evaporation experiments have been conducted with various hot-pressed and sintered SiC grades under high vacuum. The results of screening tests up to 2000°C and of more thorough measurements at 1700 °C were compared with theoretical calculations of C. H. Wu (NET-team) and foreign measurements on single crystals under argon. It seems that a maximum temperature of about 1700°C (sublimation rate ∿1mm per year) has to be observed under normal operation conditions.

Bending test specimes were cut from small SiC tiles manufactured by sintering or isostatic hot-pressing (HIP). In Fig. 30 the so-called Weibull plots of the bend strength distribution are presented, which show the superiority of the HIP material.

The thermal conductivity data of highly pure The thermal conductivity data of highly pure polycristalline Al_2O_3 and sapphire in the temperature range 300 < T < 900 K can be summarized. The characteristics of the samples are given in the Tab. 9 They follow the relationship.

$$\lambda = (a + bT)^{-1} \quad (T) = K$$

with the ccefficients as shown in table 10.

The continuous measurements of dielectric loss of ceramic insulators in the GHz domain corroborated the experience, that it appears extremely difficult to achieve the tan δ levels wanted for ECRH windows, which are at $1\text{-}3\times10^{-4}$ for Al_2O_3 and $MgAl_2O_4$, and $\lesssim 1\times10^{-3}$ for AIN. A compilation of the tan δ data that became known up to now is given in Table 11; R. Heidinger is the KfK author. The worse results for Al_2O_3-99.9 seem to be due to an unfavorable influence of very small grain size. The disappointing results for Al_2O_3 single crystal are still unexplained and require further examination.

First measurements on Al_2O_3 samples that were irradiated at low temperature (<100°C) to a fast neutron fluence of 2×10^{20} n/cm^2 indicated a considerable increase of tan δ , but have to be continued to obtain conclusive results.

The Fabry-Perot resonator system for dielectric measurements at 140 GHz has been tested and proved to be functioning. Some problems remain to be solved concerning the power and the frequency range of the microwave generator.

Facility	Start	Duration	Fast Neutron Fluence [10^{22} n cm^{-2}]	Quantity of Samples Bend Strength (B) Phys. Prop. (P) Dielectr. Prop. (E)	Partners
HFR Petten	1/86	1 month	0.02	11 P, 16 E	-
OSIRIS (Saclay)	4/86	1 year	1	16 B, 25 P	F
HFR (Petten)	7/86	1 year	1 (SiC: 1200 °C)	156 B, 108 P, 14 E	F, E, GB
LAMPF (Los Alamos)	7/86	some months (till end of 87 due to breaks)	~ 1 dpa	60 B, 53 P, 15 E	USA, D-KFA
PHENIX (Marcoule)	ca. I/87	1/2 year	3	84 B, 103 P	F
HFR (Petten)	ca. IV/87	1/3 year	0.3 (SiC: 1500 °C)	ca. 104 B, 90 P	F, D-KFA

Table 8: KfK participation in irradiation experiments on SiC and ceramic insulators

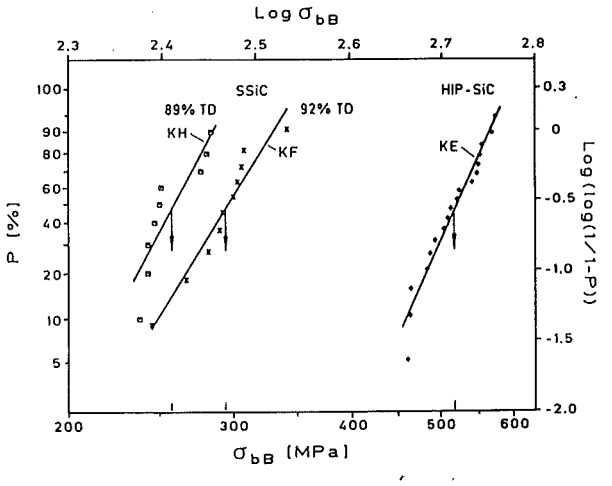

Fig. 30: Bend strength of different SiC grades

	Al2O3 (Bio) wt%	Al23 (Degussit) wt%	Al2O3 (Sapphire)	
Al_2O_3	99.9	99.5	Fe	1 - 5 ppm
SiO_2	< 0.015	< 0.03	Cr	1 - 5 ppm
Fe_2O_3	< 0.0044	< 0.03	Ti	5 - 20 ppm
CaO	< 0.008	< 0.05	Co	< 2 ppm
MgO	< 0.05	< 0.3	W	not found
CrO_2	< 0.0003			
Sample thickness (mm)	3.16 2.05	1.995 2.73	2.05 ⊥ c-axis	
Density	3.918 g/cm³	3.916 g/cm³	theoretical	
grain size (µm)	2 - 4 µm	1 - 2 µm		

Table 9: Characteristics of Aluminia Materials

	a $[W/cmK]^{-1}$	b $[W/cm]^{-1}$
Polycrystal		
Degussit	- 0.162	0.0106
Bio	0.268	0.0103
Single crystal		
C⊥	0.274	0.00981

Table 10: Thermal conductivity of polycrystallline Al_2O_3 and sapphire

Material	Author	Frequency GHz	tan δ 10^{-4}
Al_2O_3 99.5	Afsar	100-200	5-10
	Ho	135	4.5
	Frost, Ho	100	4
	Ho	35	3
	Birch	35	5.5
	Heidinger	35	5
Al_2O_3 99.5	Afsar	100-200	15-20
	Ho	135	15
	Ho	100	3.5; 13
	Ho	35	10
	Heidinger	35	10-40
Al_2O_3-SC	Afsar	100-200	5-10
	Heidinger	35	7-12
$MgAl_2O_4$	Afsar	100-200	5-10
$MgAl_2O_4$-SC	Heidinger	35	12
AlN 96.5	Heidinger	35	40-70
AlN 98.7	Heidinger	35	15-30

Table 11: Tan δ of ceramic insulator materials in the GHz domain

Staff:

Ch. Adelhelm
M. Blumhofer
W. Dienst
G. Gausmann
CH. Gosgnach
H. Haase
R. Heidinger
D. Kempf
B. Schulz
S. Winkler
H. Zimmermann

MAT 9.2 Investigation of Fatigue Under Dual Beam Irradiation

The Dual Beam Facility of KfK was developed as a research tool for materials within the European Technology Programme. The Dual Beam Technique allows the production both of damage and helium in thick specimens by simultaneous irradiation with high energy protons ($\leq$ 40MeV) and alpha particles ($\leq$ 140 MeV) produced by two KfK cyclotrons.

In order to investigate the effects of helium implantation on mechanical properties and microstructure helium was implanted into homogeneously several sheet specimens of martensitic steel 1.4914 with a gauge size 7.1 x 2.0 x 0.2 mm^3 after a heat treatment of 1075°C/ 30' + 700 °C/ 2h. The helium implantations were performed in a vacuum chamber using the 104 MeV alpha-particle beam and a corresponding moderator system. Four specimens cculd be irradiated simultaneously. The implantation rate varied between 2.0 and 3.2 appm He/h and the displacement damage due to the implantation was about 4 x 10^{-3} dpa/appm He.

Tensile measurements at test temperatures equal to the implantation temperatures (380 - 620°C), with a strain rate 1.2 x $10^{-4}s^{-1}$ and a helium content of 140 - 310 appm He indicates a strong embrittlement particularly at lower temperatures. The total elongation which for the unirradiated material drops with decreasing temperature is further reduced by the helium implantation to 1/2 to 1/3 of the initial value. The rupture mode changes from a ductile type at ~585°C to a more brittle type at lower temperatures (380-440°C). Here the embrittlement starts with crack nucleation at one specimen edge at low strains (0.4-1.2 %) which propagates in shear direction through the sample-width. During the crack propagation stage the stress-strain curve shows serrations indicating contributions via localized flow in slip bands.

The effect of He-implantation on material strength seems to be similar to that found after neutron irradiation at low fluence and helium levels in 9-12Cr-1 Mo steels.

Below $T_I \leq$470°C the yield strength increases ($\leq$130 MPA) in a more pronounced way than the ultimate strength ($\leq$ 40 MPA)Specially at 440°C the hardening could occur by secondary precipitation formed during thermal ageing. At higher temperatures ($\geq$470°C) the material softens by a decrease in yield and ultimate strength of about 28%. At 640 °C He-bubbles becomes visible in TEM observations only at large precipitates.It should be noted, that the helium content in the experiments described is rather high compared with the NET specification. By the end of phase III (fluence MWa/M^2) the estimated helium content will have reached about 80 appm in martensitic steels. Therefore, in future, we will concentrate the tensile investigations mainly on the low dose dependence of the helium embrittlement.

Staff:
G. Bürkle
A. Möslang
D. Preiniger
G. Przykutta

MAT 18 Development of Low Activation Ferritic-Martensitic Steels

First wall and blanket structures of fusion machines will get activated during operation by the high neutron fluxes, giving rise to problems in reprocessing or waste disposal. To overcome these problems, it is necessary to avoid the presence of certain alloying elements (or some isotopes therefrom) and to minimize impurity elements exhibiting unfavourable activation properties.

A literature survey has shown that in recent years 9-12% Cr ferritic/ martensitic steels have been devised in which mainly Mo and Nb have been replaced by additions of W or enhanced levels of V or Mn. The results obtained show that for the modified materials the standard of commercial alloys, like 1.4914, FV 448 or HT9, has not been reached, especially with regard of an adequate balance of tensile and impact properties. However, improvements appear possible, by varying the interstital content and by a sophisticated combination of other alloy constituents. In this connection the effects of variable δ-ferrite contents on the mechanical properties must be systematically investigated.

Six alloys of a 1.4914-like base composition, but with Cr-contents varying between 9.2 and 14.0 wt-% have been produced. By this measure the following δ-ferrite contents have been obtained:0%(100% martensite); traces of δ-ferrite; 5%; 20%; 25%. In searching for the best solution treatment temperature the alloys were annealed between 850 and 1150°C, followed by air cooling. The resulting hardness values and grain sizes are plotted in Fig. 31.

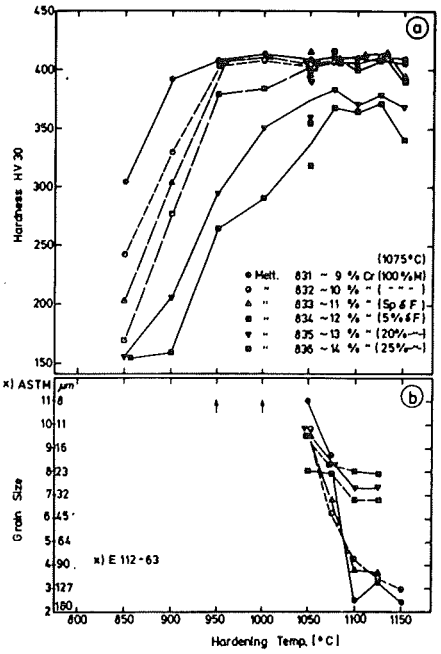

Fig. 31: Effect of hardening temperature on hardness and grain size

1075°C appears to be a good choice because the hardness maxima are reached and the (prior austenite) grain size remains below 45µm in all cases.

As the next step the tempering behaviour of these alloys will be studied.

3 martensitic low activation materials, alloyed with Ce, Ta and/or Hf, are in the forging stage.

Staff:
K. Anderko
M Schirra

N 1 Design Study of Plasma Facing Components

This task comprises design studies concerning first wall and first wall protection and the investigation of divertor concepts for NET.

1. First Wall Design
First Wall with Radiatively Cooled Protection Tiles

First Wall protection against impact of particles and mainly against plasma disruptions is considered necessary for at least the first operation phase of NET. Graphite is a short term candidate protection material. Since direct coatings can probably not be made thick enough to reach a sufficient life time, protection tiles and attachement methods are being developed. Cooling of the tiles by radiation to the first wall steel structure is probably the most reliable heat transfer mechanism.

A typical design feature of the KfK concept of gas ooled first wall with radiatively cooled protection tiles as described in (1) is the loosely fitting of small tiles between directly cooled support rails welded to the first wall front panel. It has been shown in the last semi-annual report that this concept results in acceptable graphite protection tile temperatures of less than 1400°C and maximum equivalent stresses of below 230 MPa for a heat flux of 20 W/cm^2 and small tile dimensions.

As will be shown below,the concept compares favorably with the unacceptably high stresses of some other first wall designs also at the higher heat fluxes anticipated for some areas of the first wall. herefore it seems worthwhile to elaborate this concept in more detail and also to apply it to water cooling of the first wall. In addition to design work necessary to integrate the concept into the design of a first wall box the special requirements and possibilities of thermal fatigue testing are being considered. Blackening of the austenitic stainless steel wall by coating with Al_2O_3 + TiO will be investigated to improve emissivity and stability in contact with the substratum with the graphite tile at service temperature.

Temperature and Stress Calculations for First Wall Concepts.

As discussed previously designs with radiation cooled graphite tiles in front of a First Wall (FW) made from austenitic stainless steel are presently under discussion as most favourable. In table 12 three proposals for a FW are shown

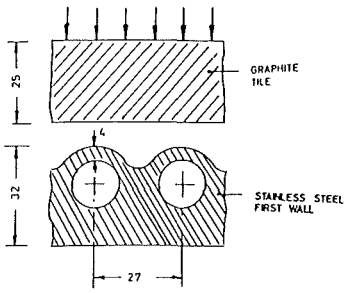

(a) water cooled

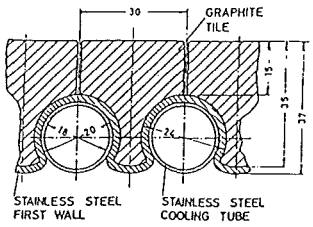

(b) helium cooled

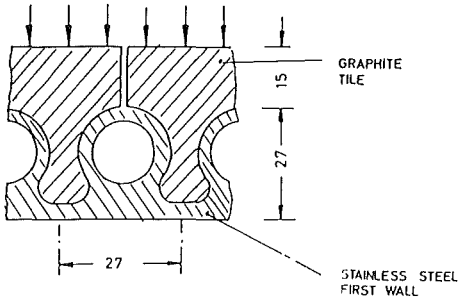

(c) water or helium cooled

Fig. 32: Radiation cooled First Wall designs

These concepts differ in the cooling, which is either water or helium, and in the direction of the cooling tubes, namely poloidal and toroidal, respectively. Concept (a) uses water, concept (b) helium cooling, whereas concept (c) is considered with both cooling media.

A comparison of these FW designs was carried out varying some geometrical data and the thermal loads. A surface heat flux of 0.4W/mm^2 was taken into account as reference load. The temperature and stress distributions were calculated using FEM (Finite Element Methods). A preliminary qualification can be made by looking at the following criteria:

maximum tile temperatures (T)
maximum (Tresca) equivalent stresses (EQ)
maximum principal stresses (P1, P3 = compressive, tensile stresses).

The data are summarized in table 12:

	Concept:			
	(a)	(b)	(c) with water	(c) with helium
T /°C/	2068	1791	1753	1740
EQ /MPa/	622	556	340	314
P1 /MPa/	-627	-332	-297	-313
P3 /MPa/	559	556	344	259

Table 12: Temperatures and stresses for different FW concepts

With respect to cyclic thermal fatigue, lifetimes of 10^5 cycles could be achieved with cyclic strain rates less than 0.2%. Furthermore primary plus secondary stresses in the wall must not exceed twice the yield strength. From these requirements stresses less than 300 MPa are acceptable.

In addition, cyclic thermal stresses and inelastic behaviour due to irradiation creep and swelling have been investigated. Based on inelastic stress distributions fatigue crack growth will be considered.

Publications:
(1) S. Malang, E. Diegele, G. Hofmann, K. Rust:"A First Wall Concept with Radiatively Cooled Protection Tiles", Proc. 14th Symp. on Fusion Technology, Avignon (Sep.1986).

Staff:
E. Diegele
G. Hofmann
K. Rust
G. Schweinfurther

2. Divertor Design

The main thermomechanical issues for the NET divertor are the high heat flux, the physical and chemical sputtering rates, and the surface erosion from plasma disruptions. Most of the divertor walls proposed so far consist of a metallic heat sink structure protected by a heat and erosion resistant surface material. In this duplex structure material compatibility, perfect bonding, temperature limits, and cycling shear stresses due to differential thermal expansion are the major features of concern.

There is a large uncertainty in the design heat flux (5-10MW/m^2). Thin walls are required to cope with this magnitude of heat flux. On the other hand the predicted erosion depths of many centimeters per full power year call for thick protection layers. Above all, the material properties and fabrication aspects (e.g., the bonding) have to be taken into account.

As a first computational approach the heat flux potential has been compared for several candidate material combinations. The temperature and stress analysis was done by use of the finite element computer code ABAQUS for a 2D linear elastic model. The geometric configuration (fig.32)is typical for a tube concept, consisting of a coolant tube and a protection sleeve, perfectly bonded to it. The critical region in terms of temperature and stresses is along the line of symmetry, designated as y-y in figure 33. Similar conditions will be expected for other designs with equivalent wall thicknesses, which in this case are 2 mm for the tube and 5 mm for the protection layer. Two different cooling conditions have been assumed at the inner tube wall, typical for water coolant and for helium gas coolant, leading to somewhat different temperature distributions. Six material combinations were chosen, which are under discussion for NET (table 13).

Typical temperature contours in the whole cross section and von Mises stress contours in the critical region are plotted in figure 33 as an example for the molybdenum-alloy (TZM)/tungsten combination at a heat flux of 8MW/m^2. The heat flux limits, where either the temperature or the allowable stress limits are reached, are summarized in table 12.

It can be concluded, that the material combinations TZM/graphite and TZM/-tungsten are the only ones promising to reach the 10MW/m^{2}heat flux goal, when cooled with water. If TZM should turn out to be not viable for reasons of embrittlement, fabricability, and activation the often proposed combination copper/tungsten water cooled provides an alternative.

The strategy for divertor testing in the predesign phase of NET has been developed in collaboration with the NET team. It consists of three test categories, i.e., sample fatigue tests, sample disruption tests, and elements performance tests. A proposal has been made to perform sample fatigue tests in an existing plasma spray device with a plasma gun as a heat source. The suitability of the device is being investigated and a test program is under discussion.

The idea of a partial coverage divertor, as opposed to the full toroidal coverage divertor belt, was pursued in order to ease the handling procedure. In a brief design study it was found that in the NET-DN configuration with a single divertor module per access port a coverage of only about 1/2 to 2/3 of the full toroidal belt can be achieved. This is not very attractive with regard to the enhanced heat flux and erosion rates. Hence, the full coverage version should remain the reference solution.

Heat flux limits for a douplex compound divertor wall for different material combinations			
Material combination tube/sleeve	max. surface heat flux (W/cm2)		limit a)
	water	helium	
1 Cu/W	690	330	SM_t
2 NB-1ZR/TZM	710	560	T_s
3 V-15Cr-5Ti/W	580	450	T_t
4 TZM/W	1000	800	SM_s, T_t b)
5 TZM/Graphite	1150	730	T_t
6 Cu/Be	410	390	SM_s

Table 13:

a) SM = Stress limited — Index t = tube
T = Temperature limited — Index s = sleeve

b) SM_s for water, T_t for helium

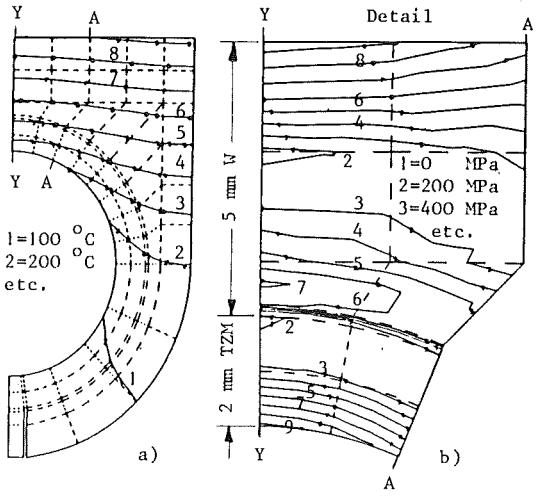

Figure 33 : Temperature (a) and v. Mises Stress Contours (b) in the TZM/W Divertor Wall at a Heat Flux of 8 MW/m^2

Staff:
K. Kleefeldt
K. Schramm

N 2 Shield Design Studies

Blanket segments for shielding are being developed and designed which will be used in the first phase of the NET operation instead of breeding blankets. This in-vessel shield blanket should be robust, failure proof during operation and capable of being produced at reasonable cost. For the time being, three directions are simultaneously pursued: concepts based on gas and water cooling, which have solely a shielding function, and, in addition, a version of the water cooled blanket which, thanks to the use of an aqueous lithium salt solution, offers the possibility of contributing to tritium generation. In all cases the blanket segments are designed in such a manner that they can be placed behind the first wall inside the segment box instead of the breeder blanket.

In the helium cooled blanket sufficient shielding effect can be achieved by a steel layer of about 275mm thickness. In order to avoid high thermal stresses this layer has been divided into four successive sheets. The coolant gas first passes through the toroidal cooling coils of the first wall and is then routed in the poloidal direction through the cooling channels integrated in the shielding plates. The states of the gas and the pressure losses correspond to those of the helium cooled breeder blanket.

In the water cooled blanket the shielding effect is achieved by neutron moderation mainly in the water and its absorption in the following steel layers. The blanket segment may consist of a cluster of pipes in poloidal configuration composed of at least three pipe sections of different diameters in order to obtain optimum covering. The space can be used still better by poloidal traversing blanket segments shaped as steel containers, almost rectangular in cross section. They are fabricated by welding of steel sheets. The water flows several times through the container in the poloidal direction at about three bar pressure and is heated during its passage from about 40°C to 70°C. At present, a study is being made on the methods and costs of fabrication of the shield blanket segments outlined here.

When the water cooled shield design is optimized for simplicity and adequate shielding performance it contains a large volume fraction of water. Then it is without any design modification very well suited for tritium production with an aqueous lithium salt solution. This possibility has been checked by extensive neutronics calculations and literature studies on corrosion and tritium recovery in order to come to a first assessment.

When compared with other concepts the aqueous lithium salt blanket has the advantage that the solution can replace water cooling also in the divertor and in segments dedicated to plasma heating and diagnostics. Fig. 34 shows the tritium breeding ratio of such a blanket versus ^{6}Li-concentration in the solution.

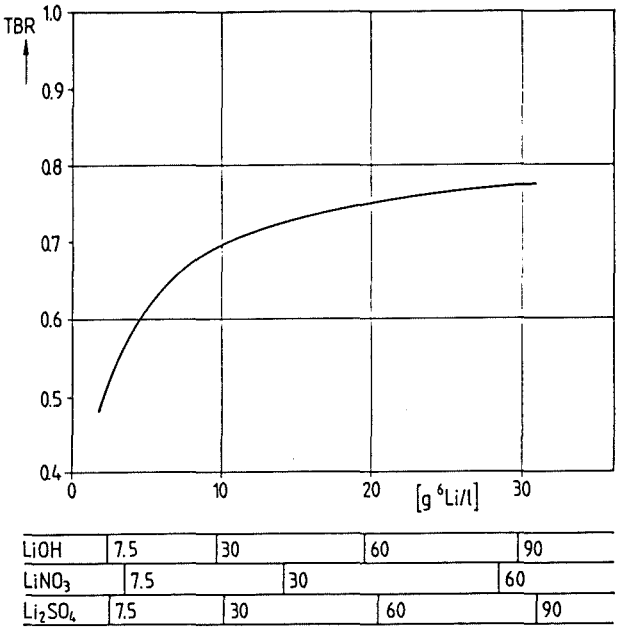

Fig. 34: Tritium breeding ratio (TBR) vs. ^{6}Li-concentration in the aqueous lithium salt blanket. Lower scales: ^{6}Li-enrichment (%) to achieve the ^{6}Li-concentration in 20° saturated solutions.

The data were obtained by three-dimensional Monte Carlo calculations (see this report under B2). The calculations refer to the situation where all segment positions are occupied by lithium salt solution blankets. All of the three-compounds seem comparable from the neutronics point of view with a slight preference for $LiNO_3$.

Although there is an indication that no major corrosion problems are to be expected in the low temperature region envisaged here (40°C-70°C), more measurements at relevant conditions and engineering tests are urgently needed before a realistic assessment and material selection can be made. This should include the impact of welds and possible improvements by inhibitors. Tritium recovery costs were estimated from literature data on the basis of a 10 Ci/l feed concentration and with buffer tanks to smoothen the tritium production in the blanket. Capitel costs of 22 Mio/ECU to 53 Mio/ECU were

obtained. Tritium production can be increased when beryllium plates are placed in the front part of the elements.
These plates are cooled by the lithium salt solution, flowing in poloidal slits. With 15cm beryllium on the outboard and 10cm beryllium on the inboard blanket a tritium breeding ratio of 0.98 is obtained in three-dimensional calculations. When only a fraction of all segments is occupied by breeding blankets the breeding ratio increases linearly with this fraction. For NET it is assumed that 15 segments will be used for the plasma heating and diagnostics, and 4 for test positions. In the following table tritium breeding ratios are given for 3d-calculations both, for all 48 segments occupied by breeding elements (TBR), and for 48-19=29 breeding segments (TBR_{eff}).

No.	blanket concepts	TBR	TBR_{eff}	a_{max} %
1	solid breeder	0.95	0.57	10.5
2	Pb-17 Li self cooled	0.83	0.50	9.0
3	Pb-17 Li H_2O cooled	0.75	0.45	8.2
4	LiOH without Be	0.73	0.56	10.3
5	LiOH with Be	0.98	0.755	18.4

Table 14: Tritium Breeding Ratio and Maximum Availability of NET for Various Driver Blanket Concepts.

Included are the ceramic breeder canister blanket (see B1), the Pb-17 Li self cooled concept with beryllium but without inboard breeding blanket, the Pb-17 Li water cooled blanket as calculated by Dänner, and the lithium salt blanket with and without beryllium. In case of the lithium salt blanket with p (^{6}Li) = 19.6 g/l it was assumed that the breeding efficiency of the 15 segments used for plasma heating and diagnostics is about half of the normal breeding blanket local TBR. The table also contains values of the maximum availability which can be achieved with the various blankets. These figures are based on the assumption that 1.5 kg tritium from external supply are available per year and that the fission power is 600 MW. Then the maximum availability limited by tritium supply is a_{max} = 0.045 without tritium breeding and

$$a_{max} = \frac{0.045}{1-TBR_{eff}}$$

with tritium breeding in equilibrium.

Even without beryllium the effective tritium breeding ratio of the lithium salt blanket is equal to the best of the other concepts. With beryllium it is clearly superior to all others. For the concept without beryllium the decision to use this option can be taken rather late in the program because it has practically no influence on the in-vessel components in the main building. But it would require a special tritium processing plant. Once NET is running well, the shield blanket can be converted to a breeding blanket just by changing the coolant. No replacement of components is needed. The beryllium plates in the front part require a different container design and have to be foreseen from the beginning, otherwise an exchange of blanket segments would be necessary.

Staff:
E. Bojarsky
S. Dorner
U. Fischer
M. Küchle
G. Reimann
H. Reiser

N 5 Development of Theory and Tools for Evaluation of Magnetic Field Effects on Liquid Breeder Blankets

Investigations of MHD in liquid metals

The governing problems in developing a selfcooled liquid metal breeder blanket for NET are pressure drop and flow distribution of the liquid metal circulating in the high magnetic field of a fusion machine. The proof that this pressure drop can be held low by an appropriate guidance of the flow will decide on the feasibility of such a concept. To overcome the lack of reliable experimental data, the program MEKKA (Magneto-Hydrodynamik Experiment in Natrium-Kalium Karlsruhe) has been initiated 1985 at KfK. Therefore a MHD laboratory was built up. In a first step experiments with straight ducts and circular or rectangular cross section, and experiments with modulated channel widths and with bends will be made. To reduce the MHD pressure drop the introduction of flow channel inserts is planned in order to reduce the electrical wall conduction ratio. The basic MHD effect of these flow channel inserts will be investigated already in 1987. A normal conducting dipole (MA) magnet (a loan of DESY-Hamburg) is used. It has a field strength of 2 Tesla and a test volume of 0.17m x 0.5m x 1.5m. The magnet has already been set up, the 400 KW direct current and the corresponding cooling water supply are installed. The Sodium-Potassium liquid metal loop NaK 1 designed and built up at KfK has been finished except the control and monitoring units. It uses some components which at KfK are used for the first time in this kind of application: A canned motor pump to circulate the liquid metal, an oil cooled double tube heat exchanger , an oil cooled cold trap and a gyrostatic flow meter with high accuracy.

Fig. 35 is a photograph of the first step of completion of MEKKA showing the movable liquid metal loop (in the foreground), the normal conducting dipole magnet and the electrical power supply (background left side), state end of 1986.

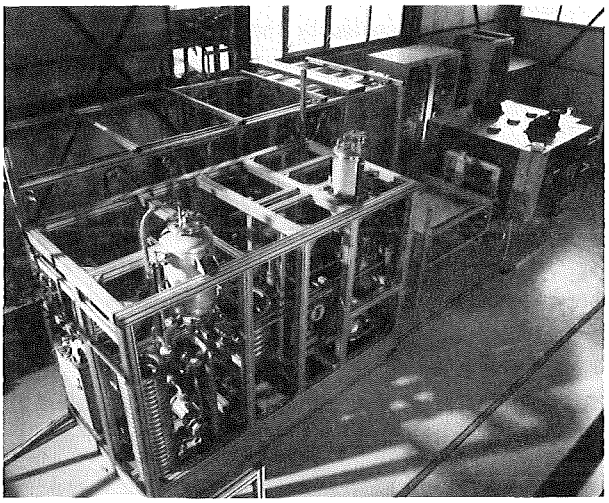

Fig. 35: MHD test facility MEKKA

The facility will start operation in the first half of 1987.

A data acquisition system which allows to collect pressure drop, electrical potential and velocity data in 60 channels has already been installed. A positioning device with stepping motors to measure the three dimensional magnetic field distribution of the MA magnet has been set up, too.

A straight duct test section with a circular cross section of 140 mm inner diameter is under construction. A superconducting solenoid magnet (CELLO-Magnet) with a field strength of 3,5 tesla and a warm bore of 400 mm has been installed in the laboratory. It is to be used for the second step of the MEKKA program, where the pressure drop and flow distribution in a poloidal-toroidal bend will be measured.

The setup includes Dewar vessels for the cryogenic supply and a helium gas backfeeding line. A literature survey has been made and investigations have been started to numerically simulate MHD flow in simple geometries. The first calculations showed satisfactory results but also revealed the limits of the used method with respect to the needed spatial resolution at high magnetic field strength.

Development of a Velocity Meter

For interpretation of MHD-pressure drop measurements a velocity meter is being developed in KfK. It applies the propagation of an artificially created temperature pulse in the fluid. Measurements in a rotating mercury channel have been carried out. Fig. 36 shows measurements at a velocity of v =0.01942 m/sec. The propagation time of the temperature pulse for a distance (r) of 2 and 4 mm is plotted as a function of the direction of convection α(α=0, convection from position of pulse creation to the sensor). The propagation time (t) is independent of the direction of convection as predicted by the analytically derived equation.

$$V = \sqrt{\frac{r^2}{t^2} + \frac{4a}{t}}$$

with "a" being the thermal diffusivity of heat. The propagation time difference between r_1 and r_2 completely agrees with the predicted value of Δt = 101.7 m/sec.

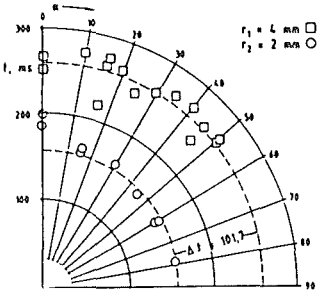

v = 0.01942 m/sec.

Fig. 36: Propagation time of a temperature pulse in flowing mercury

A computer program has been developed for data acquisition, evaluation of data and for initiating temperature pulses in the fluid. This program operating on a PC responds directly to the measuring system. A typical computer output of a measurement in a solid copper block is shown in Fig. 37. An averaged temperature-time-signal is plotted along with a fit of the analytical equation to the measured curve.

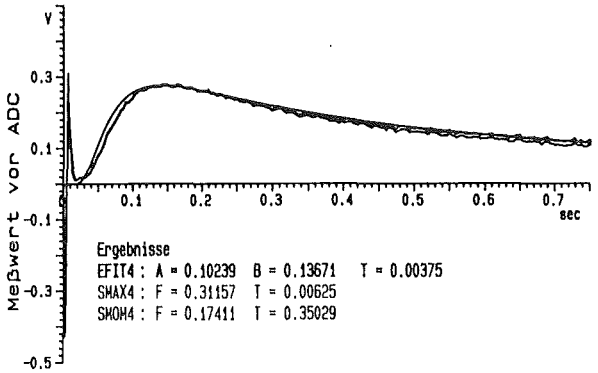

Fig. 37: Computer output of temperature signal measured in a solid copper block and a fit of the analytical equation

Staff:

G. Arnold
L. Barleon
V. Casal
R. Kirchner
H. Kreuzinger
H. Kußmaul
K. J. Mack
A. Sterl
K. Thomauske

RM 1 Background Studies on Remote Maintenance

This task concentrates on the investigation of pipe connectors (for water cooling liquid metal breeder fuelling, gas cooling, and gas purging systems), electrical connectors, and cutting and welding techniques for fusion reactors.

The work includes:

- identification of development needs,
- recommendation of a pre-testing programme,
- performance of pre-tests, identification of necessary improvements and modifications,
- design and fabrication of prototypes,
- performance a manual for licensing and standardization.

As part of a basic development of pipe connectors the possibilities to fulfill with selected available connectors the NET requirements concerning medium, pressure and temperature were investigated. Special emphasis was given to the problems of tightness and corrosion rates of the gaskets for LiPb. Based on these studies different pipe connectors were selected for modification and further development. A pre-test programme was started with a selection of JET and KfK types of pipe connectors. The tests are related to remote handling capability and tightness.

Fig. 38 shows a test rig for the demonstration of the handling capabilities of different types of pipe

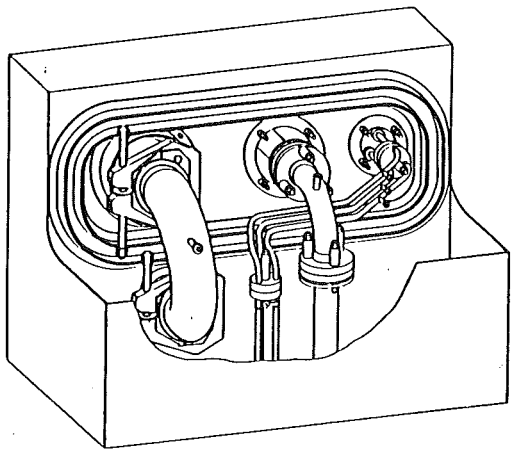

Fig. 38: Test rig for remote handling of pipe connectors

jumpers and different experimental set-ups. At present KfK types SPR-200, ERV-100, and DRV-20 (i.e. two of each) are being installed.

For the performance of tightness test under normal and elevated stress conditions another test facility (PAULA) is available. First test started with three JET wat er and vacuum connectors made available by JET. Fig.39 shows a pipe jumper equipped with a 400 mm

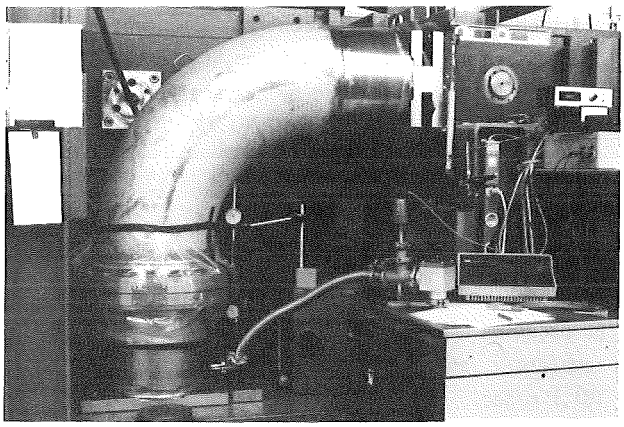

Fig. 39 : JET pipe connector during tightness test (installed in the PAULA test facility)

dia. JET connector during the tightness test in the PAULA test facility. These tests are going on.

The design and prototype fabrication of flange connectors for NET will be carried out according to the results of the pretests.

The basic test programme with these prototypes has to be performed under NET typical geometrical conditions and, if possible, with NET typical handling tools in an integral test facility. This test facility will simulate the upper part of a prototype blanket segment including its auxiliary coolant make up and supply systems. The preliminary draft worked out provides connections for the different types of blankets. Moreover, the sealing lip connections of blanket segments can be tested under realistic boundary conditions using the lip welding units currently being developed at KfK.

In the field of "remote" welding a pipe welding unit for pipe diameters >120 mm and a universal lip welding and cutting system was developed which meets the NET requirements of high pressure, elevated temperature, and low leak rate.

The lip welding system is designed to allow the implementation of exchangeable individual-purpose tools in a trolley. The meanwhile completed design allows to prepare the fabrication drawings for different components until mid 1987.

The prospective exchange of blankets requires both remote-controlled cutting and welding. Minimum tools exchange periods necessitate auxiliary equipment. Realistic tests of the respective cutting and welding units will be performed in a special test rig. This rig will be equipped with a computer control system for parallel operation of different tools. The industrial fabrication of some first system components has already been ordered.

Staff:
L. Gumb
U. Kirchenbauer
A. Schäf
M. Selig
M. Trettin
R. Ullrich

RM 2 Mechanical Components Assembly

Besides basic studies on the arrangement of blanket and divertor segments investigated within the NET contract Nr. NET/85-067/NPE, 3rd task "System Integration of Blanket Segments", the investigations were extended within the frame of this technology programme as far as it was required and possible to define assumptions for the handling of these components. In particular the integration of divertor plates in divertor cassettes inserted from the top of the vacuum vessel instead of key plugs was checked. This option has more exchangeable components than the key plug version and therefore also an increased handling complexity which is only justified if the lifetime of the upper divertor plates is significantly shorter than the lifetime of the lower ones. In this case a replacement of divertor independent from a blanket exchange would be useful and possible.

Investigations of blanket guidance, fixation and sealing of blanket/vacuum vessel will be continued in dependance on the progress of the blanket and divertor replacement studies.

Staff:
G. Böhme
B. Haferkamp
W. Link
A. Suppan

RM 3 Handling Equipment for In-Vessel Components

The investigation of an "In-Vessel Handling Unit" IVHU for inspection, repair and replacement of NET in-vessel components was continued. CEA, CEN/SCK, ENEA, JET and KfK cooperate in the development of such equipment. It consists of

- a contained transfer unit (CTU)
- a transport unit based on an articulated boom or an in-vessel vehicle movable on telescopically inserted rails
- work units with end-effectors attached to the transporter
- the control system

Out of the 9 sub-tasks of the RM3 work programme the following main activities will be reported:

Sub-Task 1: Development of a Conceptual Design

The development was mainly based on the articulated boom as a transport unit and less on the investigation of an in-vessel vehicle. The latter one has significant disadvantages with respect to the required preparation time for insertion and removal of temporarily installed rails.

The geometry and reach envelope of articulated booms with reaches of 90 and 180degr. of the torus were investigated and optimized. On the basis of NET specified tasks and requirements multi-purpose and special work units were identified for the articulated boom:

- A manipulator unit consisting of two electrical master-slave manipulators,
- a handling unit for the replacement of radio-frequency antennae, and
- a combined handling unit for the exchange of divertor plates and active stabilization coils. It consists of a large gripper combined with an electrical master-slave manipulator for dexterous work.

  The work units are equipped with lighting and TV-viewing systems.

According to the results of the November workshop for RM3 where it was decided that KfK would concentrate on the articulated boom with a reach of 180degr. of the torus. Main emphasis was given to

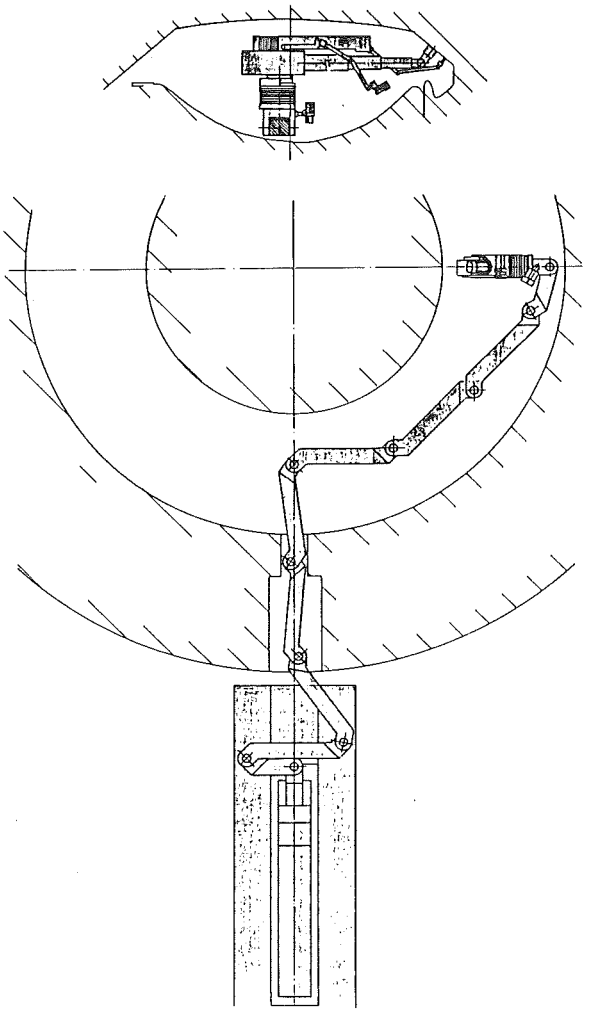

Fig. 40: Articulated boom with handling device for divertor plates and stabilization coils

- minimize the IVHU size in stowed position resulting in a possible reduction of the reactor hall size,
- perform preliminary structure mechanic calculations with the aim to suppress a support of the boom totally although the acceptable load capacity at the end-effector is kept to 10kN. The calculations showed that the main contribution for deflection originates from the torque and supporting against torsion is extremely difficult and hardly feasible,
- develop systems which allow a quick opening and closing of entry ports. A possible solution is to combine the handling device for the entry port plug and the IVHU in one common CTU. The CTU should be permanently attached to the vacuum vessel. The replacement of the IVHU or the entry port plug at the CTU is being performed by using transport flasks attachable to the CTU. A similar transport flask equipped with work units and tools for the IVHU

might be permanently attached to the CTU during execution of maintenance tasks to allow a quick exchange of tools with respect to the different task requirements.

Sub-Task 2: Overall Geometry Measurement

The subtask was split into two domains: out-of-vessel measurement and in-vessel measurement with the major difference in radiation level. The various principal methods for remote geometry measurement were analysed /2/. For out-of-vessel measurement a prototype system based on laser triangulation was designed and is being implemented (GMSYS). The system uses synergetic cooperation of an operator and a computer system. In a CAD system the operator will mark the measurement points in the model and a specially adapted abstraction of the CAD model is then downloaded to the measuring system. In the measuring process a theodolite with integrated laser and a CCTV camera will be directed to the target positions automatically. On a display the overlay of the camera image with the laser point and the synthetic image of the geometric model with the marked measuring point will be produced. The operator has to move the laser point onto the real target manually when he is prompted by the system. With a ready signal of the operator the system goes to the next point. The results are uploaded to the CAD system for further processing. The remote control of the theodolite system and the triangulation algorithms for resection and intersection are implemented and tested. The implementation of an IGES processor for communicating between the CAD data base and the measuring system was started.

Requirements definition and conceptual studies for the in-vessel system are underway.

Sub-Task 4: Conceptual Design of a Device for Removal, Replacement and Fixing of Protection on Tiles

For tile replacement it was defined to use the articulated boom equipped with the multi-purpose unit. The electrical master-slave manipulators of the work unit are suitable for this task. An improvement concerning the replacement time might be possible by using special devices. It requires the previous specification of tile fixation options.

Sub-Task 6: Boom Position Monitoring

To support the remote handling operation in controlling the boom and other remote handling equipment in a fusion reactor a general concept for a computer aided telemanipulator (CAT) system was developed. Its main purpose is to aid the operator in system state perception by computer graphics. The main component is a three-dimensional geometric and kinematic data base. The data base is used for the synthetic scene presentation, collision detection, based on the actual joint parameters, and for off-line simulation to solve ad-hoc problems and to teach new motion sequences. The CAT system shall unburden the operator from repetitive work by integrating robot-like features, general algorithms for manual operator work (e.g. geometric restriction surveillance) and special autonomous subtasks like basic transport motions of the boom. This means, that the CAT-system may work in two different modes: the manual mode, in which the operator is supported merely by an enhanced scene presentation and general manual motion supporting algorithms, and the supervisory mode, in which the operator starts and supervises automatic subtasks.

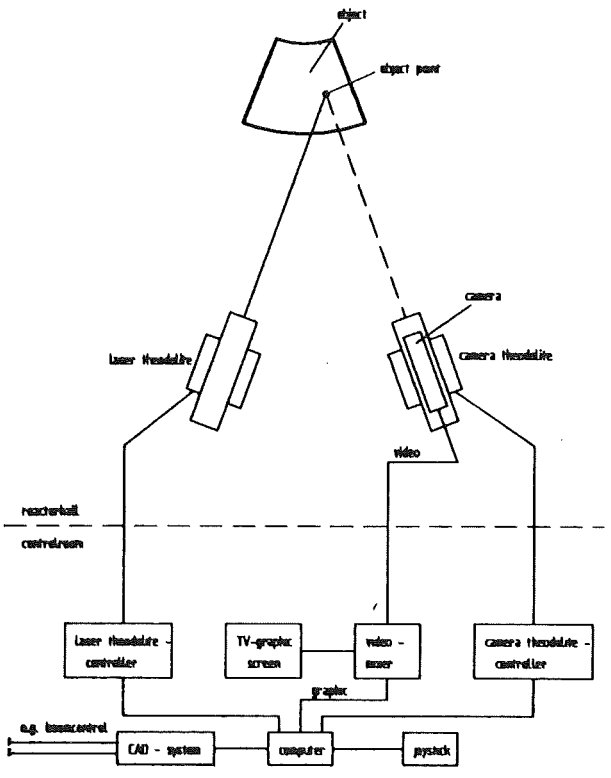

Fig. 41: Architecture of geometry measurement system (GMSYS)

To the test the various functional parts of this concept, two implementations were realized and are operational:

1. A transport and camera control system (CATSYS) for a KfK working cell with an EMSM1 master-slave manipulator mounted on a telescopic bridge crane carrier. System features: hierachical environment model with variable degree of detailling, collision detection, speech input and output (commands, warnings), wireframe low-cost graphics for scene presentation and graphical camera control, camera tracking on hand or room points.

2. A simulation system (GBsim) for the JET boom control system, based on a high performance graphics workstation (IRIS 3020). This implementation is closely related to NET environment. System features: real-time and rather realistic synthetic scene presentation, collision detection, off-line simulation and teaching, problem suited resolved motion algorithms. First tests in the real JET environment were successfull.

For geometric and kinematic model transfer from a CAD-system to the real-time CAT-system a neutral file format, closely related to the ESPRIT CAD*I Format, was defined and post-processors for the CAD system were implemented. First data transfers of manipulator data to the IRIS workstation have been done.

Based on the experiences with these prototype implementations the draft version of a more detailed and NET equipment related control system concept was documented and is presently being reviewed within KfK.

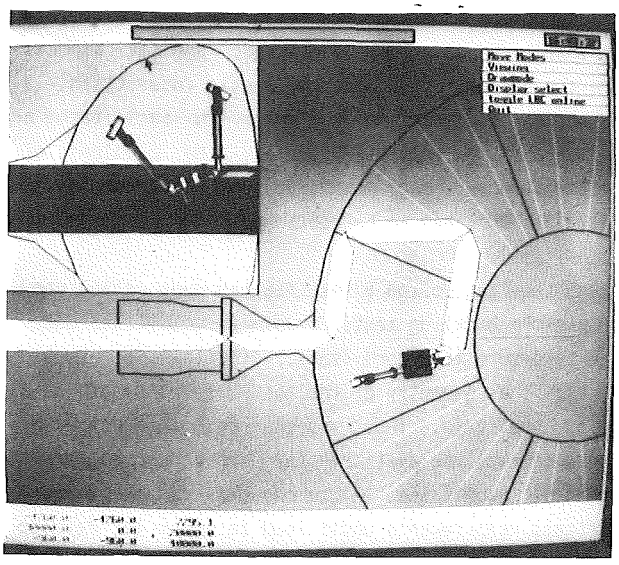

Fig. 42: Display example of JET boom simulator (GBsim)

With a prototype CAT system (CATROB) presently under development for special applications (not directly NET related) the integration of autonomous sub-tasks into a remote handling control system is being investigated (supervisory control mode).

A survey of sensors for boom position monitoring was performed /5/, investigations of the performance of the KfK whisker type proximity sensor are going on.

Sub-Tasks 8 and 9: Environmental Conditions

At present this task is closely integrated with the work related to sub-task 3. The market survey on sensors showed the necessity of radiation experiments with selected sensors. The performance of these experiments is planned to be done in cooperation with CEN/SCK.

References:

/1/ J. Hübener, W. Köhler "NET In-Vessel Handling Concepts, NET RM3-Workshop, Nov. 1986

/2/ J. Schröder , KfK, unpublished report.

/3/ U. Kühnapfel, K. Leinemann, E.G. Schlechtendahl "Graphics Support for JET Boom Control", Intern. Topical Meeting on Remote Systems and Robotics in Hostile Environments, Pasco, Washington, USA, March 30 - April 2, 1987

/4/ K. Leinemann , KfK, Nov. 1986 unpublished report.

/5/ L. Kornelson , KfK, Jan. 1987 unpublished report.

Staff:

G. Böhme	A. Ludwig
E. Holler	H.A. Rohrbacher
J. Hübener	E.G. Schlechtendahl
H. Köhler	K. Schleisieck
W. Köhler	P. Schultheiß
R. Krieg	A. Suppan
U. Kühnapfel	E. Wehner
K. Leinemann	

S+E 4.1.2 Safety Aspects of the Cryosystem

Unter this task safety aspects of the cryostat of NET are investigated. The cryostat is a shell structure surrounding the torus and all coils. It has to maintain high vacuum conditions. To guarantee the integrity of this outer pressure loaded vessel the complicated buckling behaviour has to be studied for normal and accident conditions.

In order to investigate the buckling behaviour for different accident situations a simplified strategy to calculate the buckling loads is under development. During the last period the ability of the simplified method to approximate the most important imperfection sensitivity has been studied . Fig. 43 shows

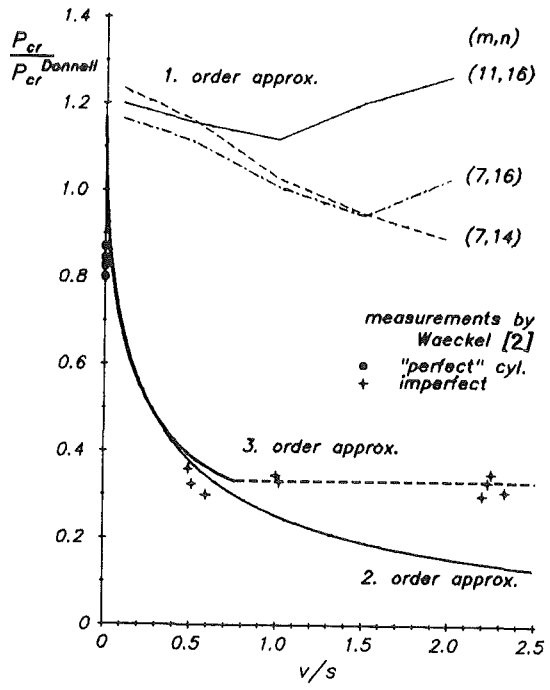

Fig. 43: Imperfection sensitivity of circular cylindrical shells under uniform axial pressure

the comparison between the results of the simplified method and measured values for nearly perfect and imperfect axially compressed circular cylinders /1/. It can be seen, that the very strong decrease of the buckling load P_{cr} by a factor of 4 due to geometric imperfections v of the order of the wall thickness s can be approximated very well by the second and third order approximation of the simplified method. An attractive advantage of the method is, that due to its special series solution approach the result does not only give the buckling load for just one imperfection amplitude but solution function for varying imperfection amplitudes which describes a family of geometry.

The reported strong sensitivity is due to a geometric imperfection having a distribution proportional to the critical buckling mode function. According to the literature this very special imperfection has the strongest influence on the buckling load. Imperfections of this worst type seem to be especially suited to the considered method. But nevertheless, in a next step other more realistic imperfections, e.g. due to manufacturing, have to be studied.

Further studies concerning the general applicability of the method have been continued. The sample problems treated up to now belong to a class where the buckling problem almost leads to a bifurcation problem. For this type the method shows good results, if the imperfections have only a weak influence on the buckling mode function. Although a lot of structures optimized against buckling belong to this type, which is characterized by a membrane stress state during rebuckling loading, this is not the most common situation. But theoretical consideration promise, that problems where the perfect geometry does not lead to a bifurcation problem may be treated too, if the problem is in a certain vicinity to a bifurcation problem. This will have to be studied further because it is expected that cryostat structures will belong to this type.

To support a proper cryostat design different possibilities have been discussed. Special aspects were the prevention of electromagnetic interaction, a segmential construction in order to facilitate a replacement of torus segments and the problems of tightness under such constructive requirements as well. This work has to be continued.

During the last period a test rig has been established to perform buckling tests for simple geometries under outer pressure load conditions. It allows to measure exactly the geometry of the test samples before and during the tests. Thus, further test data for code assessment will be available for perfect and different imperfect geometries. A second aim is to perform stiffness measurements under load in order to develop an experimental nondestructive buckling load

measurement device. Also test equipments for cryostat models up to 1.3 m diameter have been prepared.

References:

/1/ S. Raff, B. Dolensky, R. Krieg "A simplified procedure for elastic buckling analysis", SMIRT-9, Lausanne 1987, to be published

/2/ N. Waeckel, J.F. Jullian "Experimental Studies on the Instability of Cylindrical Shells with Initial Geometric Imperfections" in "Recent Advances in Nuclear Component Testing and Theoretical Studies on Buckling", PVP-Vol. 89 (1984)

Staff:

B. Dolensky
R. Krieg
T. Malmberg
S. Raff
E. Wolf

S+E 4.1.3 Safety Aspects of Superconducting Magnets

During operation of superconduction magnet systems disturbances are conceivable which could finally result in a destruction of a magnet. The energy discharged thereby into an electric arc may lead to damage of the surroundings of the magnet. Cause and course of the disturbances, their detection and identification as well as their possibly destructive consequences are to be investigated using the superconducting torus arrangement TESPE-S. Through development of codes and their verification on the TESPE-S experiment an attempt will is to be made to transform the results to other larger magnet systems.

For this purpose failures are first simulated and built-in in separate experiments, respectively, and initial non-destructive tests are performed. The work includes breakdown of the insulating vacuum current conductor short-circuits, loss of coolant, and generation of electric arcs. At the end of the series of experiments an attempt will be made to demonstrate that a destructive arc in one coil can be mastered safely.

The loss-of-coolant experiments were continued with higher operating currents and varying operating temperatures. One of the six coils was warmed by low pressure gas flow to temperatures between 5.8 K and 8.0 K. Thereafter the complete torus was ramped up to the quench current of the warmed coil. Preliminary evaluation showed stability of the coil against disturbances during current ramping even at these elevated temperatures. Furthermore it was observed that there is a considerable benefit from the large cold mass when one of the cooling loops fails. At least for partial loss of cooling (one or two cooling circuits) a fast safety dump of the stored energy is not necessary.

A vacuum breakdown may occur as a result of a destructive electric arc. Therefore the series of loss-of-vacuum experiments was continued. Before flooding the vacuum space with helium gas, the refrigerator was separated from the torus which then was connected to the a helium gas venting line. With varying rates of pressure increase a helium pressure of up to 10^4 Pa was generated in the vacuum space. The minimum flooding time was two minutes. At that pressure the heat transfer between warm and cold parts of the system is fully developed. Higher pressure values in the vacuum space up to 10^5 Pa were postponed, especially because in that case convection effects can be expected, which in principle can be kept low by design. In the helium space the pressure rise resulting from evaporation could be kept down to few 10^4 Pa, mainly due to the large cross-section of the venting line. Vacuum breakdown therefore did not lead to any risk for the torus system.

Next step on the way to arcing inside a coil is to study arcing across one coil. For this purpose a selected coil was equipped with an extra pair of current leads to room temperature surroundings. The warm ends are fed into a helium-gas filled spark chamber. The electrodes are movable and adjustable. After having started a discharge of the system, an arc will be ignited across the electrodes. These electrodes may be easily exchanged if damaged.

In continuation of studies on safety of superconducting magnet system components the next task was identified. The complex power supply and control system for the LCT-coils in the IFSMTF at Oak Ridge will be analyzed as an intermediate step on the way to the NET magnet control systems.

Publications:

K.P. Jüngst et al., "First Results of the TESPE-E Magnet System Safety, Experiments", Proc. 14th SOFT Conference, Avignon, Sept.8-12, 1986, pp. 1759

W. Geiger, K.P. Jüngst, "Magnetoelastic Buckling Measurements on the Superconduction Torus TESPE", Proc. IUTAM Symposium on the Electromagnetomechanical Interactions in Deformable Solids and Structures, Tokyo, Oct. 12-17, 1986

H. Schnauder, A. Wickenhäuser, "Potential Influence of Reliability Analysis on Component Design in Fusion Reactors", Nucl. Eng. and Design 100 (1987)

Staff:

P. Duelli
W. Geiger
L. Hütten
K.P. Jüngst
H. Kiesel
G.W. Leppelmeier
G. Obermaier
M. Oehmann
H. Schnauder
J. Seibert
E. Süss
A. Wickenhäuser

S+E 5.2.2 Behavior of Gaseous Tritium in the System Plant/Soil
(former S+E 1: Radioactive Effluents)

When atmospheric molecular tritium (HT) comes into contact with soil and plants it will be converted into the more radiotoxic tritium water (HTO) and organically bound tritium (OBT).

For investigation of the mechanism of HT uptake by plants and the distribution of tritium in the main components of organic plant material representative plants will be exposed with HT under controlled climatic conditions. Therefore a climatic chamber was build up and prepared for first experiments. Because of the known very low deposition velocity of HT on plants ($< 10^{-6}$ m/s) only low tritium concentrations in OBT are expected. Processing methods and measuring techniques were tuned to this problem. Biochemical methods for separation of the main components of organic plants material like proteins, fats and carbohydrates were established and tested with contaminated plant material. Contamination was attained by watering of wheat grass with HTO during the whole growth period.

In addition to this programme it was decided to participate in the French Tritium Release Experiment to have the possibility to expose plants and soils to molecular tritium under natural conditions. KfK experiments during the first HT-release on October 15, 1986 included air measurements by a tritium monitor and an HT/HTO-sampling device based on retention of HTO by a molecular sieve. Different plants and soil cores from Germany were exposed to the HT-plume. H-3-concentration of air at KfK-position (6.5×10^{8} Bq/m^3) was lower than measured by other participants because only the edge of the plume passed the KfK equipment. H-3-concentrations in free tissue water of plants were in good agreement with H-3-concentration measured in air moisture (6945 Bq/l) during the exposure. For that reason it is assumed that tritium in plants origins mainly from HTO of air, not from HT. About 3% of tritium in plants are organically bound, mainly to N-, O- and S-atoms as exchangeable tritium.

Deposition velocities of exposed soils ranged from 7.1×10^{-4} to 1.5×10^{-3} m/s. HT diffused into soil up to 40 cm in depth and converted to HTO. Nevertheless the main H-3-activity (70 - 94%) was deposited in the upper 10 cm of the soil.

Perspectives for the Period April - September 1987

- Participation in the second HT-release experiment in France during April/Mai 1987, analyzation and interpretation of received samples

- HT-exposure of plants under controlled conditions in a climatic chamber, comparison with results of the field experiment.

Staff:
H. Schüttelkopf
S. Diabaté
D. Honig

S+E 5.4 Overall Plant Accident Scenarios for NET

Besides the component related safety studies performed under the topic S+E 4.1 this work concentrates on the interactions of the different components and systems and the integral behaviour of the whole plant.

As mentioned in the previous report accident sequences for the blankets are identified and followed up as far as possible. A lack of knowledge was identified as to what are the reaction rates of oxygen or water with the hot graphite protection tiles of the first wall under accident typical conditions. Another reaction considered is: tungsten and water resp. oxygen. A possible result of such reactions are burnable or even explosive gas mixtures. The reaction rates of these mixtures cannot be estimated easily because they depend strongly on their distribution in the vacuum chamber.

Loss of flow considerations have already been inplemented in the blanket design. Natural convection as a passive mechanism is considered now to remove the decay heat of the steel structures, and, additionally, redundant coolant circuits are discussed.

The stored energy of the superconducting magnets may be another. A draft paper was prepared to identify the present state of knowledge and the needs in terms of safety investigations. The most severe accident sequences in this field are:

- shorts and arcing in a magnet
- missile generation
- loss of vacuum in the cryostat

While 'out of plane forces' on the toroidal coils are consequences of the first scenario, missile generation is a very late and a very rare or hypothetical event which requires at least complete separation of a coil cross section at two different locations at the same time. A breakthrough of a coil at one location and a following unclasp of a coil seems to be more probable. The last item may lead to arcing at the current bus and to a loss of superconductivity in the coils.

Since for the magnets most of the main parameters of the design are already fixed these questions will be investigated in more detail.

Staff:
R. Meyder

S+E 5.5 Development of Safety Guidelines for the Design of NET

In order to integrate safety considerations into the design of NET at an early stage and, thus, to support the general approach to safety in design the establishment of safety related guidelines is a special task of the S+E programme.

The Safety Guidelines Working Group has drafted and discussed among its members the General Design Safety Guidelines for NET. These general guidelines provide general safety objectives, the safety philosophy, and particularly radiation exposure targets for normal operations and for accidental conditions. The guidelines are intended for the designer's guidance. They shall provide a framework within which the design can proceed flexibly and effectively aiming at optimum design solutions. A working document of the General Design Safety Guidelines will be ready for discussion with the designers in the middle of 1987.

To provide the designer with safety advices of a more detailed nature in specified areas the second part of the guidelines is devoted to Specific Design Safety Guidelines. For the time being, KfK is participating in three small working parties to produce appropriate specific guidelines for the areas of Containment, Internal Hazards and External Hazards. The preparatory work is in progress.

Staff:
W. Kramer

S+E 7 Long Term Studies

Within the framework of a generic Environmental Impact Assessment for a model fusion facility individual and collective doses and risks for the public due to routine and accidental radioactive release from the fusion facility will be calculated. These calculations will be done for the local < 50 km) and for the regional (> 50 km) scale.

For routine releases, transport in air and water, chemical transformation, dry and wet deposition and transfer within the biosphere will be modelled. In addition to radiation exposure in the local and regional scale, global distribution of tritium, non-radioactive emissions and other risks from the fusion fuel cycle might be of some importance.

Quantified accidental activity releases of fusion reactor types will be used to assess probabilistically contaminated areas, individual and collective doses and health effects in the population taking into account emergency actions and countermeasures.

In 1986 an overview of methods for calculating individual and collective dose equivalent commitments was given. For normalized emissions of a specific radionuclide long range transport and resulting deposition values for a given region (e.g. the FRG) was calculated using to trajectory-puff-model MESOS. These calculations were performed for different European site conditions, using weather data from 1982 and 1983 from synoptic stations all over Europe with a time resolution of 3 hours. With assumptions for height of emission, deposition velocities, radioactive decay etc., given in /1/, for sample 2% of the emissions from a site in the UK (2°W, 53.3°N) and about 5% of the emissions from a site in France (2.5°E, 48.75°N) are deposited in the FRG as an average over the year 1982 and 1983.

Models for calculation individual and collective doses for the local region are also available.

As soon as emission data sets for fission and fusion power plants are available, individual and collective effective dose equivalents can be calculated. With these data a comparison of the radiological impact from fusion and fission power plants and for different European site conditions will be possible.

Reference:

/1/ K. R. Bräutigam, KfK, unpublished report, Dec.1986

Staff:

K.-R. Bräutigam

T 6 Industrial Development of Large Components For Plasma Exhaust Pumping

On behalf of the Commision of the European Communities (CEC) a working group of CEA and KfK elaborates the specifications and conducts the development of large vacuum components for NET. Two alternative solutions for plasma exhaust gas pumping are pursued in parallel: mechanical pumps and cryopumps. The large components required (high vacuum pumps, roughing pumps, and valves) are not commercially available at present. It is planned to develop them within T6.

A feasibility study for turbomolecular pumps is being carried out by industry. Another feasibility study contract with industry relating to all-metal gate valves has been prepared. The technical specification for roughing vacuum pumps has been elaborated and the invitation to bid formulated.

From the feasibility study conducted by industry on turbomolecular pumps of 50,000 l/s pumping speed (helium reference) the following preliminary results have been obtained by the Pfeiffer company:

Plasma disruptions in the torus vessel cause vibrations of the ducts providing connection to the gate valves and turbomolecular pumps. It is necessary to restrict the vibration amplitude of the housing to values smaller than the gap between the emergency bearing and the rotor shaft. The first design proposal provides a 1 mm radial gap between the rotor and the stator and a 0.5 mm gap between the shaft and the emergency bearing. Larger gaps must be avoided because they would lead to higher power input and power losses in the magnetic bearings and the motor drive. The preliminary values calculated by the NET-team for duct displacement during plasma disruptions of $\pm$ 0.5 mm in y-direction would cause the rotor to contact the emergency bearing. To avoid this, it is recommended to fix the pumps to a solid support and to use bellows between the pumps and the torus.

The energy input into the pump will be converted into heat which must be removed by cooling with water or other coolants. There are three main heat sources for the rotor: the magnetic bearings, the motor drive, and the outer magnetic field. The rotor can be cooled by radiation only. For the rotor version made of aluminium alloy the max. operating temperature is limited to 393 K.

For the magnetic bearings maximum heat losses of 10 KW have been calculated for the horizontal shaft and 0.5 KW for the vertical shaft. Different types of motor drives have been investigated.The thermal losses of the motor drive are limited to 2 KW. Heating of the rotor due to the external magnetic field (10 mT) attains 2.5 KW at the maximum. For the stator temperature level of 313 K the radiant heat transfer may attain 7 KW. A rotor made of aluminium alloy can be sufficiently cooled for some special magnetic bearing configurations only.

Theoretical investigations have bee carried out to provide the basis of extrapolation for determination of the "drop pressure" for large turbomolecular pumps. Similarity criteria have been found for pumping in the transition range to laminar flow. The values measured for the existing pumps in the "drop pressure" region were evaluated and an analytical mathematical model for extrapolation to larger pump sizes has been developed. The "drop pressure" for the turbomolecular pumps with 50,000 l/s pumping speed has been calculated for helium: it is 1×10^{-2} mbar at worst and 2.25×10^{-2} mbar at best.

Staff:
U. Kirchhof
H. Lukitsch
A. Mack
D. Perinic

T 10 A Plasma Exhaust Purification by Means of Cryosorption on Molecular-Sieves or Alternative Adsorbents

The fuel cycle of a fusion reactor requires processes for the removal of impurities from several gaseous streams, such as the plasma exhaust gas, the solid blanket coolant, the blanket sparge gas, etc..

Among the processes presently under discussion cryosorption may be cited. For an evaluation of this alternative, however, additional experimental data are required. To fill this gap a laboratory loop was designed to investigate the adsorption on type A zeolite of certain relevant impurities, such as CO, CO_2, CH_4, H_2O and NH_3 from a He or H_2 carrier gas is now under construction. First experiments will concentrate on the measurement of adsorption isotherms of the pure species as well as of gaseous mixtures at temperatures above 80K. During these runs particular attention will be directed towards the cosorption of hydrogen. For this purpose tritiated protium will be employed ($\geq 3.7 \times 10^{10}$Bq/l). Gaseous tritium will be determined with a small ionization chamber of own construction (detection limit >- 3.7×10^{7}Bq/1). Exchange reactions in the zeolite will be followed by liquid scintillation counting. Permanent trapping of tritium in the zeolite, which has been found to occur at about 250°C, i.e. during regeneration, and which appears to be due to phase transformation of the zeolite, will be investigated by techniques developed in our laboratories. The loop will have a volume of 1 litre, Cooling will be carried out with a two stage cryogenerator. The equipment will be placed in a glove box in a controlled area. For gas analysis a HP 5880 gas chromatograph, a VG mass spectrometer and several other specific detection methods, such as radio gas chromatography or UV second derivative spectroscopy, will be used.

To study the parameters that mainly determine the tritium inventory in molecular sieves, type 5A zeolites containing varying amounts of the cations Na, Ca and Ba were first loaded with tritiated water and then heated isobarically as well as isochorically to temperatures between 50 and 600°C for several hours under standardized conditions. After this treatment the tritium activity (liquid scintillation counting), water content (thermogravimetry) and specific BET surface area of the samples were determined. In addition, X-ray diffraction spectra gave information on structural changes of the crystalline framework, and the rate of tritium exchange in water provided data on the permanent trapping of tritium.

The results show that upon isochoric heating of Ca or Ba exchanged type 5A zeolites a change in crystalline structure occurs at temperatures between 260 and 270°C. This structural modification is accompanied by a nearly complete loss of specific surface area as well as by trapping of some of the water. The amount of trapped tritium depends upon the type of cation present in the crystalline framework. Another effect that leads to the fixation of tritium is caused by an exchange between protons in the large cavities with those present in the small ß cavities of type A zeolite.

Tritium trapped in zeolites can be completely removed. For this purpose , however, the zeolite needs to be heated, under controlled conditions, up to at least 500°C either under vacuum or under a stream of dry inert gas.

Staff:
R.-D. Penzhorn

T 10 C Plasma Exhaust Gas Purification by Use of Hot Metal Getters

1. Objectives

Investigation of hot metal getters for purification of the plasma exhaust gas as a process option besides cryogenic methods or selective permeation through a palladium/silver membrane. The main program steps are:

A) Inactive tests with a He/H_2 carrier gas to study various getter metals and alloys (e.g. Zr-Al, Zr-Fe-V) with respect to their absorption and desorption behavior of gaseous impurities, i.e. N_2, CO, CO_2, CH_4, and NH_3;

B) Active tests with tritium to demonstrate the purification efficiency under realistic operational conditions and to investigate isotopic and ageing effects.

2. Current Progress

Design and construction of the laboratory-scale tritium compatible facility TRIGA (Tritium-Gasreinigungs-Anlage) have been completed. A schematic diagram of the facility is shown in Figure 44.

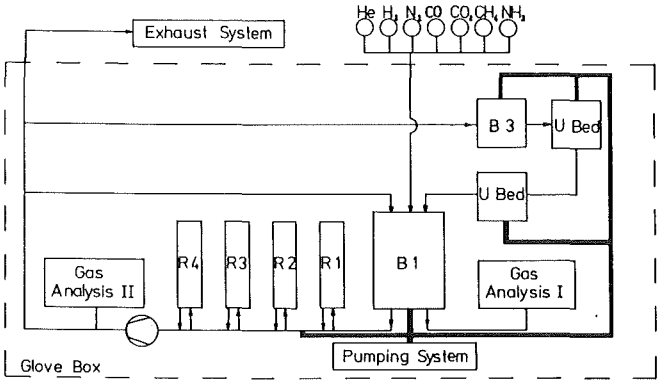

Figure 44 : Diagram showing the main components of the TRIGA facility

He and /or H_2 carrier gas containing one or several impurity gases will be prepared in a recipient of either 100 liters (B1) or 10 liters (B2, not shown in the diagram) in volume. Both vessels can be evacuated and baked at 300°C before being filled with the test gas. The initial gas composition is determined with a quadrupole mass spectrometer (Gas Analysis 1). The purifiers (R1,.., R4) containing the getter materials can be exposed to the gas either separately or in series. A gas chromatograph will be used to measure the impurity concentrations remaining in the carrier gas after passing over the hot metal getters. The gas chromatograph (Carlo Erba Fractovap 2700, Gas Analysis 2) is equipped with a highly sensitive He ionization detector which allows detection of trace gases in the sub ppm region.

After passing trough the purifiers, the test gas can be sent into the exhaust system or pumped back into the recipient B1 (B2) for recirculation. When tritium is involved in the tests, the gas will be pumped into an evacuated recipient (B3) and then stored in one of the uranium beds. The second U bed is used for independent storage of clean tritium during preparation of the test gas mixtures.

3. Results obtained

- All components needed for the step-A experiments have been procured;
- A preliminary safety report for the TRIGA facility has been accepted by the KfK-Department for Radiological and Technical Safety;
- The glovebox has been installed
- Testing of several components has successfully been carried out successfully prior to assembly.

Staff:

H. Albrecht

T. Kastner

T 10 E Adsorption of DT on Heated Metal Beds other than Uranium

Titanium is one of the metals proposed for use as a reversible tritium getter which could be used in tritium processing system of a fusion reactor.

Absorption isotherms of hydrogen in this metal were therefore measured in the temperature range 427-679 °C employing a volumetric procedure. The obtained results agreed reasonably well with data published by other investigators but showed that fairly high temperatures are necessary for the complete liberation of the immobilized hydrogen. In consequence it appeared therefore necessary to initiate a high temperature study of the effect of fusion reactor plasma-exhaust contaminants on the absorption capacity and reaction kinetics of the Ti/H_2 system.

The reaction of N_2 with Ti was found to take place at temperatures above 750 °C. The reaction rate, which can be described by a parabolic law, depends strongly upon the aggregation form of the metal (sheet, sponge, powder). The various phases appearing in the overlayers on the metallic substrate, i.e. TiN, Ti_2N and N dissolved in Ti, were identified by X-ray analysis. The thickness of the overlayers increased with reaction time. The last phase formed when Ti is exposed to N_2 for increasing periods of time is TiN. XPS and AES depth profile analysis showed continuous changes of the in-depth composition of the overlayers. This result is not surprising considering the broad ranges of stability of the titanum nitride phases formed during the reaction.

The quantitative AES analysis of the titanium/nitrogen layers is difficult due to the overlap of the relevant Auger peaks. In XPS problems arise because of the difficulty in defining the Ti 2p peak areas. In spite of these problems reasonable agreement between both surface analysis methods could be obtained.

To separate the contribution of titanum and nitrogen to the complex Auger peak at 385 eV the intensity ratios of the peaks from pure titanum as well as those from a reference titanium nitride were employed. With this evaluation procedure excellent correlation between the estimated thickness of the overlayers and the results obtained from kinetic experiments was achieved.

From the above it can be concluded that the combination of the three techniques, i.e. X-ray analysis, XPS and AES, allows a complete characterization of the overlayers: Whereas with XPS and AES the average composition of an analyzed volume together with depth profiles by argon sputtering can be obtained, the various single phases existing in the sample can be identified by X-ray diffraction.

The results of the kinetic experiments of N_2 with Ti sheets are in line with an effective activation energy of 152kJ/mol as determined by Gulbransen and Andrew(1949),(see Fig. 45).

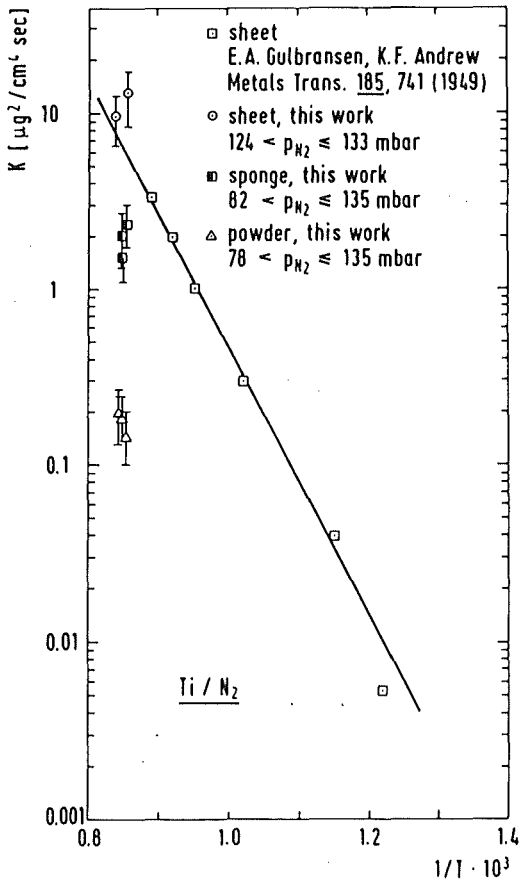

Fig. 45 Temperature dependence of the parabolic rate constants for the reaction of N_2 with Ti

For the estimation of the parabolic rate constant of these specimens the geometric surface area was used. The parabolic rate constants for the reaction of N_2 with Ti sponge and powder are too low because the specific surface aera employed for the calculation of K was determined after BET and evidently this method does not adequately describe the surface area effectively participating in the reaction.

A run with a N_2/H_2 mixture revealed that N_2 does not impede the formation of titanum hydride. Whereas at 625 °C cracking of NH_3 into the elements is the predominant reaction path, efficient nitridation of Ti occurs with NH_3 at 900 °C. In the former case absorbed ammonia strongly inhibits the absorption of hydrogen. At temperatures above 625 °C methane is cracked on Ti into molecular hydrogen and metal carbide as well as elemental carbon.

The carbonaceous surface layer that builds up on the metallic titanum has little influence on the kinetics of hydrogen absorption. The absorption capacity for hydrogen is reduced to some extent.

A few runs were devoted to the investigation of the kinetics of N_2, NH_3, CO and CO_2 with uranium powder and sheets. Parabolic rate constants and saturation concentrations were determined for the corresponding reactions in the temperature range 370 - 851 °C. Ammonia reacts very slowly with U at 370 °C. If the getter is heated up to 590 °C a rapid cracking reaction takes place with the production of an overstoichiometric partial pressure of hydrogen with respect to nitrogen, which can be explained by a slow removal of N_2. Quantitative gettering of N by U is therefore only possible at considerably higher temperatures. CO_2 is not completely absorbed by U at 750 °C, a fraction is converted into CO.

Currently the properties of a Co/Zr alloy are being investigated. In addition, a substantially improved new apparatus is being installed in a glove box for work under radioactive conditions.

Staff:
Dr. Moers
Dr. Noppel
Mrs. Pfennig
Dr. Penzhorn
Mrs. Sirch
Dr. Willin

T 10 H Plasma Exhaust Purification Applying Catalysts

The present report concentrates on the selective oxidation of carbon mcnoxide by Hopcalite, a mixed oxide catalyst composed of manganese dioxide and cupric oxide as well as traces of other oxides. Experiments were carried out in an all metal UHV tight closed loop. Typically 5 - 50 mbar CO diluted in up to 1 bar He were passed with a flow rate of several l/min over 10g of the catalyst placed in a 20 mm Ø stainless steel reactor. During kinetic studies high space velocities were employed. Under these conditions the conversion per pass over the catalyst was low and the system could be treated as an ordinary ideal batch reactor. In general, the reaction was followed gas chromatographically. Complementary analytical techniques were quadrupole mass spectrometry and Fourier transform infrared spectroscopy.

The results obtained show that Hopcalite not only catalyses the CO oxidation by O_2 but can also act as an oxygen donator. In fact, it is possible to oxidize CO diluted in He quantitatively with Hopcalite in the absence of O_2 at temperatures in the range 20-200°C. At low temperatures only a fraction of the CO is converted into CO_2, the rest remains chemisorbed on the catalyst surface. The mechanism of the chemisorption can be described by the reactions.

$$CO + O_2 \rightarrow [CO] \times O_s \qquad (1)$$
$$CO + O_s \rightarrow CO_{2s} \qquad (2)$$

where O_s represents the surface oxygen of the catalyst. Hopcalite with chemisorbed CO on its surface will liberate this gas quantitatively as CO_2 when heated up to 200°C. Thermogravimetric analysis indicates that at temperatures above 220°C the mixed oxide begins to decompose with liberation of molecular oxygen. The weight loss observed up to 100°C suggest that Hopcalite is largely composed of MnO_2 (CuO is stable up to $\nu \geq 1000$°C.

A systematic study of the oxidation of CO by Hopcalite at 200°C reveals that after the initial and fast coverage of the catalyst surface both oxides are reduced by CO with different reaction rates, possibly by steps such as

$$MnO_2 + CO \rightarrow CO_2 + MnO \qquad (3)$$
$$CuO + CO \rightarrow CO_2 + Cu \qquad (4)$$

With the catalyst employed at least 0.23 bar x l CO/g Hopcalite) can be oxidized to CO_2. Numerous experiments carried out at temperatures between -20 and 200°C are presently being evaluated for the calculation of rate constants and an estimation of the effective activation energy. The reduced oxide can be reoxidized by contact with oxygen, but the reaction is slow and incomplete.

In experiments in which approximately 50 mbar NH_3 diluted in a He carrier gas (total pressure 1 bar) were circulated over Hopcalite at 200°C a slow and incomplete reaction with formation of N_2O, N_2 and H_2O as products took place. Under these conditions a reasonably good nitrogen material balance between the reactant and the products was obtained. Therefore it was concluded that no other important product is formed. An increase in the partial pressure of ammonia up to 150 mbar was accompanied by a further reduction in the degree of the conversion. The same effect was noticed when the reaction was carried out at temperatures below 200°C. There is evidence that the fraction of the ammonia, retained by the solid in chemisorbed form, can be expelled again at moderate temperatures. Exposure of Hopcalite to ammonia and reconditioning by heating under vacuum does not impair the oxygen donating properties of the catalyst.

A few runs were devoted to the investigation of the effect of ammonia on the oxidation of carbon monoxide by Hopcalite. Still preliminary results show that at room temperature 35 - 50 mbar CO diluted in He up to 1 bar total pressure are rapidly and selectively oxidized in the presence of 22-23 mbar NH_3 by 10 g Hopcalite. None of the characteristic oxidation products of ammonia were observed under these conditions. They only appeared when the catalyst temperature was raised up to 200°C. For the identification of N_2O in the presence of CO_2 high resolution mass spectrometry ($M/\Delta M = 4.620$) together with the other analytic techniques were used.

Among the major contaminants that need to be considered for the design of a fuel clean-up system hydrocarbons may be cited. It was therefore of interest to examine the possible influence of methane on the oxidation of carbon monoxide by Hopcalite. The results show, that at temperatures between - 22°C and 150°C the oxidative activity of Hopcalite for carbon monoxide (50 mbar) is not impaired by the presence of 20 -33 mbar of CH_4 in He carrier gas.

First screening tests carried out with a $La_{0.8}Sr_{0.2}CoO_3$ Perovskite indicate that fairly high temperatures, i.e. $T \geq 300°C$, are needed for a rapid oxidation reaction of carbon monoxide to occur. Further experimental work with other Perovskites is presently in progress.

Staff:
Mrs. K. Günther
R.-D. Penzhorn

Studies for NET/INTOR

Design of TF Coils for NET

The NET TF Coil Design Study was continued with the aim of identifying critical paths and components for design and construction of the toroidal field coils and by preparing solutions for the identified problems.

After settling the general coil design features special components of the TF coil system are being studied. One significant component is the 16kA current lead between room temperature and liquid helium temperature. The current supply concept of NET foresees such current leads for each coil. Therefore a very economic, reliable and safe design is required. In a first phase the electrical and thermal parameters were optimized. The optimum copper cross section was found to be 50 cm^2 applying copper with a residual resistance ratio of 4. This low RRR is recommended for lowering the temperature rise in case of excess currents and for stable operation and control for enhanced coolant flow.

Staff:
K.P. Jüngst
J. Lühning

Availability of the TESPE Device

The availability study of the TESPE device was completed. It was clearly shown that the superconducting magnets and their discharge control were fully available. Maximum unavailability was only six days originating from a failure of a refrigerator component. While there was considerable amount of failure of instrumentation (sensors, leads, measuring equipment and operation control) observed, availability was not effected due to appropriate redundant lay-out.

Staff:
K.P. Jüngst

Availability of the LCT Plant

The progress on the LCT experimental program is already described under item M1. Within this study the availability and the reasons for its limits should be analysed. Fig. 46 gives a survey on the cumulated availability of the facility until end of 1986. The different activities in outage times will be evaluated and an attempt for extrapolation to later facilities will be done.

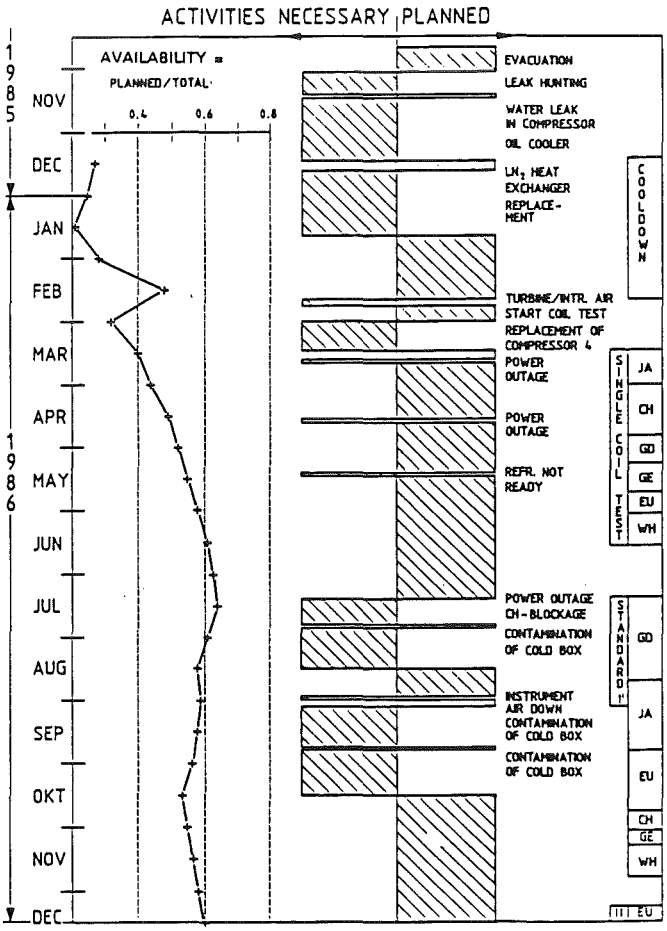

Fig. 46: Cumulative availability of the IFSMTF (LCT) plant

Staff:
A. Ulbricht

Study on the NET TF Pancake Tests

The considerations and calculations in order to develop a model coil test facility relevant for NET coils were continued. The prototype lengths of the conductors (about 1.5 to 2 km of each conductor developed by industry) should be used in the TOSKA cryostat. Two configurations were investigated in detail (Fig. 47):

Both configurations were investigated with respect to forces and stresses in order to determine not only the limits but also the values which can be simulated. More over the possibility of installation into the TOSKA cryostat was examined . The result of this examination was that for the cluster configuration the cryostat wall and the LN_2 shield must be removed in order to install the model coils. Due to the difficult access the installation and pretests would be very

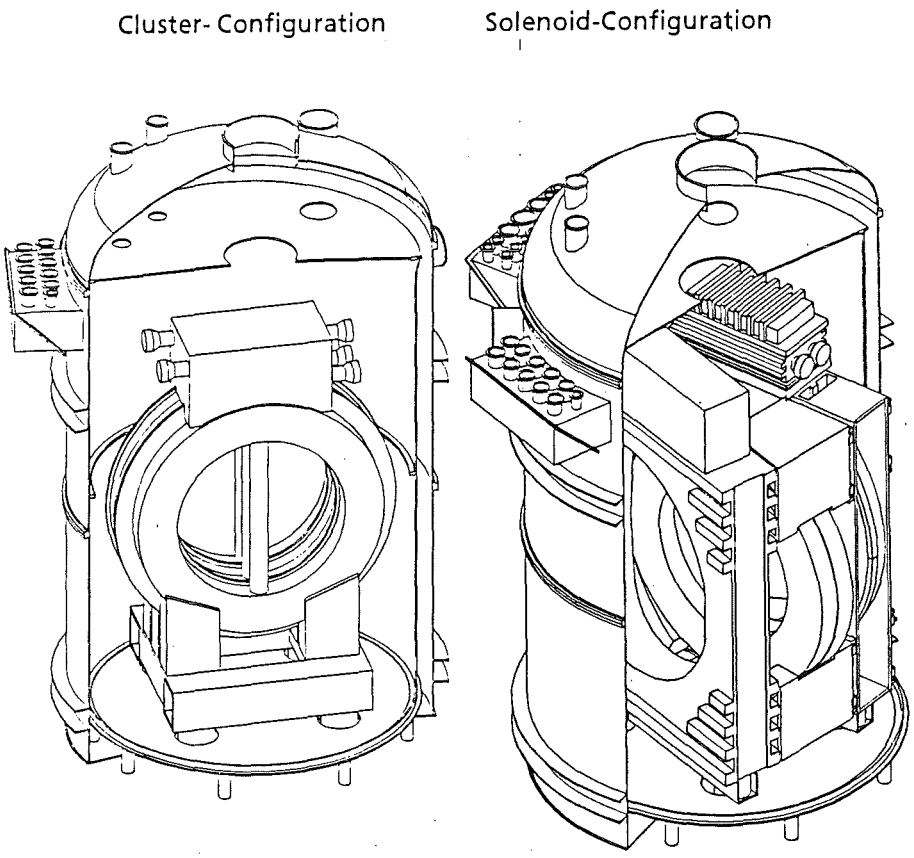

Fig. 47: Alternative test configuration

a) "Cluster-Configuration" with 2 LCT coils generating the background fields and in between test coils with the TF-conductors or OH-conductor for testing. A configuration could be found, which provides the required 11T at the conductor of the test coils , taking into account the geometrical boundary conditions and the electric and magnetic maximum allowed values of the LCT-coils.

b) "Solenoid-Configuration" consisting of three solenoids (two with TF-conductors and one with the OH-conductor) with about 3m diameter and a maximum field of 12T.

time consuming. Preliminary flow schemes for the coils and current leads were worked out and the optimum He mass flow and also the required cooling power were estimated. The cluster configuration requires due to the LCT coils a larger mass flow with an inlet temperature of 3.5K compared with 4.2K for the solenoid configuration. A 4.5K equivalent cooling power of about 2.7kW is needed for both configurations. The mass to be cooled down is 130 metric tons for the cluster configuration and 80 tons for the solenoid configuration.

The further work comprises a comparison of test possibilities, of costs, and of time schedules. The work is done in collaboration with the laboratories of ECN, ENEA Frascati, SIN and the NET-team.

Staff:
W. Herz
K. Jentzsch
W. Maurer
G. Zahn

Investigations of the Vacuum and Exhaust Performance of NET

The previous studies about the evacuation behaviour of NET design alternatives (impact of NET material outgassing and leak rates for two different blanket design concepts) were extended to include dwell time pumping. The modifications in the design of the plasma chamber internals, as e.g. introduction of graphite first wall protecting tiles, and new vacuum duct onfigurations are taken into account.

This work is carried out within the new NET study contract "Simulation of the Vacuum Performance of NET-DN": In an introductory report all design figures and design assumptions of the actual NET design used to execute this contract were specified. The conductivity values of new vacuum duct configurations were calculated using the Monte Carlo code MOVAK 3D. The results of a duct geometry with enhanced helium dissipation are shown in Figure 48.

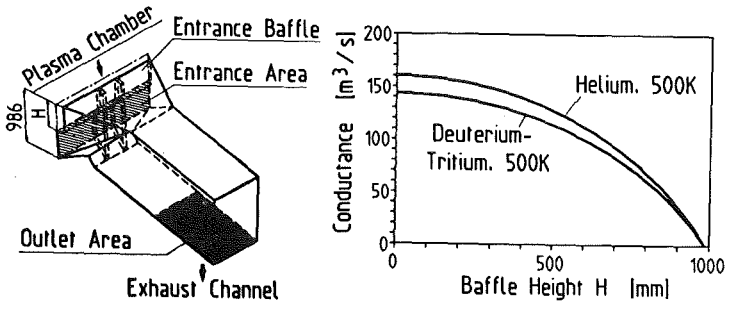

Fig. 48: Reduction of conductance of the divertor channel by an entrance orifice plate

A thorough literature survey was started to gather and interpret the knowledge published about the gas-solid interaction phenomenon of graphite which is envisaged for the first wall protection tiles. In the course of this work the information available at present about the outgassing behaviour of other kinds of structural materials is also completed and updated. For storage and easy retrieval of this information suitable data banks based on the d-Base system were implemented on a personal computer.

Staff:
R. A. Müller

Development of Helium Cryopumping Materials and Preliminary Design Concept of Cryocompound Pumps for NET

Experimental investgations are under way at KfK with the aim to develop and optimize porous active cryosorption surfaces for helium pumping from the plasma exhaust gas. In these investigations a multitude of combinations of materials for the sorbent, bond , and the cold wall are tested and the bonding techniques are investigated to select the best suited candidates.

After elaborating the test matrix which incorporates the promising, technically feasible material combinations for the sorbent, the bond and the cold wall, specimen preparation was started.

Till now, sorbent materials have been attached to more than 200 metal platelets of 50 mm diameter simulating the cold wall. Various bonding techniques have been used:

- Bonding through thermal spraying techniques (plasma spraying) has been ordered from industry.
- Brazing in air with phosphorous bearing brazing metal and in vacuum with active brazing metal has been performed.
- Cementing using inorganic cements, with and without heat conducting additives, has been carried out successfully.

Assembly has been completed of the TARZAN temperature cycling facility and operation has started. The facility can be run both manually and automatically. It is operated as follows:

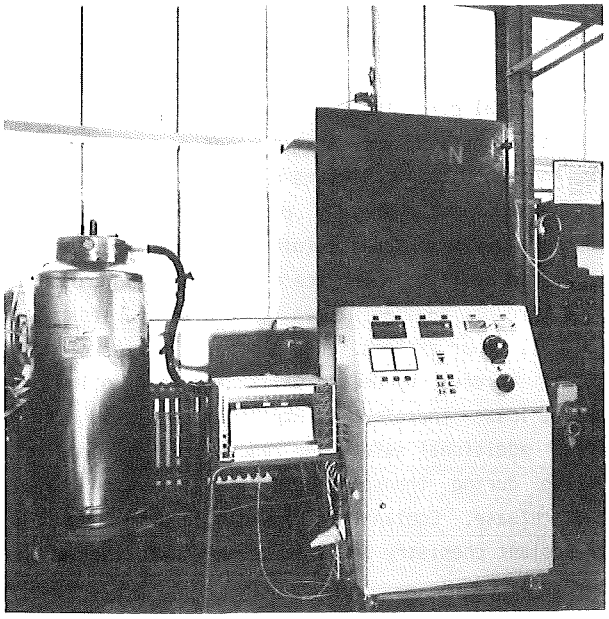

Fig. 49: TARZAN thermal cycling facility

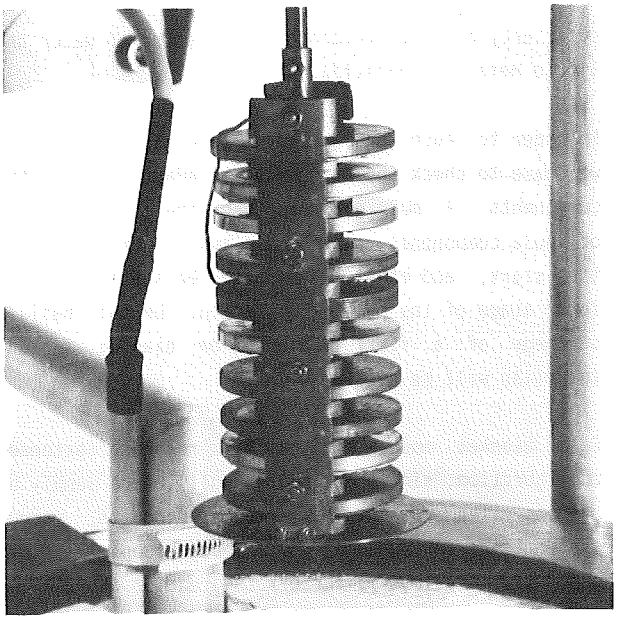

Fig. 50: Specimen holder with sorption specimens to be used in the cycling tests.

A specimen holder accommodating up to ten sorption specimens (50 mm in diameter) can be fixed to the piston rod of a pneumatic cylinder which is mounted to operate vertically. By temperature-dependent control the specimens are alternately heated in an annular furnace in nitrogen atmosphere (150-350 °C) and immersed into an LN_2 bath (78 K). This cycle is repeated 100 times. Specimens surviving these cycling tests without defects are used further, the rest is sorted out. The failure rate has been ∿50% until now. In principle, it seems possible to achieve a sufficiently good thermal cycling resistant and sorbent bonding on the cold wall by use of the preselected bonding techniques (thermal spraying, brazing and cementing).

In the next step of the test programme the rest of the specimens will be exposed to He-gas at 4.2K and their helium absorption capacity will be measured. This will be done in the HELENE testing facility which is presently under construction.

The subsequent tests on a technical scale (sorption panels with 400mm diameter) will be carried out at the TITAN testing facility. They will include comprehensive experiments involving vacuum pumping under simulated operating conditions of a fusion reactor. The specifications have been elaborated for the components of the TITAN facility and most of the orders have been placed.

Staff:
H. Haas
J. Hanauer
W. Höhn
U. Kirchhof
H. Lukitsch
A. Mack
D. Perinic
D. Zimmerlin

Engineering Problems of NET Blanket Testing and Blanket Insertion Strategy

The only chance for testing advanced NET blanket types in a realistic reactor environment is the use of the NET reactor itself as a test facility. Because of the growing radioactivity of the reactor torus and the coolant and breeder circuits during reactor operation, remote handling can only be chosen as the handling method for maintenance and blanket exchange purposes. Flexible blanket insertion must therefore be a basic design goal of NET. Standard blankets for the first operation period of NET are water cooled LiPb elements. Gas cooled blankets with ceramic breeder material and selfcooled liquid metal breeder blankets are candidate advanced blanket types to be tested. Main advantage of these types are a higher breeding

efficiency and the avoidance of risky use of water and liquid metals in parallel.

In order to reach such a blanket insertion flexibility we have to check and eventually to adapt all related components. A main goal has to be the identification of those components, which have just to be present at the start, and others, which may be supplied in a later stage of the reactor operation. On this basis a strategy of a flexible blanket or blanket segment insertion will be developed.

Each blanket module in the NET reactor (extended configuration, single and double null) needs supply by systems like coolant or breeder circuits, vacuum system and instrumentation. These supply systems generally are located far off the reactor torus and joined at the top of the blanket modules, claiming a lot of space around the top of the reactor torus. Also some of the space there must be kept free for the transport routes for blanket segment replacement. Additionally some space is claimed by devices for plasma heating and diagnostics. Therefore we conclude the space problem is a critical NET design issue.

In a first step a tentative design for the pipe arrangement in the mentioned critical space region, was developed using the watercooled LiPb-blanket as a reference. This design was based on the following assumptions: 4 separate circuits fo cooling of each outboard blanket segment and 3 circuits for each inboard segment, and permanent coolant availability for after heat removal. This demands valves on both sides of the disjoin location of the coolant tubes, and a connection for the transport cooling system is required in addition. This reference solution is based on "cutting and welding" for the tube dismounting and reassembling, respectively. The multiplicity of connections leads to a time consuming blanket exchange process.

In order to reduce the time consuming manipulations, an adapter is proposed as an alternate to the single tube joints, providing automatic multiple tube clamping. It serves for automatic clamping of conical tube flanges equipped with metallic seals. All tube connections of one blanket segment are assembled in a common casing, where each pair of flanges owns individual clamping mechanism.

Attempts were made in order to reduce the number of pipe connections. The NET team proposes 2 sets of 3 primary circuits each: the outboard segments are connected to one circuit for first wall cooling, one for blanket cooling and one for emergency cooling. One liquid metal circuit serves for tritium removal. The inboard segments do not contain breeding material and are connected to 2 circuits only, one main cooling system and one emergency cooling system. These proposals are discussed as follows: Because of safety reasons we see the preference of such a design, where the emergency cooling system is completely separated from all other systems. Not all parts of the circuit can be covered by double walls for prevention of coolant loss. Therefore a completely separated system offers additional safety and reduces the problems of cooling during transporting of segments with decay heat release. Coolant mixing would lead to problems for coolant chemistry and leak detection in addition.

The number of valves needed for the isolation of one circuit for one segment are not reduced markedly. Like in the case of our reference design we state that the use of more valves would simplify the replacement procedure and vice versa.

A further way aiming in a plant simplification may be the use of intermediate headers. This means drums, in which the coolant streams of different segments of the same blanket sector are collected or distributed, respectively. In this case a reduction of the number of components results in a markedly increased number of operating steps necessary for segment replacement, and in a shortage of redundancy too.

Staff:
G. Class
K. Schramm

Design Study of Plasma Facing Components

a. First Wall with radiatively cooled protection tiles (see also task G1, N1)

At least for the physics phase of NET a ceramic protection of the First Wall (FW) seems necessary. Graphite is considered the only short term protection material, because of its irradiation data base available and inspite of open questions concerning tritium uptake. Radiative heat transfer between the protection tiles and the FW steel structure is favoured since it seems the most reliable mechanism under cyclic conditions and despite of the fact that these results in relatively high graphite

temperatures. The principle of forming with the coolant channels rails in front of the FW steel structure by welding on tubes or by corrugating the wall itself results in two benefits: firstly, the coolant channels serve as attachment rails for the protection tiles loosely fitted in between and free to expand, and secondly the coolant channels are close to and almost surrounded by the heat radiating tiles such that temperature differences causing stresses in the steel structure are minimized.

FE evaluations of the temperature and stress distributions showed that surface heat fluxes of up to 40 W/cm^2 together with representative volumetric heat sources seem to result in tolerable stresses and in maximum graphite temperatures near 1800°C. There are design proposals for coolant channels in toroidal direction (preferred for gas - or LiPb-cooling of the FW) as well as in poloidal direction (preferred for water cooling of the FW); additional design work on details and optimization with repeated temperature and stress calculations are necessary. As for other FW concepts the gain in vacuum tightness should be compared from a view point of reliability between the limited possibilities of double containing the coolant along with a sufficiently high heat transfer and a single containment with a minimum number of welds in lowly loaded zones.

There is a need of blackening parts of the FW steel structure for improved radiative heat transfer; this may be achieved by plasma-spray-coating with Al_2O_3 + TiO. Diffusion and chemical reaction processes with the substrate and with the contacting graphite tile will be investigated but are not expected problematic. Development of suitable tiles and investigation of their irradiated properties is expected to be covered by a different task.

Manufacturing tests will be initiated as soon as the design seems sufficiently consistent and reliable.

Thermal fatigue testing must proof the crucial issue of lifetime of FW samples under cyclic loads. In such a test for the KfK FW concept the inclusion of tiles and of vacuum seems necessary to provide a typical temperature distribution on the curved steel surface and at the tile contact points. If in the thermal fatigue test facility at JRC Ispra temperature limitations for the quartz tubes do not allow that kind of high temperature and vacuum conditions an additional test facility should be considered.

Staff: G. Hofmann

Development of ECRH Power Sources at 150 GHz

The KfK gyrotron started microware operation in October 1986. An output power of 120 KW during pulses up to 5 ms was achieved in the TE_{031}-mode at 149,5 GHz with an effciency of about 20%. Several adjacent modes existed; both stable single mode and multimode operation was observed. This experimental achievement was an significant step in the long-term development of MW power sources for future fusion devices like NET.

The resonator used in this experiment was selected from extensive parameter studies and manufactured by KfK. It includes a slightly tapered (0,05 degree), 19 mm long midsection with calculated resonances at 146,56 GHz (TE_{231}), 149,57GHz (TE_{031}) and 154,64 GHz (TE_{521}). Up to 50% effiency was expected with this resonator.

During the initial experiments, the parameter settings for a maximum output power and mode determination were major objektives. For this purpose, a low average power calorimeter and a frequency measuring system were installed. The magnetic field was varied between 5.42T and 6.08T and the output power was measured for various beam voltages and currents.

The frequencies measured for the main modes

146.5 Ghz - TE_{231}
149.5 GHz - TE_{031}
154.5 GHz - TE_{521}

are in excellent agreement with the theoretical predictions. Beside of stable single mode operation, ode jumping or multimode operation has been provoked by suitable adjustment of the magnetic field.

The maximum output power of > 120 KW achieved so far and the related efficiency of 20% are still below expectation. One possible reason is a lateral isplacement of the beam inside the resonator of about 0,4 mm, which is concluded from the assymmetry of the beam observed by X-ray photography on the collector surface. Therefore, magnetic steering of the beam will be installed in the next future.

The modes were regularly identified by frequency measurement. In addition, the modes have been visualized by thermopaper and by liquid crystal. A relatively high mode purity has been estimated from this observation.

Under certain circumstances, small frequency jumps from pulse to pulse around the frequencies related to the modes involved have been observered (e.g. 50 MHz). A mismatch in the transmission line is a virtual explaination.

During this initial experimental phase, several improvements became necessary. The short pulse (10 µs) power supply for the beam voltage showed excessive instability. After successive modifications, a regulated power supply with independent modulation anode control provides now highly stable beam parameters for an extended pulse length (100 µs to 5 ms). Thereby the stability and repeatability of the microwave signal was essentially improved. Similarly the magnet power supplies needed additional stabilisation. This was solved via computer based calibration and control procedures.

In parallel to the experimental activities, progress in gyrotron theory was achieved mainly in three areas:

- the parameter studies have been completed for several resonators from TE_{03} to TE_{06} modes using the using the self consistent code.
- complex cavities have been calculated for arbitrary transition angles between cavities. The mode conversion at the transition is included.
- the influence of the beam on the behaviour of the output taper has been calculated. A significant deterioration of the mode purity can be explained by this effect.

The development of microware diagnostics concentrated on the calibration of the far field mode analyzer and on improvement of the frequency mesurement.

Staff:

W. Baumgärtner
E. Borie
H. Budig
G. Dammertz
U. Feißt
P. Grundel
G. Haubrich
R. Hietschold
G. Hochschild
A. Hornung
B. Jödicke
M. Kuntze
R. Lehm
A. Möbius
N. Münch
H. Oppermann
B. Piosczyk
G. Redemann
H. Stickel
R. Vincon
H. Wenzelburger

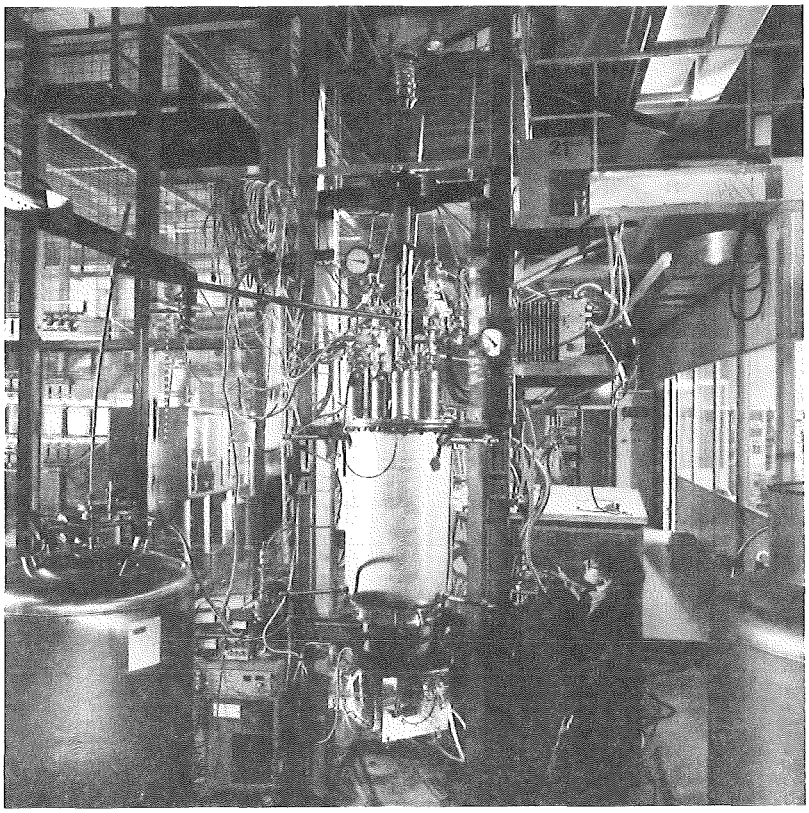

Figure 51: The 150 GHz gyrotron under test operation

External Contributors:

H. Flügel et al. (TU, Hamburg-Harburg)
M. Kitlinski et al. (IHE, Univ. Karlsruhe)
M. Thumm et al. (IPF, Univ. Stuttgart)
O. Dumbrajs (Abas, Leopoldshafen)

Publications:

M. Kitlinski, W. Wiesbeck, G. Hochschild:
Measurements of Mode and Frequency Spectra for 150 GHz Gyrotrons.
11. Int. Conf. on Infrared and Millimeter Waves, Pisa, October 20 - 24, 1986

E. Borie:
Self Consistent Calculation for a 150 GHz Gyrotron
ibid.

M. Thumm, H. Kumrić, H. Stickel:
TE03 - to - TE01 Mode Converter for use with a 150 GHz Gyrotron
ibid.

G. Hochschild, Gyrotron Team:
Initial Experiments with a 150 GHz Gyrotron operated in TE_{031} Mode
ibid.

B. Jödicke:
Startup and Mode Competition in a 150 GHz Gyrotron
ibid.

E. Borie, O. Dumbrajs:
A complex Cavity with Mode Conversion for Gyrotrons
ibid.

H. Stickel, B. Jödicke:
Generation of TE_{on}- Modes by Diameter Steps in Circular Waveguides
ibid.

E. Borie, B. Jödicke, O. Dumbrajs:
Parameter Studies for a 150 GHz Gyrotron operating in the TE 031 Mode
Int. Journal of Elektronics, Vol. 61, No. 6, p. 735, December 1986

E. Borie:
Self Consistent Code for a 150 GHz Gyrotron, Int. Journal of Infrared and Millimeter Waves, Vol. 7, No. 12, December 1986.

Appendix I: Table of Fusion Technology Contracts

Task Code No.	Title	KfK Departments
B 1	Blanket Design Studies	IMF III, INR, IRB, IT
B 2	Development of Computational Tools for Neutronics	INR
B 6	Corrosion of Structural Materials in Flowing Pb-17Li	IMF I, IMF II
B 6.3	Fatigue of Structural Steel in Pb-17Li	IMF I, IMF II
B 9	Tritium Extraction based on the Use of Solid Getters	IT
B 11-16	Development of Ceramic Breeder Materials	IMF I, IMF III, INR, IRCH
B 15.3	End of Life of Solid Breeding Materials in Fast Neutron Flux	IMF I, IMF III, INR
M 1	The Large Coil Task (LCT)	ITP
M 3	Development of Composite High Field Superconductors	ITP
M 4	Superconducting Poloidal Field Coil Development	ITP
M 8	Design and Construction of a Poloidal Field Coil for TORE SUPRA as NET-Prototype Coil	ITP
M 9	Structural Materials Fatigue Characterization at 4 K	ITP
M 12	Development of Low Electrical Conductivity Structures	IMF IV, ITP
MAT 1.6	Development and Qualification of Type 1.4914 Base Metal Properties	IMF II
MAT 1.9	Pre- and Post-Irradiation Properties of 1.4914 Martensitic Steel	IMF II
MAT 1.11	Post Irradiation Fracture Toughness of Type 1.4914 Martensitic Steel	IMF II
MAT 2.2	In-Pile Creep-Fatigue Testing of Type 316 and 1.4914 Steels	IMF II, IMF III
MAT 6/ MAT 13	Ceramics for First Wall Protection and for rf Windows	IMF I
MAT 9.2	Investigation of Fatigue under Dual Beam Irradiation	IMF II
MAT 18	Development of Low Activation Ferritic-Martensitic Steels	IMF II

N 1	Design Study of Plasma Facing Components	INR, IRB, IRE
N 2	Shield Design Studies	IMF III
N 3	Development of Procedures and Tools for Structural Design Evaluation	IMF IV
N 5	Development of Theory and Tools for Evaluation of Magnetic Field Effects on Liquid Breeder Blankets	IRB
N 6	Studies of Pepple Beds of Ceramics Compounds	INR
RM 1	Background Studies on Remote Maintenance	IT
RM 2	Mechanical Components Assembly	IT
RM 3	Handling Equipment for In-vessel Components	IDT, IRE, IT
S+E 4.1.2	Safety Aspects of the Cryosystem	IRE
S+E 4.1.3	Safety Aspects of Superconducting Magnets	IDT, IRE, ITP
S+E 5.2.2	Behavior of Gaseous Tritium in the System Plant/Soil	HS
S+E 5.4	Overall Plant Accident Scenarios for NET	IRE
S+E 5.5	Development of Safety Guidelines for the Design of NET	IRE
S+E 6	Licensing Activities	PKF-PL
S+E 7	Long Term Studies	AFAS, INR
T 6	Industrial Development of Large Components for Plasma Exhaust Pumping	IT
T 10 A	Plasma Exhaust Purification by Means of Cryosorption on Molecular Sieves or Alternative Adsorbents	IRCH
T 10 C	Plasma Exhaust Gas Purification by Use of Hot Metal Getters	IRCH
T 10 E	Adsorption of DT on Heated Metal Beds other than Uranium	IRCH
T 10 H	Plasma Exhaust Purification Applying Catalysts	IRCH
Development of ECRH Power Sources at 150 GHz (This task is part of the Fusion Physics Programme of the EC.)		IDT, IK

Appendix II: Table of NET Contracts

Theme	Contract No.	Working Period
TF-Coil Design	183/84-12/FU-D/NET	12/84 - 3/87
Availability of the LCT Plant	210/85-9/FU-D/NET	10/85 - 12/87
Availability of the TESPE Device	211/85-9/FU-D/NET	10/85 - 12/86
Development of Helium Cryopumping Materials and Preliminary Design Concept of Cryocompound Pumps for NET	224/86-4/FU-D/NET	6/86 - 12/86
Study on the NET TF Pancake Tests	240/86-6/FU-D/NET	5/86 - 4/87
Engineering Problems of NET Blanket Testing and Blanket Insertion Strategy	243/76-6/FU-D/NET	7/86 - 7/87
Evaluation of Crack Growth Delay in Multilayer Sheets	253/86-11/FU-D/NET	11/86 - 12/87
Simulation of the Vacuum Performance of NET-DN	254/86-11/FU-D/NET	10/86 - 12/87

Appendix III: KfK Departments contributing to the Fusion Project

Kernforschungszentrum Karlsruhe GmbH
Postfach 3640
D-7500 Karlsruhe 1
Federal Republic of Germany

Telephone (07247) 82-1
Telex 7 826 484
Telefax/Telecopies (0)07247/82 5070

KfK Department	KfK Institut/Abteilung	Director	Ext.
Applied Systems Analyses Department	Abteilung für Angewandte Systemanalyse (AFAS)	Dr. H. Paschen	2500
Central Safety and Security Department	Hauptabteilung Sicherheit (HS)	Prof. Dr. H. Kiefer	2660
Institute for Data Processing in Technology	Institut für Datenverarbeitung in der Technik (IDT)	Prof. Dr. H. Trauboth	5700
Institute for Nuclear Physics	Institut für Kernphysik II (IK)	Prof. Dr. A. Citron	3502
Institute for Materials and Solid State Research	Institut für Material- und Festkörperforschung (IMF)	I. Prof. Dr. F. Thümmler II. Dr. K. Anderko III. Prof. Dr. K. Kummerer IV. Prof. Dr. D. Munz	2918 2902 2518 4815
Institute for Neutron Physics and Reactor Engineering	Institut für Neutronenphysik und Reaktortechnik (INR)	Prof. Dr. G. Keßler	2440
Institute for Reactor Components	Institut für Reaktorbau-elemente (IRB)	Prof. Dr. U. Müller	3450
Institute for Radiochemistry	Institut für Radiochemie (IRCH)	Prof. Dr. H.J. Ache	3200
Institute for Reactor Development	Institut für Reaktor-entwicklung (IRE)	Prof. Dr. D. Smidt	2550
Central Engineering Department	Hauptabteilung Ingenieur-technik (IT)	Dr. H. Rininsland	3000
Institute for Technical Physics	Institut für Technische Physik (ITP)	Prof. Dr. P. Komarek	3500

Appendix IV: Fusion Project Management Staff (PKF-PL)

Nuclear Fusion Project - Project Management Group	Project Manager	Dr. J.E. Vetter	ext. 5460
	Secretariate	I. Sickinger, I. Pleli	5461/5466
	Project Administration, Documentation	BW. G. Kast	5462
	International Affairs	Dr. F.W.A. Habermann	5520
	Studies, NET Contacts	Dr. J.E. Vetter	5460
	Blanket Development, Test Facilities	DI. H. Sebening	5464
	Superconductiong Magnets, Gyrotron Development	N.N. (Dr. J.E. Vetter)	5460
	Tritium Technology, Structural Materials	Dr. H.D. Röhrig	5463
	Safety and Environmental Impact, Remote Handling	DI. A. Fiege	2668/5465